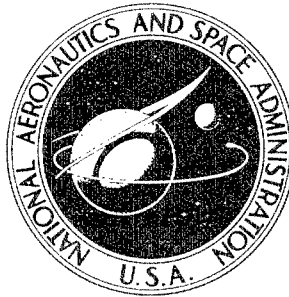


NASA CONTRACTOR
REPORT

NASA CR-165



NASA CR-165

INVESTIGATION STATEMENT A
Approved for Public Release
Distribution Unlimited

OK

(CAVITATION DAMAGE OF MECHANICAL PUMP IMPELLERS OPERATING IN LIQUID METAL SPACE POWER LOOPS)

by R. S. Kulp and J. V. Altieri

Prepared under Contract No. NAS 3-2541 by
PRATT & WHITNEY AIRCRAFT DIVISION
UNITED AIRCRAFT CORPORATION
Middletown, Conn.
for

20011210 129

NATIONAL AERONAUTICS AND SPACE ADMINISTRATION • WASHINGTON, D. C. • JULY 1965

CAVITATION DAMAGE OF MECHANICAL PUMP IMPELLERS
OPERATING IN LIQUID METAL SPACE POWER LOOPS

By R. S. Kulp and J. V. Altieri

Distribution of this report is provided in the interest of information exchange. Responsibility for the contents resides in the author or organization that prepared it.

Technical Film Supplement CRC-1 available on request.

Prepared under Contract No. NAS 3-2541 by
PRATT & WHITNEY AIRCRAFT DIVISION
UNITED AIRCRAFT CORPORATION
CANEL - Middletown, Conn.

for

NATIONAL AERONAUTICS AND SPACE ADMINISTRATION

For sale by the Clearinghouse for Federal Scientific and Technical Information
Springfield, Virginia 22151 - Price \$4.00

FOREWORD

This report describes the work done under Contract NAS3-2541 for the National Aeronautics and Space Administration, Lewis Research Center, Cleveland, Ohio. The work reported was done at CANEL (Connecticut Advanced Nuclear Engineering Laboratory), Middletown, Connecticut, a facility operated by Pratt & Whitney Aircraft Division of United Aircraft Corporation for the United States Atomic Energy Commission.

Work was conducted by the CANEL Pump Group, supervised by Mr. Robert W. Kelly, Component Development and Major Test Systems Manager, and Mr. Glenn M. Wood, Head of the Pump Group. Mr. Robert S. Kulp was Project Manager of the contract, and Mr. James V. Altieri was Senior Engineer. Technical direction for NASA-Lewis Research Center was by Mr. James P. Couch, Nuclear Power Technology Branch.

ABSTRACT

A three vaned centrifugal pump impeller, designed for high suction specific speeds, was endurance tested as part of a turbopump in 1400F potassium at a suction specific speed of 20,000 to determine the extent of cavitation damage. The endurance test was terminated after 350 hours due to performance deterioration and increased vibration. Post-test examination of the impeller showed mild cavitation pitting on inlet pressure surfaces of the vanes and variable amounts of damage on back channel pressure surfaces with a maximum penetration of about 0.050 inch. Complete water calibration of the impeller was done prior to the liquid metal test to determine cavitation patterns and tentatively select test conditions for the endurance test. Attempts were made to correlate cavitation noise with visual data during the impeller test. The complete turbopump was tested in water to determine collector effects on impeller performance and to finally select the endurance test point.

TABLE OF CONTENTS

		<u>Page</u>
I.	Summary -----	1
II.	Introduction -----	3
III.	Test Impeller, RI-7C3 -----	5
IV.	Turbopump -----	7
V.	Test Facilities -----	9
	A. Impeller Water Test Stand -----	9
	B. Water Pump Test Stand -----	9
	C. Liquid Metal Pump Test Stand -----	10
VI.	Impeller Calibration in Water -----	13
VII.	Turbopump Tests in Water -----	16
VIII.	Turbopump Test in High Temperature Potassium -----	19
IX.	Discussion -----	25
X.	Conclusions -----	29
XI.	Appendices -----	30
	A. Nomenclature -----	30
	B. Orifice Calculations -----	31
XII.	References -----	33

I. SUMMARY

The success of a nuclear Rankine cycle space powerplant throughout its required long life-time depends on many things, not the least of which is limited or no cavitation damage. A ultimate or net performance relies on high performance components; in mechanical pumps, this may mean designing for very high suction specific speeds and operating in cavitation. To what degree a pump can be allowed to cavitate without sustaining damage and endangering the system is unknown. This report describes an investigation which takes the first steps in that direction.

A mixed flow centrifugal pump impeller was used in an investigation of cavitation damage in liquid metals. This investigation was conducted to determine the feasibility of operating a pump at very low inlet pressures which resulted in a high degree of cavitation being established on the impeller and the consequent danger of cavitation damage. The investigation was conducted in the following three phases to provide detailed information for a thorough analysis of the hydraulic and cavitation performance of the impeller and of the impeller and diffuser combination: 1) a visual study and calibration of the impeller with water, 2) a water test of the pump, and 3) an endurance test of the pump with 1400F potassium. 1729

The hydraulic performance data of the test impeller both in and out of cavitation were obtained from a series of water tests. The tests were conducted in a test stand which had a clear plastic housing surrounding the impeller. This allowed direct visual observation and photographic recordings of the cavitation bubble formations at various test conditions. A motion picture supplement, CRC-1, has been prepared and is available on loan. A request card and a description of the film are included at the back of this report.

Sound emanating from the cavitating impeller was recorded and analyzed for variations of both frequency and intensity levels. The sound intensity curve thus obtained was used as an additional guide for determining the degree of cavitation existing in the liquid metal experiment. Tentative selection of the conditions for the liquid metal experiment were made from the data of the impeller test. These selected conditions were confirmed by a water test of the complete liquid metal turbopump. This turbopump test was run to determine changes in performance caused by the pump collector since the impeller tests were conducted with a long conical diffuser rather than a pump collector. The flow orifices used in the main flow circuit of the liquid metal loop were also calibrated during these water tests.

The water pump tests of this investigation showed moderate changes in cavitation performance from the impeller data. These changes were characterized by a gradually declining head rise beginning at relatively high values of net positive suction head (NPSH) for the pump compared to a sharper drop-off in head rise below the break-off point for the impeller tests.

An extensive record of the impeller condition was made before each of the water tests and before and after the liquid metal test. This record included dimensional and zyglo inspections, radiography, chemical and metallographic analyses, surface roughness profiles, and rubber molds of the impeller vanes. These same inspection and analytical procedures were repeated after the liquid metal endurance test, and the records were compared for any indication of cavitation damage.

The liquid metal turbopump endurance test was conducted with 1400F potassium. The parameters for this test were selected after carefully reviewing all of the documented water test results. A shaft speed of 6375 rpm was chosen to correspond to the water tests, which produced a non-cavitating head rise of about 200 feet at a flow of 700 gpm. This level of head

rise is of interest in Rankine cycle space powerplants. The flow rate of 700 gpm appeared near optimum from the water tests as it permitted operation at minimum NPSH around the head rise drop-off point on the cavitation curve with relatively stable and well defined cavitation patterns. This flow rate was also near the best efficiency point for the RI-7C3 impeller. From visual studies of the cavitation patterns, it did not appear that the cavitation bubble implosions in the rear channels of the impeller collapsed on the vane surfaces for suction specific speeds as high as 20,000. Although bubble implosions were observed to occur on the vane surfaces near the leading edge at these suction specific speeds, they were not judged to be as potentially damaging as cavitation implosions occurring in the rear channel regions where high pressure gradients existed. Also, since no evidence of cavitation pitting attack was found after several hundred hours of water testing in cavitation, it was decided to test the impeller at a suction specific speed of 20,000 with 1400F potassium.

The establishment of the liquid metal operating point in cavitation involved a slight compromise in flow rate resulting from a higher head rise with 1400F potassium than was predicted. A cold impeller tip clearance of 0.017 inch had been established based on the prediction that this would increase to about 0.030 inch at 1400F to correspond to the performance of the water pump test. Due to the higher head rise, an average flow rate of 708 gpm was obtained at the established suction specific speed operating point of 20,000 with 1400F potassium rather than the desired 700 gpm. The drop-off in head rise was about 4 percent of the maximum head rise at a shaft speed of 6375 rpm at this fixed throttle condition.

The high temperature potassium endurance test was terminated after 350 hours due to an increase in vibration and a moderate performance deterioration. Examination of the pump after shutdown revealed that the impeller had rubbed on the collector during operation. The cause of this rubbing contact could not be determined. Additional minor damage to other pump parts was observed, and an exact cause and effect relationship could not be established.

The test showed that the selected test conditions were too severe; they resulted in excessive cavitation damage. Several areas of cavitation damage were found; the most severe damage occurred on the pressure surface near the vane channel exits. The most severely damaged area was measured during metallographic examination to have a depth of penetration of 0.050 inch. Minor damage found on the inlet pressure surfaces was judged to consist of single event pits. The suction surface of one vane at the impeller inlet had cavitation damage induced by two small projections above the blade surface.

The mechanism by which small metallic particles are removed from the surface of the impeller vane was not revealed by metallographic examination. The examination did show a reorientation of carbon and recrystallization along all areas exposed to the liquid metal, including those surfaces exposed by removal of material by cavitation. Electron beam microprobe examinations did not show a selective removal of any constituent of the impeller material, leading to the conclusion that very little, if any, chemical reaction was involved.

II. INTRODUCTION

The low specific weight (lbs/Kwe) required of electric propulsion systems for space vehicles appears to be most easily attained by the use of a nuclear Rankine cycle turbogenerator system. Cavitation damage of centrifugal pump impellers, its prevention or control, plays an important role in the final reliability and ultimate specific weight of these space powerplants. Present systems of this type use mercury as the primary working fluid with condensing temperatures of around 600F. Development of these Rankine cycle systems to higher power levels will require condensing temperatures of around 1300F to 1500F which precludes the use of mercury. These high condensing temperatures may be obtained with alkali metals such as potassium or sodium.

This report describes a detailed investigation into cavitation and cavitation damage occurring on a centrifugal pump impeller operating in 1400F potassium. The objective was to conduct a well documented investigation at as high a suction specific speed as possible, consistent with insignificant cavitation damage in high temperature potassium. The work was accomplished using an existing, investment-cast, type 316 stainless steel impeller designed for high suction specific speeds. Existing test facilities and equipment were also used in this program.

The two-phase liquid metal circuit of these Rankine cycle powerplants will require the condensate (or boiler feed) pump to be supplied with an inlet net positive suction head sufficient to suppress cavitation. Net positive suction head, or NPSH, is defined as

$$NPSH = H_T - H_V$$

where H_T is the total pressure at the pump inlet which is fixed by system requirements, and H_V is the liquid vapor pressure at the temperature of the liquid being pumped. An NPSH sufficient to suppress cavitation can be obtained by increasing H_T through use of a jet pump or by decreasing H_V by subcooling the liquid leaving the condenser. Both of these actions result in an increase in powerplant specific weight. The jet pump adds weight directly and indirectly by reducing the over-all powerplant efficiency. Increased subcooling would require increased radiator surface and a consequent increase in total powerplant weight. Jet pumps may possibly be omitted, subcooling may be minimized, and a low NPSH attained by allowing the pump to operate with some degree of cavitation. The extent to which a pump may be allowed to cavitate without sustaining objectionable damage is not known; and, currently, conservative values of suction specific speed must be used by designers of pumps for long service.

Suction specific speed is a parameter used to classify impellers regarding their NPSH requirements. It is defined as

$$N_{SV} = \frac{N \sqrt{Q}}{NPSH^{3/4}}$$

where N is the pump shaft speed in rpm, Q is the flow rate in gpm, and NPSH is the net positive suction head in feet. It is desirable to design a pump with as high a suction specific speed as possible within limits of cavitation damage. At present, suction specific speed values of about 6000 are used for pumps required to render long service. Some attempts have been made to go beyond this value for long service pumps as evidenced by the work of Grindell (Ref. 1) in molten salt and liquid alkali metals and Grennan (Ref. 2) in mercury.

Most pumps which are allowed to cavitate produce small metallic particles which are dislodged from the impeller under the action of cavitation. These particles are abrasive and can erode pipe walls, nozzles, valve seats, liquid metal bearings and other components in the system. The erosive action may accelerate rapidly by producing more abrasive particles, thus wearing out the system from the inside at an ever-increasing rate. The larger particles may become lodged in narrow reactor heat transfer passages, reducing or completely blocking liquid flow. Extremely high local temperatures could thereby be developed and melting and rupturing of the fluid passage could follow.

Cavitation damage can eventually cause a decline of pump performance by eroding away complete sections of the impeller vanes. The time required for this to occur has not been established since it is a function of the degree of cavitation the impeller material may sustain.

Many investigations have been concerned with finding a cavitation damage resistant material. A highly resistant material may allow higher suction specific speeds or an increased degree of cavitation on the impeller for a given time period. However, most materials testing devices do not represent the complex flow patterns or the pressure fields of an actual impeller. The materials problem is further complicated by the lack of a parameter by which the damage resistance of materials may be correlated. While materials investigations should and must continue, little effort has been directed toward cavitation patterns within pump impellers. Studies of cavitation patterns within impellers, such as those reported by Wood (Refs. 4, 5 and 6), Hartmann and Soltis (Ref. 15) and by Dodge and Langteau (Ref. 16), should also be continued.

III. TEST IMPELLER, RI-7C3

The impeller chosen for this program was designed for high suction specific speed operation. It was the seventh research impeller (RI-7) design of the CANEL Pump Group, in a continuing investigation of the effects of design parameters on impeller performance, dating back to the early days of the Aircraft Nuclear Propulsion program (ANP). The development programs conducted by CANEL have included numerous water tests of impeller designs and high temperature liquid metal tests of pumps and pump components.

The RI-7 impeller, shown in Fig. 1, was made by investment casting type 316 stainless steel. Three impellers of this design were cast from one heat of material. The first, or A casting (RI-7A), was tested extensively with water for both hydraulic and cavitation performance. Part of the test program was optimization of the impeller with respect to cavitation. This program showed that a 15 percent cutback of the blade leading edge on the meridional profile provided increased cavitation performance without loss of hydraulic performance. The impeller was then redesignated as the RI-7A3. The impeller used for the investigation described in this report was the third or C cast impeller, which also utilized the cutback leading edge and was, therefore, designated RI-7C3. The RI-7C3 impeller is shown in Fig. 2, with a sketch of its meridional profile dimensions.

The design procedures, which are based on the stream filament technique of Hamrick et al. (Ref. 3), are programmed on a digital computer to expedite calculation. No attempt was made in the analysis to account for the real fluid effects in the derivation of the velocity and pressure distributions; however, vane blockage effects are included. Complete vane coordinates are obtained from the computer printout.

The vane tip as seen in the meridional profile was chosen as the reference station (Fig. 2). The vane angle distribution, or angle of intersection of vane and meridional vane tip, was determined from the equation

$$\beta^* = \beta^*_{1t} + (\beta^*_{2t} - \beta^*_{1t}) (S/S_T)^n$$

where β^*_{1t} and β^*_{2t} were the inlet and discharge vane tip angles. S/S_T was the fractional linear distance along the meridional tip measured from the inlet (Fig. 2), and n was an arbitrary exponent. The inlet and discharge tip vane angles were 8.0 and 7.3 degrees, and a value of unity was chosen for n .

The hub station was generated by assuming a smooth variation in the through-flow velocity from inlet to discharge. The vanes were described by extending perpendicular elements from the tip meridional reference station to the impeller axis. Vane thickness was then specified for a finite number of hub and tip stations and the vane contours produced by a fairing process.

The RI-7C3 impeller water tests of this program showed that two separate and distinct areas of cavitation were present. An area of cavitation at the impeller inlet generated by the leading edge appeared first as the NPSH was decreased. A second area of cavitation began forming in the rear channels at low NPSH values. Static pressure readings along the vane tips taken during water tests of the RI-7A impeller in 1960 (before the leading edge was cut back) are plotted in Fig. 3 and definitely show a discontinuity in the vane tip static pressure rise through the impeller. Fig. 3 shows the impeller tip static pressure rise as a function of distance along the meridional reference station (Fig. 2). The discontinuity in the static pressure rise occurs at approximately 62 percent of the distance through the impeller. This point corresponds with the beginning of the rear channel area

of cavitation as determined by visual observations of the RI-7C3 impeller in cavitation. Vane tip static pressure rise is probably not affected by cutting back the vane leading edge. Any effects which do occur would be confined to the immediate inlet area.

The RI-7C3 impeller, used in this investigation, was machined from its as-cast condition, similar to Fig. 1, by cutting the tip arc to the radius of 3.93 inches, by cutting back the inlet leading edge 15 percent of the meridional dimension, and by machining the splines required for mounting. In addition, vane surfaces were hand finished to provide a smooth surface at the impeller inlet. A surface finish of approximately 10 rms was obtained in the immediate inlet area. This fine a surface finish could not be obtained beyond the inlet area due to the difficulty of working in the narrow space between the vanes.

Extensive inspection using several techniques was performed on the RI-7C3 impeller to completely document its pretest condition. Mechanical inspection was made to determine the impeller geometry, dimensions and surface roughness. All dimensions, including vane location, were within the casting and machining tolerances specified by the CANEL Pump Group. Surface roughness measurements were made of both suction and pressure surfaces of each vane at four specified vane coordinate stations. These measurements were recorded on a paper tape for permanent record as shown in Fig. 4.

The material removed from the vane leading edge in order to form the cutback was examined metallographically as pretest material to determine the microstructure and hardness. These data were used in post-test comparisons in an effort to determine the mechanism of cavitation damage.

Other internal and external methods of examination and documentation used included radiography, fluorescent inspection, photography, and rubber molds of all vane surfaces. Radiographic and fluorescent inspections revealed no defects of the impeller vanes. An area of surface porosity was revealed by fluorescent inspection, and it was photographed to retain a permanent record. This area was on the impeller hub near the vane root of vane 3 and is shown in Fig. 5. This porosity was produced during the casting process and may be classified as extensive surface roughening.

A macroscopic record obtained by photography was made of only that inlet area visible when looking directly into the impeller inlet. This area was photographed at magnifications of two and four times. Enlargements of as high as twenty times could be made from the negatives for detailed visual inspection if needed. Fig. 6 is a sample photograph of the vane surface at four magnification. A record of the entire vane surface, including that photographed, was obtained by using room temperature vulcanizing silicon rubber. This material was applied to the surface, allowed to harden and then stripped from the surface. This process produced a remarkably accurate record of the vane surfaces, including such details as polishing marks and the trace marks left by the surface roughness measurement technique. A photograph of a typical rubber mold is shown in Fig. 7.

IV. TURBOPUMP

A turbopump originally designed for liquid metal operation in the Aircraft Nuclear Propulsion program (Refs. 7, 8 and 9) was selected as the drive vehicle for the RI-7C3 impeller. This turbopump (CANEL designation TP-1) is shown in Fig. 8. The turbopump had most recently been operated in the liquid metal stand chosen for this test series; and, therefore, a minimum of changes to both pump and stand was required.

The turbopump was designed about 1957 and required minor design changes to reflect advances in liquid metal pump technology developed at CANEL. A sketch of the turbopump in Fig. 9 shows the design changes necessary for the RI-7C3 impeller and for improved operating characteristics with 1400F potassium. These changes are described briefly in the following paragraphs.

The turbine, originally designed for several hundred horsepower, requires only 56 horsepower when operating with the RI-7C3 impeller at its best efficiency point in water. A partial admission plate was added to the turbine inlet which reduced the inlet area by 60 percent. This permitted the turbine to operate more efficiently at the reduced pressure ratios of the cold air system used as the power source.

A sweep gas system is used in this pump to control liquid metal vapor and prevent its condensation in close clearance, low temperature areas. The gas is admitted under the lower oil seal (Fig. 10), sweeps down the shaft and is vented overboard through the dynamic seal area. The sweep gas vent system was enlarged to handle the high vapor load when operating at 1400F with potassium.

The dynamic seal was changed from the original single rotor to the more efficient double rotor. The double rotor design is a more advanced design which operates effectively under high vapor conditions. A liquid metal-gas interface is established on the lower seal, while the upper seal aids the sweep gas system in removal of liquid metal vapor (Fig. 10).

An insert in the scroll to adapt to the RI-7C3 impeller was also required. The impeller originally designed for this turbopump was of larger inlet diameter than the RI-7C3 and had a different tip radius. The scroll adapter was designed for the RI-7C3 to minimize hydraulic losses. The adapter provided a bell-mouth inlet to the impeller and a contoured discharge passage to allow the impeller fluid discharge angle at 700 gpm to match as closely as possible the diffuser vane angle.

A new bolt, used to attach the impeller to the shaft, was designed since creep stress calculations indicated the original design was marginal. The new bolt was of larger diameter and was made of a material with greater creep resistance at 1400F.

Fabrication of parts for these changes was completed and turbopump assembly began with the shaft assembly shown in Fig. 11. The shaft assembly was balanced to 0.01 ounce-inch and indexed for correct orientation on assembly into the turbopump. The completely assembled turbopump, less the pump scroll, is shown in Fig. 12.

Impeller tip clearance settings in the turbopump were difficult to obtain accurately due to the inherent axial play of the deep-groove ball bearing used in the turbopump assembly. The clearance problem was further complicated by the inability to check clearance settings directly. To set the clearance, it was necessary to preload the shaft and take measurements of the impeller position with reference to mating surfaces of scroll and pump. Backup spacers behind the impeller were ground to the proper thickness to provide the desired clearance.

The liquid metal test assembly of the turbopump required spacers different from those used in the water test assembly to account for clearance changes which would result from thermal expansion of the pump parts. The anticipated thermal growth was calculated from data of previous tests of the TP-1 turbopump and other high temperature pumps tested at CANEL.

V. TEST FACILITIES

The three phases of this program were conducted in three separate test stands. In Phase I, the impeller was calibrated in the Water Impeller Test Stand; Phase II used the Water Pump Test Stand for a full configuration test and to calibrate the orifices used in the liquid metal test; the Phase III experiment in 1400F potassium utilized the Liquid Metal Pump Test Stand.

A. Water Impeller Test Stand

The Water Impeller Test Stand is a two leg closed loop and is shown in Fig. 13. The arrangement of the various loop components and some auxiliaries is shown in the schematic of Fig. 14.

The stand contains provisions for supplying deaerated and demineralized water to the test loop. Additional deaeration of the water can be accomplished using a vortex generator and gas pickup tube assembly built into the test stand. This equipment produces water having a dissolved air content of 3 ppm.

Water flow in the system is controlled by a throttle valve located in each of the two legs of the loop. Each leg is sized for a different range of flows so that a wide range of impellers may be tested. Flow in each leg is measured by a flow tube with the output read on a slant-tube manometer.

Loop pressures are controlled through accumulators mounted on the piping leading to and from the test impeller. Either the impeller inlet or discharge pressure may be controlled by air pressure applied to the accumulators. Measurement of pressures requiring highest accuracy is done by precision Bourdon tube gages which are periodically calibrated. The gages on this stand were calibrated at the beginning of this test program.

Water temperature is controlled at a constant value by a water-to-water heat exchanger built into the loop. Temperature is maintained through a pneumatic proportional band controller at a preset value.

Impeller speed is regulated by controlling the DC output of a motor-generator which supplies power to the impeller drive motor. Speed was measured by a proximity probe triggered by a two-tooth gear on the drive shaft and read on a digital counter. Speed control is excellent in this arrangement with a variation of only ± 3 rpm at 6375 rpm occurring during the tests.

B. Water Pump Test Stand

A water test of the turbopump liquid metal configuration with the RI-7C3 impeller was run in the Water Pump Test Stand. This test stand, shown in Fig. 15, is a single closed loop. Component and auxiliary layout is shown in the schematic of Fig. 16. The turbopump required the addition of a high pressure cold air line to the test stand for operation of the turbine and some changes of loop pipe sizes to adapt to the impeller flow rate. Orifice flanges were added to the test loop to provide means of calibrating the orifices for the liquid metal test stand.

This water stand has provisions for supplying demineralized and deaerated water to the loop. The deaerator tower can be connected into the loop circuit with partial bypass flow for additional deaeration of loop water as needed. Degaeration operations before testing resulted in water with 5 ppm dissolved air.

Water flow in the test loop was controlled by a pneumatically operated throttle valve located on the pump discharge pipe. The flow was measured by a venturi type flowmeter whose output was read on a vertical mercury manometer, slant-tube mercury manometer and, through a differential pressure transmitter, on a precision Bourdon tube gage. The flowmeter was calibrated after the test and was found to be within 5 gpm over the test range.

Pressure control of the loop was accomplished by regulating the air pressure supplied to accumulators connected to the pump inlet and discharge pipes. All loop pressures were read on precision Bourdon tube gages at the control panel.

Loop water temperature was controlled by a pneumatic proportional band controller regulating the cooling water through a water-to-water heat exchanger built into the loop. Water temperature was also measured by thermocouples attached to the loop piping at the pump inlet. A precision millivolt meter with internal calibration was used to indicate these temperatures.

Pump speed was sensed using a proximity pickup and a six-tooth gear on the pump shaft. Output of the pickup was read on a digital counter. The pump speed was controlled by varying air pressure in the turbine air line using pneumatically operated throttle valves. The speed control system was not sensitive enough to provide accurate control and allowed speed variations of up to 200 rpm. This system was refined by installing a vernier valve on a bypass line around the main throttle valve. Through this method speed variations were reduced to \pm 20 rpm at 6375 rpm.

C. Liquid Metal Pump Test Stand

The 1400F potassium test was run in the Liquid Metal Pump Test Stand shown in Fig. 17. A schematic representation of this stand is given in Fig. 18 which also shows arrangement of system components. This test stand required considerable rework in order to prepare it for this test. The test loop had been loosely capped with argon gas inside for the two year period since its last operation; and it, therefore, required complete dismantling and acid cleaning. Figs. 19 and 20 indicate the extent of this rework program.

The developing liquid metal technology at CANEL had obsoleted most of the control panel installation of the Liquid Metal Pump Test Stand. The control panels were reworked to provide centralized grouping of the more critical controls. The control panel arrangement around the operator's station is shown in Fig. 21.

Changes to the test loop were made to increase reliability and improve measurement techniques. The throttle valve used in this loop was removed entirely and a long radius elbow installed in its place. Previous experience with bellows sealed liquid metal valves of this size has shown very low reliability due to bellows failures. Therefore, flow control for this test was changed to a calibrated orifice, since the test would be conducted at one flow for the test duration.

The liquid metal flow measurement was changed from a flow tube using two pressure transmitters to an electromagnetic flowmeter. Pressure transmitters in high temperature liquid metal service have not shown the required accuracy, nor are they reliable. The electromagnetic flowmeter does not require penetration of the loop piping in any way, thus assuring high reliability. Ideally, electromagnetic flowmeters are accurate to one percent of range, but due to installation techniques, the inaccuracies can range above five percent of range. The installation on this stand was estimated to have an

accuracy of three percent of range, since positioning of both the magnet and output wires was done with considerable care. However, the turbulent flow through the pipe in the area of the flowmeter caused a fluctuating reading. Flow measurements recorded were the observed average of indicator fluctuations amounting to ± 5 gpm.

A potassium oxide control station in the form of a hot trap, which included a liquid metal sampling station, was included in the test loop. The hot trap was an eight inch pipe packed with titanium sponge. Part of the loop flow was to be channeled through the hot trap to react potassium oxides with the titanium. Hot trap temperature was to be held around 1500F to insure the reaction. The hot trap became inoperative due to a faulty control valve sticking shut during early phases of the test and the system was not used during the endurance test.

The liquid metal sampling station was made from small diameter piping and tubing and was installed in parallel with the hot trap. Liquid potassium flow was established through the sampling station by heating the piping with propane torches to melt the potassium which was then allowed to flow for a period of 15 to 30 minutes. Flow was then stopped by closing two valves ahead of and behind a ten inch long section of removable tubing. The sampling lines were then forced cooled to room temperature and the tube containing the sample was removed. A new section of tubing was then connected to the lower fittings and flushed with argon gas for five minutes. Final connections were made, and the sampling station remained this way until the next sample was required at which time the procedure would be repeated.

Chemical analysis of liquid metal samples was done by the mercury amalgam technique for oxygen and spectrographic analysis for other contaminants. The mercury amalgam technique for oxygen determination has been used extensively at CANEL and is developed to an accuracy of ± 10 ppm.

Critical system pressures were read on precision Bourdon tube gages having an accuracy of 0.1 percent of full scale. Pressure measurements were obtained by reading the argon gas pressure required to maintain a given liquid level in two tanks connected to the loop. One tank was connected at the pump inlet and also served as a loop liquid level indicator as well as inlet pressure sensor. The second tank was connected to the pump discharge pipe. A liquid level indicating "J" type probe was used in both tanks for level measurement. To arrive at the pump inlet head a correction of 0.375 feet of potassium was subtracted from the pressure gage reading (converted to head, in feet) to account for the head of potassium above the impeller inlet, as noted by dimension "x" in Fig. 10. Liquid levels were maintained within $\pm 1/2$ inch during the test. The inlet pressure was automatically controlled with a pneumatic proportional band controller to within ± 0.15 foot of potassium. Gage fluctuations on the discharge pressure gage were less than one gage division, or one quarter psi.

Temperature measurements on the test loop were made by thermocouples attached to the outside of the loop piping. The wires used in these thermocouples are purchased to a CANEL specification which gives the metallurgical requirements of the wires. A complete chemical analysis is conducted on samples of the wires when received to assure their compliance with the specification. Temperature measurement errors using specification wire are: thermocouple plus installation error, ± 3 F; extension lead wire from thermocouple to instrument ± 4 F; instrument error, ± 4 F, which gives a total error of ± 11 F. Indicating instruments used in these applications are of the internal calibrating type with an accuracy of 0.2 percent of full scale reading.

Argon gas, used as inert cover on system potassium, was purified to remove water vapor and oxygen before introduction into the loop system. The gas purification system was comprised of two purifiers of CANEL design. Water was removed from the gas by a molecular sieve trap. Oxygen removal was accomplished by heating the gas to 1500F in the presence of titanium sponge. These purification units are capable of supplying purified argon gas at a rate of 40 scfh per unit. Typical analysis of the gas during test was 1.1 ppm oxygen and 3 ppm water vapor.

The solubility of argon gas in potassium was calculated from theoretical considerations for temperatures up to 1400F. These calculations showed a possible argon content of 2.26 ppm (by volume) per atmosphere at the 1000F filling temperature. The gas-potassium surface available in this system and the outgassing features of the dynamic seals of the turbopump limited the addition of argon to the system at higher temperatures. This quantity of argon in solution is considered well below that necessary to affect cavitation data.

Gas analysis for water vapor and oxygen was done by continuous reading instruments on the gas supply line from the purifier. The instruments were thoroughly purged of air and other contaminants and calibrated in the CANEL Instrument Laboratory to insure reliability. Accuracy of these instruments is stated by the manufacturer to be \pm 5 percent of full scale. The water vapor instrument functions by passing a gas sample into an electrolytic cell over a thin film of phosphoric acid supported by two spirally wound platinum electrodes. The acid film absorbs the water vapor and it is then dissociated into hydrogen and oxygen gas by an electric potential between the two electrodes. The current produced by this dissociation is a measure of the concentration of water vapor.

The measurement of oxygen content of the argon gas is accomplished in another instrument. The gas flows into a specially designed cell containing a porous silver electrode and a cadmium rod which supply an ionization potential. Ionization of the oxygen occurs within the pores of the silver electrode with the resulting current being a measure of oxygen concentration.

VI. IMPELLER CALIBRATION IN WATER

The RI-7C3 impeller was calibrated in water by determining its cavitation patterns and performance. These tests supplied information as to where the cavitation formed as a function of NPSH and the general nature of the cavitation to be expected, i.e., small or large bubbles, vortices, etc. In addition, the air borne sound from the test unit was recorded and the intensity of this sound was noted.

The test impeller (RI-7C3) was installed in the Water Impeller Test Stand in a clear plastic housing as shown in Fig. 22. The vane tip clearance was set at 0.028 inch instead of the design clearance of 0.032 ± 0.002 inch in anticipation of the plastic housing expanding under pump discharge and datum pressures. A dial indicator was mounted against the plastic housing to measure its deflections and to provide data for clearance dimensions in the turbo-pump. The design clearance of 0.032 inch is the maximum allowable clearance without appreciable performance penalty as determined from previous impeller tests. This clearance dimension is used extensively at CANEL in high temperature liquid metal pumps to provide a margin of safety when considering thermal expansion. The difficulty of accurately predicting temperature gradients and thermal expansion between parts of the hot running pumps dictates the need for this relatively large clearance.

The impeller water tests were begun by filling the test loop with water from the demineralizer and deaerator. The drive motor was started and the water circulated by means of the test impeller for additional deaeration within the test loop. This process continued until dissolved air in the water was reduced to 3 ppm or approximately 15 percent of saturation. This low level of dissolved air prevented the formation of air bubbles which would give erroneous cavitation data.

Hydraulic performance tests of the RI-7C3 impeller were conducted at shaft speeds of 4250 rpm and 6375 rpm and are shown in Fig. 23. The lower speed tests were run to provide data to be compared with test data of the RI-7A impeller obtained about 1960. Any effects caused by physical difference between the two impellers as a result of the casting technique would be evident. However, these effects, if any existed, were masked by the effects of using two different impeller housings in the water impeller test stand. The RI-7A impeller was tested with a reinforced aluminum housing which provided a constant blade tip clearance as opposed to the pressure dependent clearance in the RI-7C3 tests using the plastic housing.

Cavitation tests of the RI-7C3 impeller were run for five flow rates at a shaft speed of 6375 rpm. These data are shown in Fig. 24. The 700 gpm flow selected as the best choice for this investigation was determined from the extensive cavitation testing of the RI-7A3 impeller about 1960 at 4250 rpm. This was the best efficiency point of that test series scaled up to 6375 rpm. To bracket the area of possible orifice error (expected to range between 1 and 3 percent) and to allow for unforeseen circumstances, four other flow rates were also tested. These flows were selected to be at approximately 3 and 6 percent either side of the 700 gpm best efficiency point. The cavitation patterns on the impeller observed during these tests were recorded by still and high speed motion picture photography. The arrangement of the motion picture equipment is shown in Fig. 25.

Some of the still photographs taken during this test series are shown in Figs. 26, 27, 28, 29 and 30 for the flows of 660, 680, 700, 720 and 740 gpm, respectively. These photographs clearly show the cavitation patterns on the impeller as a function of NPSH. Fig. 28 shows that cavitation exists on the impeller to NPSH values of 150 feet at a shaft speed of 6375 rpm. Photographs were taken using a 35 mm camera with a 55 mm lens at NPSH values of 150, 100, 60, 35, incipient head loss, 15 and 8 feet for each of the five flows. The incipient head loss point is that point just before a drop in pump head rise is observable as NPSH is decreased.

The flow rate of 700 gpm was tentatively selected for the liquid metal test based on direct observations of the cavitating impeller and the still photographs. The reason for this choice can be seen by noting the following things from Figs. 24, 27, 29 and 30. In Fig. 24, the 700 gpm flow appears to reach the lowest value of NPSH of all flows run before performance begins to fall off. The inlet cavitation cloud seen in Fig. 27 appeared cyclic, reaching well into the impeller passages at times. This effect can be seen in the photograph for NPSH of 19 feet. The photographic procedure utilized two strobe lights for illumination which were synchronized and operating at a lower harmonic of the shaft speed to maintain light intensity. The 35 mm camera and film used to take the pictures required a shutter speed which allowed two to four flashes of the strobe light to occur while the shutter was open. The cyclic action of the cavitation cloud is, therefore, less well lighted in the photograph than is the steady formation. This cyclic action is not apparent at 700 gpm (Fig. 28, 17.7 NPSH). Further, the rear channel cavitation at 700 gpm and 17.7 feet NPSH does not appear to be as intense as that for 720 gpm and 21 feet NPSH (Fig. 29).

The tentative selection of NPSH for the liquid metal tests was partly based on the sound intensity curve which indicated a minimum sound intensity at 17.7 feet NPSH. If sound intensity and cavitation damage are related, then minimum sound would indicate minimum damage. In addition, this value of NPSH provides a wide range of cavitation patterns active on the impeller. These observations are also evident in the high speed motion pictures (up to 8000 frames per second) taken using a 16 mm camera with a 35 mm lens. These motion pictures have been edited into a film report, CRC-1. A request card and a description of the film are included at the back of this report.

Sound recordings and sound intensity readings of the air borne sound were made during the cavitation tests. Two locations of the microphone were used to determine variations in the sound patterns. These locations varied in distance only, with the angular location remaining constant. The data obtained are shown in Figs. 31, 32 and 33. These curves indicate that the absolute sound intensity readings may not be used directly since they vary with distance, but the general shape of the curve may hold some significance.

The shape of the sound intensity curves can be explained from the direct observation and photographs of the cavitating impeller. As the NPSH was lowered from relatively high values, allowing cavitation patterns to form and increase in intensity, the general sound level increased. The cavitation generated on the leading edge of each blade moved into the impeller passages with further decreases in NPSH. When this was done, the sound intensity decreased reaching a minimum value. As NPSH was further reduced, the rear channel cavitation increases in intensity causing an increased sound level.

The sound was recorded on magnetic tape which was then analyzed for frequency components (Ref. 10). Four methods of analysis were attempted in order to determine a relationship between cavitation noise and the degree of cavitation on the impeller. These methods are: an analysis of the instantaneous frequency spectrum of the noise; filtering the noise with a wide band pass filter, then integrating the filtered voltage; filtering with a narrow band pass filter and integrating the filtered voltage; and integrating the entire frequency spectrum. The latter method proved to be the most successful by indicating that there are frequency bands which increase in amplitude as cavitation progresses. These frequencies are generally within the resonant frequency range (2KC to 6KC) of the impeller vanes. It appears that increasing cavitation intensity causes an increasing sound intensity which is coupled to the resonant frequency of the impeller vanes. A general relation of increasing amplitude for frequencies within the range of 2KC to 6KC can be seen in the oscilloscope photographs of Figs. 34 and 35. Fig. 34 shows the calibration of the oscilloscope trace, while Fig. 35 shows the actual recorded data.

Examination of all data from the water impeller tests indicated that a flow of 700 gpm at a net positive suction head of 17.7 feet would be a desirable test point. The water pump tests were to provide further verification of this selection of conditions for the liquid metal pump test in 1400F potassium. The selected parameters would yield a suction specific speed of 19, 500, well above present acceptable limits for long term tests. The sound data were intended to serve as an additional check when setting the desired test conditions.

VII. TURBOPUMP TESTS IN WATER

Development tests of liquid metal pumps and impellers at CANEL have shown definite performance differences between impeller tests in the Water Impeller Test Stand and the full pump configurations. These performance differences, which are usually a drop in performance, are attributed to the effects of the scroll or collector on the impeller. The pump scroll is designed with space and weight limitations imposed by powerplant requirements in mind and is, therefore, not idealized. Scroll designs often incorporate internal structural members, sharp turns, and convenient rather than optimum diffusion angles, all of which introduce losses in the over-all pump performance.

The scroll of the turbopump used in this investigation was designed for flows on the order of 3000 gpm and for an impeller having a much shorter meridional profile vane tip arc. This pump was adapted to the RI-7C3 impeller by an insert in the scroll which was machined to the proper vane tip arc. The adapter was machined at the exit of the impeller to provide a fluid discharge angle which would match the angle of the diffuser vanes existing in the scroll. The water tests of the turbopump were planned to provide pump performance data which included the losses incurred using this scroll arrangement. In this way a calibration of the pump and impeller was to be accomplished before operating in 1400F potassium.

The turbopump was installed in the Water Pump Test Stand, as shown in Fig. 36, and the test loop filled with demineralized and deaerated water. Hydraulic and cavitation data were recorded and are shown in Figs. 37 and 38. These figures also include redrawn curves of the hydraulic performance of the impeller operated in the Water Impeller Test Stand. The data presented in Fig. 37 show that the combination of the oversized scroll and carefully designed insert did not produce noticeable losses. The slightly increased performance of the turbopump is due to smaller tip clearance. A comparison of the cavitation performance obtained from the turbopump and the impeller water tests is presented in Fig. 38. It is noted that the results from the two test programs agree most closely at the lowest flow rate of 660 gpm and progressively diverge at the higher flow rates. The cavitation patterns below 700 gpm were not considered since these patterns showed the onset of stall in the impeller (flow separation and recirculation evident at the vane tips in the inlet). Similar differences have been noted at CANEL in previous comparisons of pump and impeller tests where, in all cases, the pump cavitation performance is inferior to the impeller test. The most plausible explanation offered for this is that the velocity and pressure distributions in the pump are not as symmetrically uniform as for the impeller tests, and this initiates cavitation at somewhat higher NPSH values in the pump. A comparison of the cavitation noise recordings at 700 gpm is shown in Fig. 31 for the turbopump and impeller water tests, and a common trend in the shapes of the curves is noted. It appears logical to assume that qualitatively the cavitation patterns in the pump and impeller water tests would be quite similar.

The sound intensity readings were greatly attenuated in the water pump tests. The attenuation was due to the extended path followed by the sound waves in the pump test as compared to that in the impeller test. The sound transmission path of the pump was through water, stainless steel, a second stainless steel part, water, stainless steel, and finally to the air. In the impeller test the sound transmission path was through water, plastic, and air. Each interface reduces the intensity of sound reaching the microphone. The background noise level in the test cell contributed to the difficulty, since it was significantly higher in the pump test due to the turbine drive.

A microphone initially placed in a position similar to the impeller tests yielded completely unsatisfactory results. The turbine and pump scrolls had to be covered by a sound absorbing insulating material to reduce turbine noise levels and other extraneous noise in a successful

attempt to record useful sound data. Further definition of the impeller noise was obtained by placing a cardboard tube over the microphone and inserting the end of the tube in a hole cut through the insulation under the pump scroll (Fig. 39). The sound pattern thus obtained is given in Fig. 40.

The test results with the turbopump did not cause the initial choice of 700 gpm flow and 17.7 feet NPSH as conditions for the liquid metal test to be changed. On this basis, the orifice to be used for flow control of the potassium test was designed, machined and inserted into the Water Pump Test Stand for calibration.

The calculation procedure for the orifice is given in Appendix B. These calculations were based on an NPSH of 16.6 feet, which is 1.1 feet less than the point indicated by water tests. This NPSH adjustment was obtained from considerations of the thermal properties of water and 1400F potassium as presented by A. J. Stepanoff (Ref. 11).

Calculations indicated that an orifice diameter of 1.97 inches would produce the necessary pressure drop required for the liquid metal test conditions. When this orifice was tested in the Water Pump Test Stand to check its flow and pressure drop, it cavitated violently, causing excessive vibration of the entire test stand. Earlier tests conducted in this stand indicated that an orifice of 2.5 inches diameter would not cause vibration, although some cavitation might be present. This orifice would be placed at the inlet to the elbow immediately downstream of the pump outlet in the liquid metal pump test stand. A second orifice would be installed at the pump discharge to limit the pressure drop across the 2.5 inches diameter orifice and provide the needed additional pressure drop to insure a flow of 700 gpm (Fig. 18). In this way, excessive vibration caused by cavitating orifices would be eliminated.

The Water Pump Test Stand did not contain a length of straight pipe similar to the liquid metal stand. It was necessary, therefore, to calibrate both orifices in the same position in the water stand. This was done by installing the 2.5 inches diameter orifice and measuring pressures upstream and downstream (including the elbow) with the required flow and downstream pressure established. The measured upstream pressure and pump discharge pressure were then used to calculate the diameter of the second orifice. The second orifice was calculated to be 2.1 inches diameter. This orifice was machined and installed in the test stand and pressures measured across it. This pressure measurement was within 0.4 psi or 0.5 percent of the predicted value. This error was considered satisfactory because of the limited accuracy of the pressure drop calculations of the Liquid Metal Pump Test Stand.

Upon completion of the pump tests and orifice calibrations, the turbopump was removed for disassembly and inspection. Visual inspection of the RI-7C3 impeller revealed scoring marks on the impeller (Fig. 41) and scroll insert (Fig. 42) where the two had contacted during the test. Analysis of the probable cause of rubbing contact led to the conclusion that it was caused by synchronous transients of vibration set up in the pump during tests of the 1.97 inches diameter orifice which cavitated violently. (The accuracy of this analysis is questionable in light of the liquid metal test results described in Section VIII.) The score marks were smoothed off, but not entirely eliminated before reassembly of the turbopump for the liquid metal test.

A complete inspection of the impeller was again performed to establish its condition prior to the 1400F liquid metal test. These inspection procedures showed no signs of identifiable cavitation damage resulting from the water testing. Roughness measurements indicated a slight leveling of the surface had occurred as shown in the two traces of Fig. 43. This effect was further verified by the fluorescent inspection which failed to show the porous area

at the root of blade 3 indicated by the previous inspection (Fig. 5). Photographs of the inlet suction surfaces were again made at magnifications of two and four times size. Rubber molds of the entire impeller surface were made using the silicon rubber compound.

VIII. TURBOPUMP TEST IN HIGH TEMPERATURE POTASSIUM

The objective of this phase of the investigation was the determination of the amount of cavitation damage sustained by the RI-7C3 impeller after operating in 1400F potassium at a predetermined degree of cavitation for a period of up to 1000 hours. The parameters for the liquid metal test were selected after carefully reviewing all of the documented water test results. A shaft speed of 6375 rpm was chosen to correspond to the water tests, which produced a non-cavitating head rise of about 200 feet at a flow rate of 700 gpm. This range of head rise is of interest in Rankine cycle space powerplants. The flow rate of 700 gpm appeared near optimum from the water tests as it permitted operation with minimum NPSH around the break-off point of the cavitation curve with relatively stable and well defined cavitation patterns. This flow rate was also near the best efficiency point for the RI-7C3 impeller. As shown in the visual cavitation studies in Figs. 26 and 27, the cavitation patterns for flow rates lower than 700 gpm exhibited increasingly complex stall patterns as the flow rate was reduced. Such patterns would be very difficult to interpret in terms of the possible resulting cavitation damage and were, therefore, excluded from consideration for the liquid metal test. On the other hand, although the cavitation patterns were well defined for flow rates greater than 700 gpm, as shown in Figs. 29 and 30, the break-off points on the cavitation curves occurred for higher values of NPSH.

The cavitation pattern selected from the impeller water tests is shown in Fig. 28 corresponding to an NPSH of 17.7 feet and a suction specific speed of 19,500. At this condition, the cavitation bubble implosions in the rear channels of the impeller did not appear to collapse on the vane surfaces. Although bubble implosions were observed to occur on the vane surfaces near the leading edge, they were not judged to be as potentially damaging as cavitation implosions occurring in the rear channel regions where high pressure gradients existed. Also, since no evidence of cavitation pitting attack was found after several hundred hours of accumulated water testing in cavitation, it was decided to test the impeller in potassium at this high value of suction specific speed. A correction of 1.1 feet of NPSH was introduced on the basis of the thermal cavitation criterion derived by Stepanoff (Ref. 11), which accounts for the differing thermal properties of cold water and 1400F potassium as related to cavitation bubble formation. Therefore, the NPSH of 17.7 feet for the water test was adjusted to an NPSH of 16.6 feet for the potassium test to produce an equivalent cavitation pattern in the impeller for both tests. This corresponded to a suction specific speed of about 20,000 for the endurance test with 1400F potassium.

The turbopump was assembled with the RI-7C3 impeller following complete inspection of all parts. The clearance of the impeller vane tips was set cold at 0.017 inch in anticipation of temperature gradients along the pump shaft and housing increasing the clearance to the design value of 0.032 inch. Analysis of all available data regarding temperature gradients of high temperature pumps and, in particular, the previous operation of this turbopump indicated the clearance would increase at high temperature.

The turbopump was installed in the Liquid Metal Pump Test Stand as shown in Fig. 44. All gas line connections to the loop were made to finally isolate the loop from the atmosphere. A vacuum pump was connected to the loop through one of the gas lines, and the loop was evacuated. The evacuation was done with the loop at a temperature of 600F to insure complete drying and elimination of water vapor. Argon gas was admitted to the loop following the evacuation procedure.

A complete checkout of the turbopump operation was done while the test loop contained only argon to insure proper functioning of all controls. First, the pump lubrication system was turned on and checked for possible oil leaks. The air controls to the turbine were then checked and the pump brought up to speed slowly to wear-in the oil face-seals and check vibration levels. All controls and operation were satisfactory so liquid metal charging of the system was started.

The potassium used in the test loop was purchased as high purity potassium with low sodium and oxygen. The "as-received" potassium contained less than 25 ppm sodium and 800 ppm oxygen. The sodium content was within the 0.5 percent stipulation, but oxygen level greatly exceeded the less than 40 ppm stipulated for this test. An existing purification facility at CANEL was used to reduce oxygen levels.

The purification facility was a large externally heated tank in which a measured amount of titanium sponge was placed. After filling with potassium, the tank was heated to 1500F and held for 48 hours. Two successive analyses for oxygen, using a mercury amalgam method, indicated oxygen levels of about 10 ppm. The potassium was then placed in transfer containers and brought to the Liquid Metal Pump Test Stand. Potassium purity, as determined by spectroanalysis for metallic impurities, mercury amalgam for oxygen, and chemical analysis for carbon, is given in Table I for all samples taken.

With the loop interior and dump tank dried and under argon gas cover, the temperatures were held at 400F to 500F for transfer of a flush charge of NaK into the dump tank. The tank was completely filled with NaK and was then heated to 1000F as a further step in obtaining a completely clean system. This step was necessary since acid cleaning of the dump tank could not be accomplished during test stand construction. The tank had been cleaned by using a commercial solvent and a cleaning method used to clean central steam power station equipment. This procedure was not considered sufficient to clean the dump tank as required for this liquid metal program. Therefore, the NaK cleaning was necessary.

The NaK was held in the dump tank at 1000F for a period of 24 hours and agitated periodically by bubbling argon through it. At the end of the 24-hour period the NaK was removed and potassium was transferred into the dump tank. Only enough potassium to completely fill the test loop, with no reserve, was admitted to the tank. This potassium was raised into the test loop by differential argon pressure and venting of the loop argon. When the loop was filled with potassium to the proper level, the turbopump was started and circulation of the potassium begun. This procedure was done to flush out the loop interior to remove foreign matter and react the potassium with any residual contaminants remaining in the loop.

The potassium was circulated at temperatures to 1000F for approximately six hours, after which it was drained into the dump tank. A sample of the potassium in the dump tank was taken to determine the sodium content resulting from a mix with any residual NaK from the previous dump tank flushing cycle. This sample under spectroanalysis indicated 1.5 percent sodium. Since additional potassium over the amount already on hand was needed to allow a reserve in the dump tank, it was decided to continue flushing of the loop while awaiting the purification of the additional potassium. The additional time offered by the continued flushing was used to evaluate the hydraulic performance of the pump. Some degree of flow control was offered by the hot trap valve which allowed a short span of the performance curve to be investigated. These data are given in Fig. 45. The increased performance is due to the tight clearances set in anticipation of thermal expansion differences along the pump shaft and housing. The hot trap valve seized during this period and prevented further hydraulic testing. Upon completing the purification of the additional potassium, it was added to the system.

The potassium was raised into the test loop and the pump started. The system temperature was raised to 1000F using external trace heaters and was increased to 1400F primarily by pump work input. Loop temperature was maintained at 1400F by removing approximately three feet of loop pipe insulation between the electromagnetic flowmeter and pump inlet while the turbopump was operating at a constant shaft speed of 6375 rpm.

TABLE I

Impurity Analysis of Potassium

	Spectro Analysis						Mercury Amalgam Analysis		Chemical Analysis			
	ppm Fe	ppm Ni	ppm Cr	ppm Ti	ppm Al	ppm Si	ppm Mg	ppm Na	ppm Ca	ppm Rb	ppm O ₂	ppm C
Vendor analysis	15	< 5	< 5	< 5	3	< 25	3	< 25	9	-	< 800	-
P&WA analysis as-received	< 1	< 5	< 1	30	-	-	< 10	28	27	11	352	275
Purified 48 hrs. at 1400F	64	< 5	< 1	< 1	-	-	< 10	58	-	15	10, 10	-
Loop dump tank after transfer at 1000F 4-24-64	13	< 5	< 1	< 1	-	-	< 10	520	18	46	9, 11	-
Zero test time at 1000F 4-29-64	-	-	-	-	-	-	-	700	-	-	13, 14	-
24 hrs. test at 1000F 4-30-64	4	< 10	< 5	< 9	-	-	< 5	700	-	-	14, 15	N.D. D-4562
100 hrs. test at 1000F 5-3-64	-	-	-	-	-	-	-	800	-	-	9, 8	-
240 hrs. test at ~ 800F 5-8-64	-	-	-	-	-	-	-	800	-	-	7, 9	-
Post-test from dump tank	-	-	-	-	-	-	-	-	-	-	31, 35	-
N. D. - not detectable												

Cavitation performance of the turbopump was recorded after maintaining a loop temperature of 1400F for about two hours. The cavitation curves for two different test runs are shown in Fig. 46, which includes the sound intensity readings. It is noted that the sound intensity curve for the second run generally agreed with the first run except for the point near an NPSH value of 26 feet. From the comparison of the constant throttle cavitation curves shown for potassium and water in Fig. 47, it is evident that the head rise started to decline at higher values of NPSH for the potassium test. These data suggest that the inlet flow conditions for the liquid metal test may not have been as uniform as for the water tests.

The endurance operating point was set in accordance with the selected suction specific speed of 20,000, which corresponded to an NPSH of 17 feet and a flow rate of about 705 gpm. The drop-off in head rise at this fixed throttle condition was about 4 percent of the maximum head rise at a shaft speed of 6375 rpm.

These test conditions were set for the endurance test, and running time was logged beginning at 2300 hours on April 29, 1964. The test operated smoothly for 250 hours during which conditions were held within the limits specified in Table II.

TABLE II

Operating Limits

Flow Rate	710 \pm 5 gpm with variations due to thermal changes affecting clearance in the early hours.
Head Rise	95.9% of maximum head rise determined from constant throttle curve.
NPSH	17 feet, controlled within \pm 0.15 feet.
Speed	6375 rpm, controlled within \pm 20 rpm.
Temperature	1400F \pm 5F measured at pipe surface.
Potassium	Oxygen content less than 15 ppm. Sodium less than 800 ppm.

In the next 100 hours a gradual deterioration of head and flow was noticed. No adjustments were made to pump speed or inlet pressure throughout the test period. Toward the end of this 100-hour period the head and flow were beyond acceptable limits. Within the last three hours of this period a very noticeable jump in vibration levels occurred. (A plot of all hourly readings of important parameters is given in Fig. 48.) It was decided to terminate operations at 350 hours and to bring the pump out of cavitation to determine if the vibration was originated by cavitation. Cavitation conditions were terminated by increasing the inlet pressure above that required to sustain cavitation. This procedure required approximately 35 minutes to complete. Before it was determined that the vibration was originating in cavitation and after about 20 minutes of increasing pressures had elapsed, a liquid metal fire was discovered in the test cell. The potassium in the loop was immediately dumped into the dump tank. The fire was brought under control and caused no damage to either the test loop or cell. The fire was caused by the high temperature potassium leaking from a vibration induced crack at the junction of the hot trap line and sampling station line. Subsequent analysis of the potassium in the dump tank showed no significant increase of oxygen as a result of the leak. Oxygen contamination of the potassium increased from 9 ppm at 240 test hours to only 35 ppm after the dump.

When the turbopump was removed from the test loop, it was immediately apparent that the cause of increased vibration was rubbing contact between the impeller and scroll insert. A photograph of the impeller shortly after removal from the scroll is shown in Fig. 49. Two views of the impeller were obtained in this figure by placing a mirror at an angle under the pump. Several areas of cavitation damage were also noted, one of which can be seen in Fig. 49.

Complete disassembly of the pump revealed additional rubbing damage of the rotating parts. The damage on the impeller is shown more clearly in Fig. 50. It should be noted that the damage is not uniform around the impeller. Very little material was injected into the fluid stream, as evidenced by the apparent flow of metal at the blade tips. Scroll damage from contacting the impeller is shown in Fig. 51. Again, the unsymmetrical pattern of damage should be noted. The cause of the rubbing contact cannot be fully determined from the evidence uncovered, due to the difficulty of separating cause and effect relationships of the damage. However, the unsymmetrical pattern of damage leads to a tentative conclusion that the shaft moved to one side during operation. This is further confirmed by the rubbing damage noted on the dynamic seals shown in Figs. 52 and 53. The cause of this apparent shaft movement has not been satisfactorily determined.

The principal areas of cavitation damage were located on the pressure surfaces of the vanes in the rear channels. These areas are shown in Figs. 54, 55, and 56. An area of secondarily induced cavitation damage was found on the suction surface of vane 2 and is shown in Fig. 57.

A complete program of inspection was performed on the impeller using all techniques previously noted. The surface roughness measurements made along the same vane stations as those in pretest indicated a slight smoothening of the surface had occurred. This can be seen in the surface roughness traces shown in Fig. 58. This smoothening action was apparently caused by a slight erosive action of the liquid metal.

Fluorescent inspection of the entire impeller showed all areas of cavitation damage. A general photograph of the impeller under ultraviolet light is shown in Fig. 59. A slightly angled view which shows the inlet area pressure surface is given in Fig. 60. No heavy concentration of damage is evident in this photograph. The suction surface of the impeller vanes in the inlet is shown in Fig. 61 under ultraviolet light. These vane surfaces appear completely clear of any cavitation damage.

Photographic enlargements were also made of the inlet suction surfaces. A typical photograph is shown in Fig. 62. These photographs were taken at enlargements of two times and four times size and have the potential of enlargement to 20 times size.

A typical rubber mold is shown in Fig. 63 of the entire pressure surface of vane 2. Fig. 63A is the heavy cavitation damage area of vane 2 photographed at 11X with the mold laid over a sharp edge. Fig. 63B is the rear channel damage of vane 1, photographed by the same technique but at higher magnification (23X). The partial translucence of the rubber material does not allow surface features to stand out in sharp contrast when looking directly at the surface, even under high magnification. The best method of interpreting the rubber molds appears to be the technique employed in photographing.

Vane 3 was cut from the inlet of the impeller in order to inspect the pressure surface in more detail. A section of this vane is shown at 3 1/2 magnification in Fig. 64. Small single pits are apparent on the surface in this photograph. These pits are shown at 23 magnification in Fig. 65. A count of pits of all sizes in Fig. 65 shows approximately 30 pits per square inch. A similar examination of pits on the suction surface of the vane showed only two pits per square inch, all occurring within the impeller flow channel. Examination of the area of the impeller vane suction surface as seen when looking directly into the inlet revealed no cavitation pits.

The large pit and one of the smaller ones were sectioned to obtain their profiles. These are shown in Figs. 66 and 67. It is assumed that these pits were caused by a single event, or implosion of one bubble. This assumption is based on the following facts: 1) X-ray revealed no subsurface pockets containing gas which would have blown out under high temperatures, 2) fluorescent inspection revealed no small holes in this area at pretest inspection, 3) the carbide stringers are distorted slightly around the hole, which indicates deformation after solidification of the impeller material, and 4) the surface of the blade, at least one hole diameter either side of the hole, is displaced upwards.

Metallographic examination of the cavitation damage areas in the impeller rear channels was done in an attempt to determine a mechanism of damage. This examination failed to show conclusively any mechanism by which cavitation damage propagates. A microsection of the "as cast" structure is shown in Fig. 68. This figure shows the typical large grain cored microstructure normally associated with cast type 316 stainless steel. Widmanstatten carbide precipitation observable in this figure is typical of all surfaces and results from the casting process. A microsection of post-test material undamaged by cavitation is shown in Fig. 69. The time and temperature effects are noted in the more homogeneous dispersion of the carbide phase throughout the matrix. The light band along the surface is shown at higher magnification in Fig. 70. This band shows a tendency toward recrystallization to extremely small grains with spheroidal carbide precipitation at the grain boundaries. This effect was noted in microsections of deep cavitation damage to exist on all surfaces exposed to the liquid metal.

Two sections through the most heavily damaged area of vane 2 are shown in Fig. 71. The top of the figure is a transverse section, and the bottom is a longitudinal section. The maximum depth of penetration on this section was 0.050 inch. Higher magnifications of these areas are shown in Figs. 72 and 73. A definite deformation of the material can be seen in Fig. 72 by noting the curvature of the carbide phase. The recrystallization effect is evident at the surface. The recrystallization and spheroidal carbide precipitation along the surfaces is very evident in Fig. 73.

One of the two small areas of secondarily induced cavitation damage, noted earlier on the suction surface of blade 2, is shown in microsection in Fig. 74. This pit does not resemble the pits identified as single event pits. It contains very sharp corners and no deformation of adjacent carbide phase. It is concluded that this area contained an inclusion with a slight overlay of the base metal. At some time in the operation of the test the inclusion was removed and the overlay was forced up to project into the fluid stream. This projection generated a small vortex behind it which produced the comet tail areas of damage as shown in Fig. 57. The two inclusions were present in the impeller surface before testing and can be seen in a pretest photograph of the impeller shown in Fig. 75. Further evidence that these are not cavitation damage pits is obtained from Fig. 76. The light band along the bottom edge of the pits was found by microprobe to be extremely nickel rich. Microprobe analysis of the other damage areas showed no change in the basic material compositions throughout the area.

Microhardness measurements across the sections indicated no significant change from matrix to the surface. The hardness values were essentially the same pretest to post-test. The nickel-rich area of Fig. 76 showed the only change of hardness being softer than the matrix as would be expected.

IX. DISCUSSION

The water test phases of this program were conducted to obtain as much background data as possible for evaluation of the high temperature liquid metal test. The first test series conducted in the Water Impeller Test Stand allowed the form and location of cavitation on the impeller to be observed directly and to be photographed. The existence of cavitation formations on the impeller at NPSH values up to 100 feet was clearly seen. The ability to observe growth and behavior of these formations proved to be a valuable tool in analyzing the damage found on the impeller after the potassium test.

Cavitation streaming from the impeller vane leading edge tip formed a mild vortex action which apparently dissipated mostly in mid-channel. The relatively large single vapor cavity which formed near the hub at the vane leading edge shed bubbles into the vane channels. These tip and hub formations caused very minor damage on the vanes as single widely scattered pits. No heavy concentration of damage was found around the inlet areas of the impeller. The relatively low vane angle and mild pressure gradients in this area of the impeller are probably the reasons for this very minor damage. In addition, the very mild vortex probably did not allow the bubbles comprising it to be concentrated sufficiently to cause heavy damage.

The cavitation formation occurring in the vane channels at the impeller exit were very strong vortices. This action kept the bubbles concentrated into a tight area within a high pressure zone of the impeller. Pressure gradients in this zone probably forced more rapid collapse of the bubbles with greater energy release.

The physical properties, such as tensile and yield strengths, of the type 316 stainless steel material of the impeller were probably reduced by the elevated temperatures of the liquid metal test as evidenced by the damage sustained in 350 hours. Water tests of the impeller were conducted for over 300 hours with, at times, greater degrees of cavitation and no damage of any type was found.

The noise, or sound intensity level, produced by a cavitating impeller was considered to be a possible method of determining the degree to which the impeller was cavitating. If this were true, it could be used as an aid in setting the conditions of the liquid metal test. It was also considered that the frequency of the noise might indicate the collapse or implosion rate of the cavitation bubbles. These ideas were investigated to a limited degree during the water test phase of this work. It was found that the sound intensity level did vary with the degree of cavitation existing on the impeller. The sound intensity level for this impeller was characterized by a double peaked curve. The first peak occurred at a relatively high value of NPSH and the second peak occurred at the knee of the cavitation curve. This double peak curve is considered to be characteristic of the RI-7C3 impeller design in which two distinct zones of cavitation occur on the impeller unrelated or connected in any way. It is felt that these two cavitation areas and their behavior in the impeller cause the sound curve to have its double peak shape.

Frequency analysis of the sound showed an increasing amplitude (or sound intensity level) within the frequency range of 2 to 6 KC. The amplitude increase was over this whole range as the degree of cavitation increased. There was no discernible shift in the amplitude of certain frequencies from low to high frequency as cavitation increased as might be expected if the rate of bubble collapse increased with increasing cavitation. A check of the resonant frequencies of the impeller vanes showed a resonance between 2 and 6 KC which may be only a coincidence where the impeller resonates at the cavitation frequencies. Work at the University of Michigan (Ref. 14) which analyzed the noise of a cavitating venturi in water also

showed an amplitude increase in the 2 to 6 KC frequency range, as the degree of cavitation increases. Here again, there was no noticeable shift in frequency, only in signal amplitude of the 2 to 6 KC frequency range. The real significance of sound with respect to cavitation will require more extensive study than was possible during this program.

A water test of the turbopump was conducted after the impeller tests. This test was felt to be justified by past experience with pumps tested at CANEL which showed a definite performance deviation between the pump test and impeller test. This performance shift was attributed to effects on the impeller caused by the diffuser and the collector of the pump. In the water impeller test, optimization of fluid discharge channels is maintained. Diffusion angles are held within optimum, and no obstructions, such as structural supports, are permitted in the flow channels. Practical design of pump collectors does not allow such a high degree of optimization, and performance deviations do occur. The turbopump collector was adapted to this particular program by a machined insert. The water pump test was necessary to be sure the calculated fluid discharge angles from the adapter matched the diffuser vane angles existing in the collector, thereby limiting extraneous losses. The hydraulic performance test of the pump in water verified the accuracy of these calculations. Collector effects on the cavitation performance, however, were evident and characterized as a much more gradual drop in head rise as NPSH was decreased. The impeller tests indicated a sharp drop in head rise at low NPSH would occur.

The liquid metal test point was selected after analysis of all the water data. The strong vortex formation in the back channel area at 700 gpm flow and 17.7 feet NPSH did not appear to contact the vane surface and the inlet cavitation did not appear to enter the flow channels. Based on these observations and the lack of any signs of cavitation damage after a 24-hour run in water at these conditions, this test point was selected. The water test conditions were adjusted to the physical properties of 1400F potassium on the basis of thermal criterion developed by Stepanoff. This work suggested an adjustment of 1.1 feet NPSH which changed the liquid metal test conditions to 700 gpm flow and 16.6 feet NPSH.

The pump water tests included calibration of the flow control orifice of the liquid metal test loop. The orifice initially selected to produce the desired head loss cavitated so violently in the water test that severe vibrations of the entire test stand occurred. Two orifices in series were finally used in the liquid metal test following calibration in the water pump stand.

The vibration of the water pump test stand resulting from the cavitating orifice was considered responsible for the rubbing contact of the impeller and collector insert during the water pump test. This damage, discovered upon disassembly of the pump, was slight. No additional investigation as to the cause of the damage seemed warranted at the time.

The liquid metal test was conducted with very little trouble. The major problem which arose during this test was impeller vane tip clearance. Analysis of thermal expansion of the pump parts indicated the vane tip clearance should increase. Operating data from another test pump in high temperature liquid metal also indicated the vane tip clearance would probably increase, but it was difficult to determine by how much. It was decided to set the vane tip clearance cold at 0.017 inch in anticipation of thermal growth increasing the tip clearance to approximately 0.032 inch. These calculations were based on estimated temperatures and temperatures measured during previous tests of this particular turbopump in high temperature liquid metal. The rubbing of the impeller and collector which occurred during the 1400F potassium test now appears to have been the result of a combination of occurrences. It is felt, in retrospect, that the rubbing which occurred in the water pump test and the liquid metal pump test resulted from the use of the deep groove radial bearing with its inherent play and was amplified by the long shaft overhang from the bearing. Thermal expansion is also suspected as playing a part in the resulting damage. The rubbing contact is now considered to

have occurred early in the test, since the vibration level almost doubled between the dry run-in of the pump and initial startup with liquid metal. This increase of vibration was disregarded at the time since it was only about 0.75 mil for a total vibration level of 1.5 to 1.8 mils. A vibration level of 4 mils was being approached rapidly when the test was terminated at 350 hours.

The nature of rotation finally assumed by the impeller in the scroll during the test offered a unique opportunity to study the effects of vane tip clearance on cavitation damage in this impeller. The impeller appears to have rotated eccentrically about a centerline offset from the collector centerline. (Part of this eccentricity was due to an 0.005 inch machining error in location of the splines of the impeller with respect to the vane tip.) The variation in the degree of damage found on the rear channel pressure surface appears to be a function of the vane tip clearance. The largest tip clearance causes the most extensive damage.

It has been widely held that most cavitation damage occurs at the impeller inlet; however, this test impeller showed relatively little damage in the inlet regions. The damage that did occur consisted of widely scattered single event pits. The more extensive damage occurred in the back channel and was the result of cavitation completely isolated from that generated at the inlet region. The low pressure gradients of the inlet are considered among the reasons for the widely scattered and minimal damage. The extensive rear channel damage was enhanced by the vortex formation and by the steeper pressure gradients existing in this area of the impeller.

The selected test conditions were not followed in the liquid metal test. The location of the damage sustained by the impeller indicates the test point actually run was extremely close to the desired point, but that the back channel cavitation was probably more advanced than desired. The hydraulic and cavitation performance data obtained in the liquid metal test showed some variation from the water test data. The liquid metal cavitation performance curve obtained by constant throttle methods showed a steadily declining head rise with decreasing NPSH, beginning at about 60 feet. The constant throttle cavitation curve taken in the water pump test shows a slight increase in head rise, to about 35 feet NPSH, before beginning a steady decline. The cause of this difference between water and liquid metal pump tests is not precisely known.

A difference was also noted between the sound intensity curves for the water pump and potassium tests. This difference is characterized by the location of the first maximum sound intensity point occurring at a relatively high value of NPSH (near 48 feet) in potassium while that for water is much lower (near 28 feet). This tends to indicate that cavitation in the impeller was initiated at a higher value of NPSH for the liquid metal test. Unsymmetrical flow conditions at the pump inlet are believed to be the cause. The NPSH value selected for the endurance test was chosen at a point where the sound intensity seemed to be rising again after it had declined with decreasing NPSH and where the calculated suction specific speed was about 20,000. The NPSH value was 17 feet.

The inspection procedures used to document the impeller's condition were employed with varying degrees of success in determining the areas of cavitation damage. The least successful was the surface profile or roughness measurement. These measurements were made only at selected vane stations in the inlet area where hand finishing of the surface had been done. Any roughness measurements in "as-cast" areas were so irregular as to preclude discovery of minor cavitation damage. In the inlet area, the damage would have had to occur on the exact line the profile tracing head had followed. Of the 18 surface roughness profile measurements made, none showed any discernible cavitation damage. The surface roughness measurements did, however, show a general leveling of the vane surfaces to have occurred; this is attributed to very mild erosion.

Radiography of the impeller vanes was done to locate internal defects. Considerable difficulty was encountered in obtaining the X-rays due to the geometry of the impeller. The

X-rays showed no internal defects, either pre or post-test. The X-rays were taken using dental size films and required almost 30 set-ups and exposures. This inspection method is quite necessary for the location of any internal defects since no other non-destructive technique can currently be used. Further work should be done on ways to improve this inspection method.

Fluorescent penetrant inspection is an excellent method of locating surface irregularities. The indications from this inspection method can be photographed, although extremely long exposure times (on the order of 10 to 15 minutes) are required. It must be remembered that a defect cannot always be accurately located on a complex surface by this technique.

A most effective method of preserving a record of the surface is by room temperature vulcanizing silicon rubber impressions. The compound is applied to the impeller surface as a liquid and it solidifies into a rubbery substance after approximately 24 hours. It can be stripped from the surface of the impeller vanes and retained for an indefinite period. Some difficulty arises when trying to read the rubber molds to determine surface irregularities. The method finally used at CANEL was mild intensity side lighting under a 30 power microscope with a dark background. The rubber mold was folded so that surface irregularities stood out in relief against the dark background. The partial translucence of the rubber material prevents seeing anything when looking directly at the surface.

Weight loss measurements of the impeller were not taken during this investigation. An initial weight was recorded, but the final disassembly method used to remove the impeller also removed material which grossly affected any accurate and meaningful weight data.

The most extensively damaged area of the test impeller showed a very similar pattern to that of a rotating disk cavitation test specimen. A specimen of type 316 stainless steel from a water rotating disk test operated at CANEL (Ref. 12) is shown in Fig. 77 for comparison. This type of damage appears to result from a strong vortex action in both the impeller and the disk tests.

Metallographic and chemical examination (Ref. 13) of the damaged areas of the impeller showed no change of structure or composition of the base material which could be attributed to cavitation. Material removal appeared to be a purely mechanical action, since no evidence of a chemical depletion or reaction of material and liquid metal was found.

X. CONCLUSIONS

The data obtained in the course of this investigation of cavitation lead to the following conclusions:

1. Direct observation and high speed photographs of a test impeller pumping water are very enlightening with respect to the location and severity of the cavitation formations.
2. A study of the sound emanating from a test pump can be helpful in monitoring the intensity or degree of cavitation.
 - a. Sound intensity levels may indicate the intensity of cavitation but must be combined with other knowledge of the variation of cavitation with NPSH.
 - b. The frequency spectrum of the sound of cavitation may be a function of the resonant frequencies of the impeller (or system) rather than a characteristic of cavitation.
3. Cavitation produced on the vane leading edge of an impeller designed for high suction specific speed can collapse in the liquid stream away from the vane surface and not cause extensive cavitation damage. (Damage attributed to leading edge patterns of the RI-7C3 impeller consisted of only widely scattered single pits.)
4. Streamlining and surface finishing are important in the production of a high suction specific speed impeller which will be required to operate in or near cavitation. (Surface projections on the RI-7C3 impeller induced isolated cavitation with some damage occurring.)
5. Cavitation vortex formations produce the most concentrated and extensive damage when they collapse on the flow boundaries, such as impeller vanes. (This has been further substantiated by results obtained with rotating disks in water.)
6. Vane tip clearance effects are very important in controlling the extent and intensity of the damage producing cavitation vortices in centrifugal pumps (for the RI-7C3 impeller, the least damage observed in the rear flow channels corresponded to the smallest tip clearance).
7. It appears that cavitation damage of a type 316 stainless steel impeller tested with 1400F potassium is principally due to a mechanical process with little, or no, chemical reaction involved. (Recrystallization of the impeller material was noted during metallographic examination in both the damaged and undamaged surfaces.)
8. Long-time operation of pumps in high temperature potassium at suction specific speeds approaching 20,000 with impellers of similar design to the RI-7C3 model is probably too ambitious. (A study of the water test data indicates a good possibility of operating this impeller at suction speeds of 12,000 or more for long periods with little, or no, damage.)

XI. APPENDICES

A. Nomenclature

A	=	area	ft ²
DB	=	sound pressure	decibels
d	=	diameter	inches
f	=	friction factor	dimensionless
F	=	temperature	degrees Fahrenheit
H _{REF}	=	static head rise at impeller reference station (vane tip)	feet
H _T	=	total head	feet
H _V	=	vapor pressure	feet
Δh	=	head rise	feet
L	=	length of pipe	feet
N	=	shaft speed	rpm
NPSH	=	net positive suction head	feet
N _R	=	Reynolds number	dimensionless
N _{SV}	=	suction specific speed	rpm
P ₀	=	head of fluid at point 0	feet
P _{T1}	=	inlet datum pressure	psi
P _S	=	tip static pressure	psi
Q	=	flow rate	gpm
S	=	impeller height (inlet to back face)	inches
S _T	=	dimension along impeller vane tip (inlet to selected station)	inches
S/S _T	=	ratio of impeller height to distance of selected station from inlet	dimensionless
β	=	diameter ratio (orifice to pipe)	dimensionless
β *	=	impeller vane angle	
ρ	=	density	lbs/ft ³
μ	=	absolute viscosity	centipoise

B. Orifice Calculations

The design of the orifice plates was based on the test conditions to be established in the 1400F potassium test. These conditions were determined from the pump water tests. The conditions of 700 gpm through-flow at the impeller and an inlet pressure of 16.6 feet were set.

Other requirements of the test loop were:

1. Hot trap flow to be 3 to 5 percent of main stream.
2. Dynamic seal coolant flow to be 5 gpm.
3. Loop temperature to be 1400F.

The liquid metal test loop is shown in Fig. 78 with dimensions and expected flows and pressures indicated. These values were determined by the following calculation procedure:

A. Pressure loss from P_0 to P_1

$$N_R = 50.6 \frac{Q \rho}{d \mu}$$
$$= 1.411 \times 10^6$$

From Crane Technical Paper No. 410, page A-25, the value of the friction factor (f) is determined

$$f = 0.0147$$

The head loss per foot of pipe is found from

$$\Delta h/L = 0.0311 \frac{fQ^2}{d^5}$$
$$= 0.0068 \text{ ft/ft}$$

Q in this equation is 695 gpm since the dynamic seal coolant flow is recirculated from the impeller backface to the impeller inlet.

Multiplying this factor by the various lengths yields the pressure drop for each straight section of pipe. For the section from pump discharge to the hot trap inlet:

$$\Delta h = 0.0068 (11.5) = 0.078 \text{ ft.}$$

This value is then subtracted from the discharge head of the pump, which is the pump head rise plus the NPSH of 16.6 feet, or 273.2 feet. The pressure available at P_1 is then

$$P_1 = 273.2 - 0.078$$
$$= 273.12 \text{ ft.}$$

The flow rate of 695 gpm is reduced by four percent, which is the median required hot trap flow, giving the flow through the orifice.

Pressure loss calculations similar to those above are repeated to determine system losses from impeller inlet to the downstream side of the orifice. The calculations now show the flow and required pressure drop of the orifice, and sizing calculations can be made.

B. Orifice size calculations are based on the unrecovered head loss required in the system by the orifice. In this case it is 195.07 feet.

Assume the unrecovered head loss is 87 percent of the maximum orifice pressure difference. Then Δh_{max} for the orifice is

$$\Delta h_{max} = \frac{195.07}{.87} = 224.3 \text{ ft.}$$

and assuming an orifice coefficient for a sharp edged orifice of $C = 0.61$, then

$$\begin{aligned} A &= \frac{Q}{C \sqrt{2g\Delta h}} \\ &= 0.0206 \text{ ft}^2 \end{aligned}$$

and $d = 1.94$ inches

The β ratio (diameter of orifice to diameter of pipe) is 0.243. A check of the ASME Fluid Meters Handbook indicates the unrecovered head loss for an orifice of this β ratio is 91 percent. Adding elbow effects raises this to 92 percent. Then

$$\Delta h_{max} = \frac{195.07}{.92} = 212 \text{ ft.}$$

and $A = 0.02118 \text{ ft}^2$

or $d = 1.968$ inches

A check of β yields 0.2464, indicating this orifice is calculated close enough to be tried in the loop.

Additional analysis was performed on the resistance effects of the hot trap operating in parallel with a portion of the main stream, and these were taken into account in the final sizing of the orifices.

XII. REFERENCES

1. Smith, P. G., DeVan, J. H. and Grindell, A. G., "Cavitation Damage to Centrifugal Pump Impellers During Operation With Liquid Metals and Molten Salt at 1050-1400F", Transactions ASME, Series D, Journal of Basic Engineering, Volume 85, Number 3, September 1963, pp. 329-337.
2. Grennan, C. W. and Lewis, R. A., "Cavitation Damage in a Liquid-Mercury Centrifugal Pump", ASME Paper Number 63-WA-215, 1963.
3. Hamrick, J. T., Ginsburg, A. and Osborn, W. M., "Method of Analysis for Compressible Flow Through Mixed Flow Centrifugal Impellers of Arbitrary Design", NACA Report 1082, issued 1952.
4. Wood, G. M., "Cavitation Research in Mixed Flow Centrifugal Pumps", Pratt & Whitney Aircraft-CANEL, Technical Information Memorandum, TIM-721, October 1962.
5. Wood, G. M., Murphy, J. S. and Farquhar, J., "An Experimental Study of Cavitation in a Mixed Flow Pump Impeller", Transactions ASME, Series D, Journal of Basic Engineering, 1960, pp. 929-940.
6. Wood, G. M., "Visual Cavitation Studies of Mixed Flow Pump Impellers", Transactions ASME, Series D, Journal of Basic Engineering, Volume 85, Number 1, March 1963, pp. 17-28.
7. Murphy, J. S., Lombard, R. S., Sutherland, J. D. and Farquhar, J., "Development of Pump Components for the Pratt & Whitney Aircraft Liquid Metal Turbopump, TP-1", Pratt & Whitney Aircraft-CANEL, PWAC-298.
8. Marman, H. V., Lombard, R. S., Standley, P. G., Grennan, C. W., Sarrett, H. J. and Butler, J. P., "Development Tests of the TP-1 Liquid Metal Turbopump and Components", Pratt & Whitney Aircraft-CANEL, PWAC-318, June 1961.
9. Kelly, R. W., Wood, G. M. and Marman, H. V., "Development of a High Temperature Liquid Metal Turbopump", Transactions ASME, Series A, Journal of Engineering for Power, Volume 85, Number 2, April 1963, pp. 99-107.
10. Bennett, D., "Cavitation Noise Analysis Techniques", Pratt & Whitney Aircraft-CANEL, Technical Information Memorandum, TIM-837, July 1964.
11. Stepanoff, A. J., "Cavitation Properties of Liquids", ASME Paper Number 63-AHGT-22, 1963.
12. Kelly, R. W., Wood, G. M., Marman, H. V. and Milich, J. J., "Rotating Disk Approach for Cavitation Damage Studies in High Temperature Liquid Metal", ASME Paper Number 63-AHGT-26, 1963.
13. Potts, J. R., Woodward, C. E. and Schenck, G. F., "Post-test Examination of Type 316 Stainless Steel Pump Impeller, RI-7C3", Pratt & Whitney Aircraft-CANEL, Technical Information Memorandum, TIM-842, December 1964.
14. Garcia, R., Hammitt, F. G. and Robinson, M. J., "Acoustic Noise from a Cavitating Venturi", Technical Report Number 1, 06110-1-T, The University of Michigan, June 1964.

FIG 1

BASIC RI - 7 IMPELLER CASTING

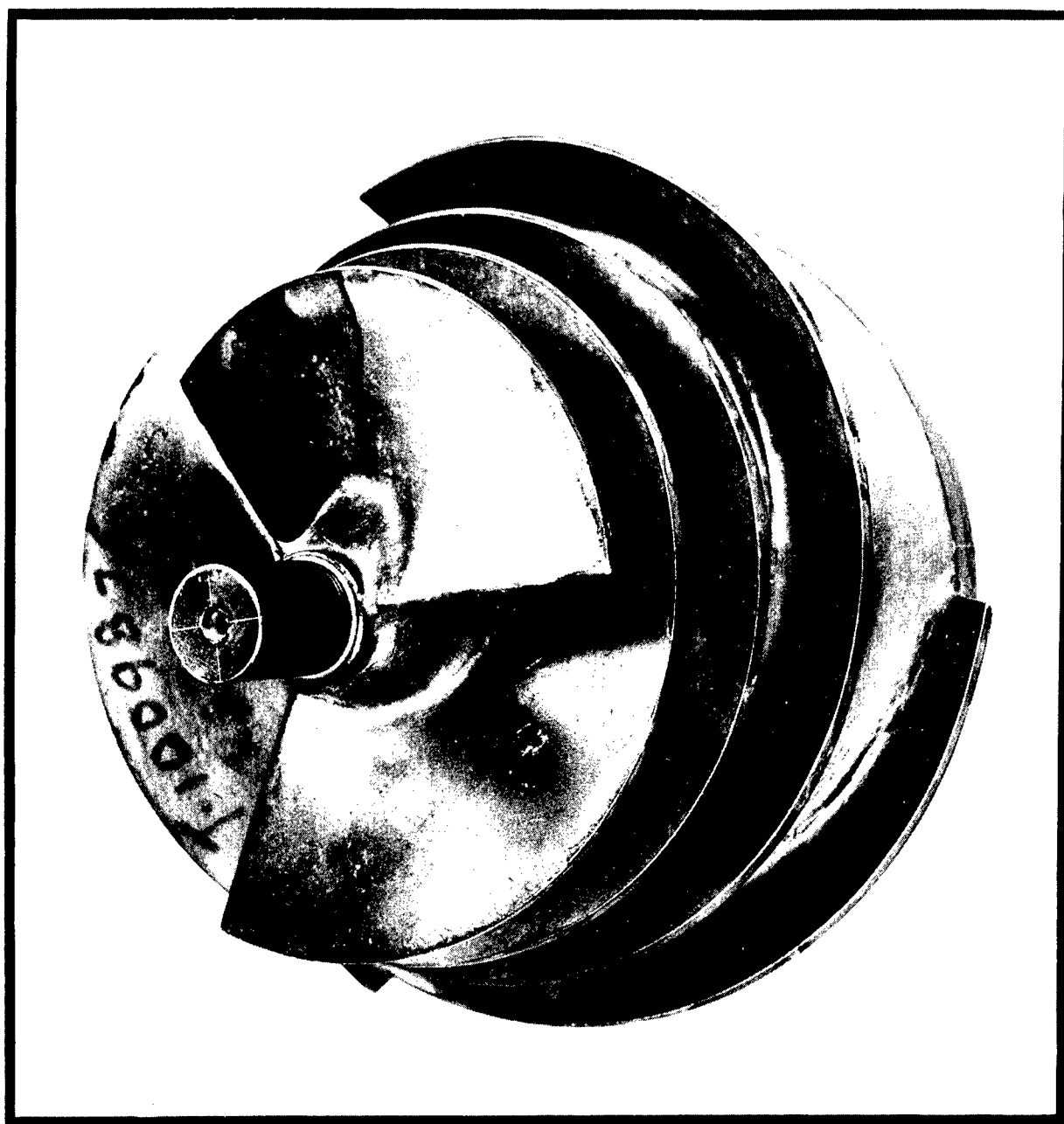


FIG 2

RI-7C3 RESEARCH IMPELLER

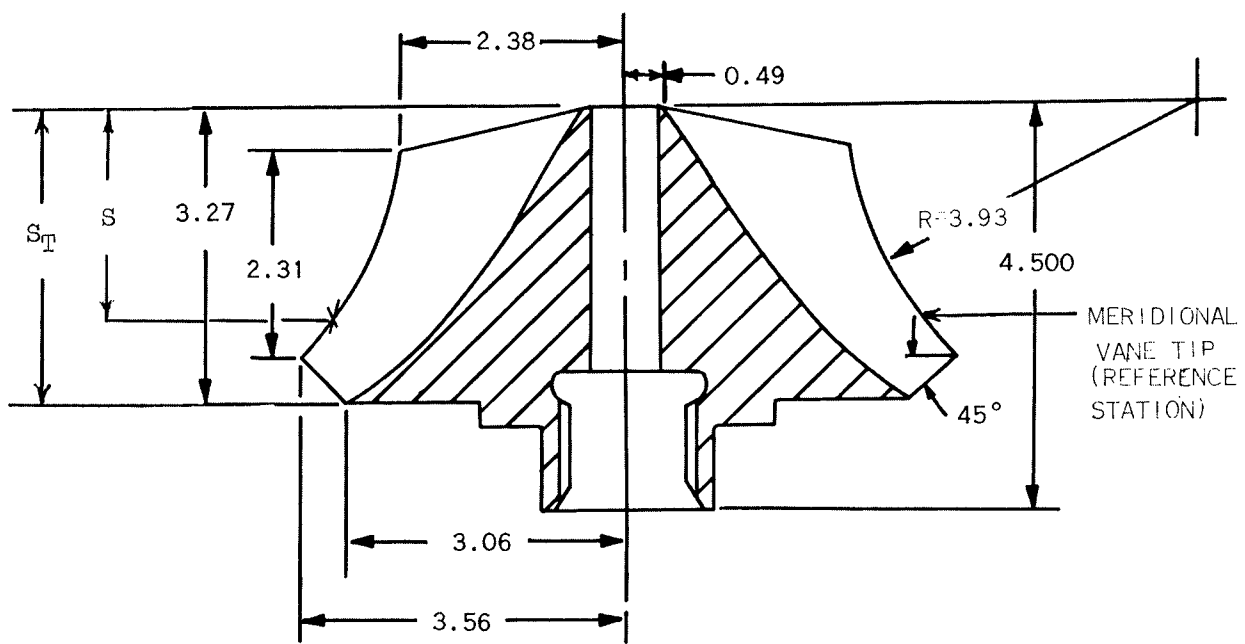
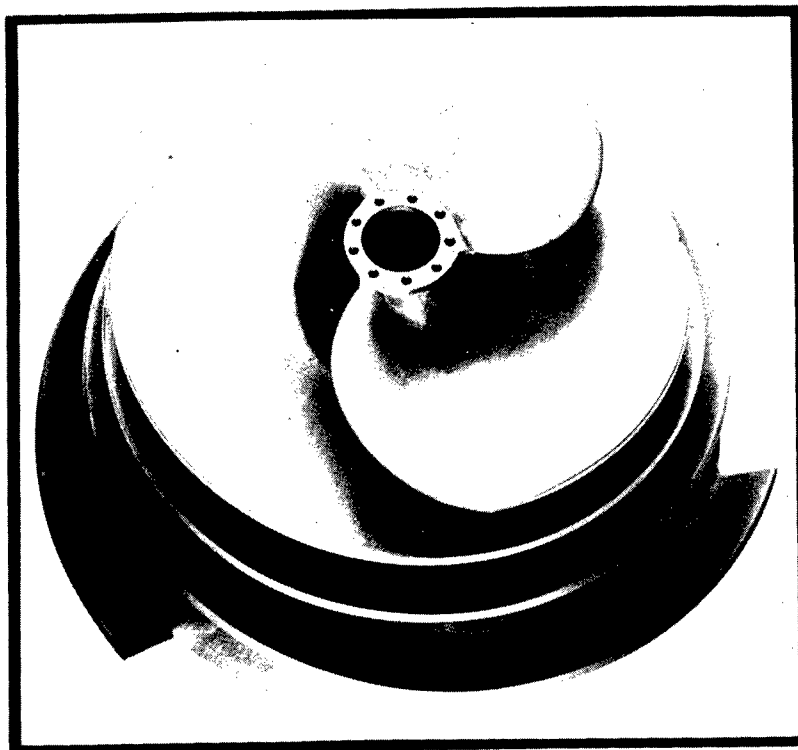
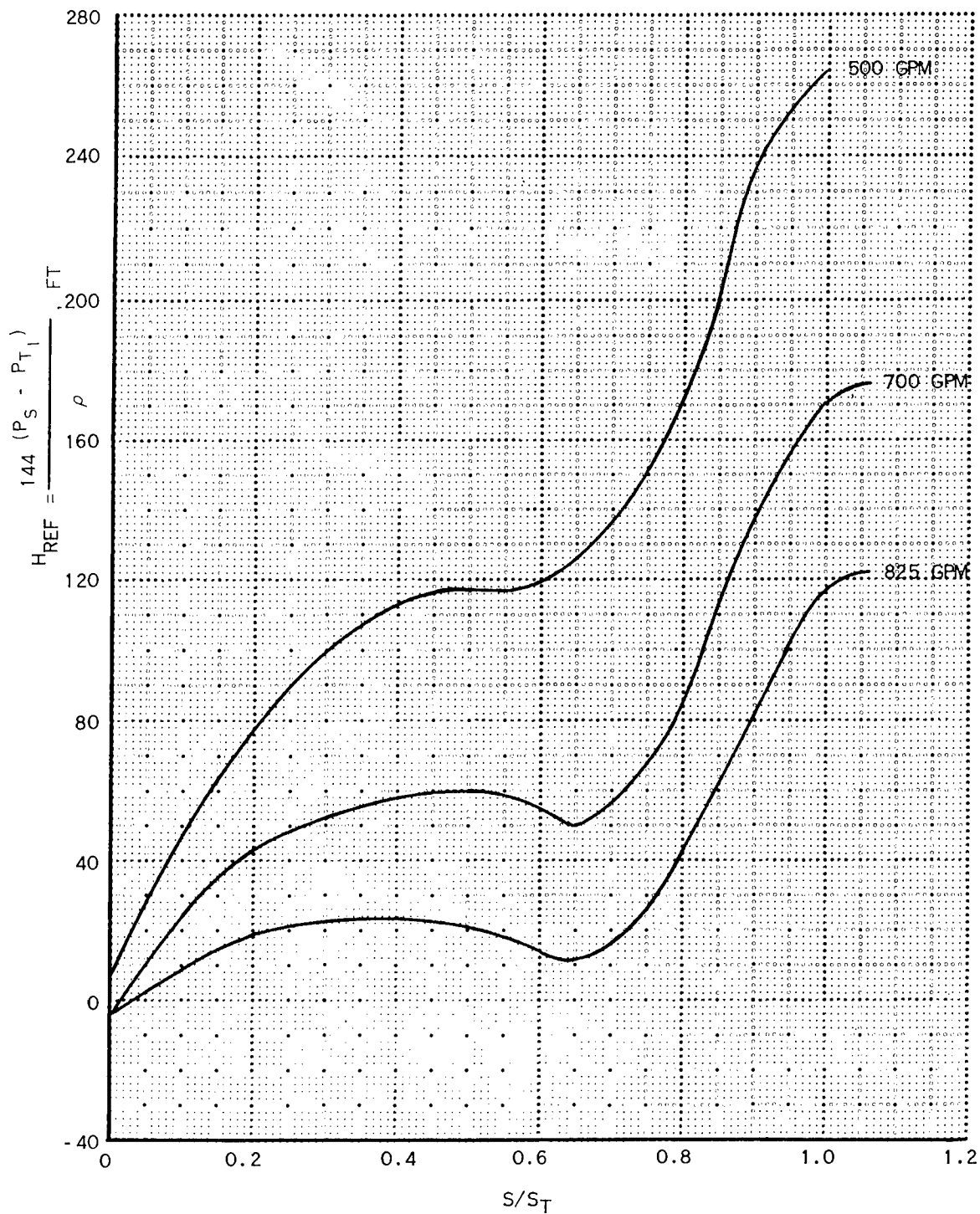


FIG 3

IMPELLER TIP STATIC PRESSURE RISE DISTRIBUTION

PREVIOUS TESTS OF RI-7A IMPELLER
SPEED: 6375 RPM



SURFACE ROUGHNESS MEASUREMENT OF RI-7C3 RESEARCH IMPELLER
BEFORE TEST

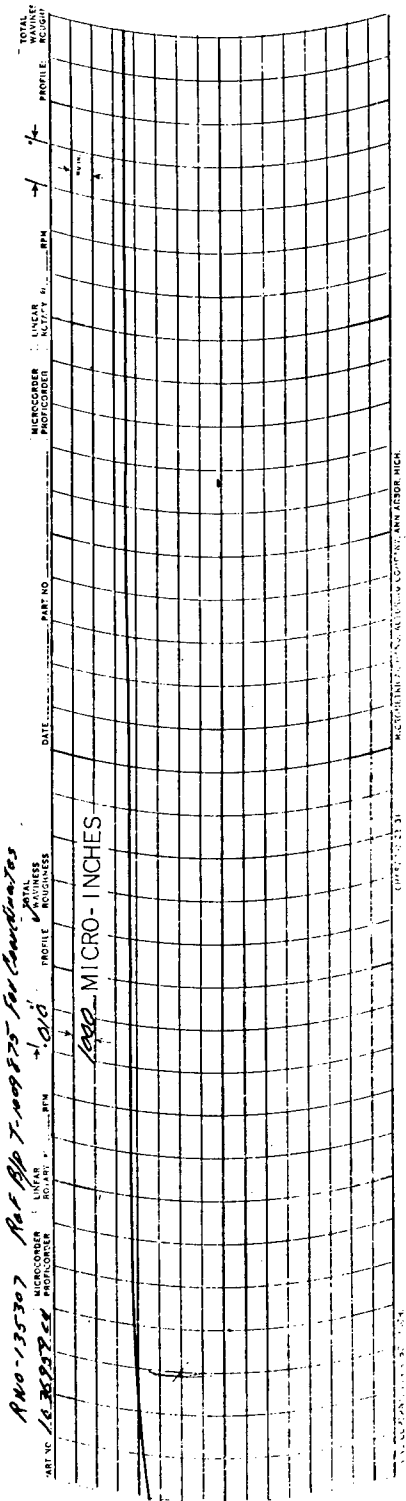


FIG 4

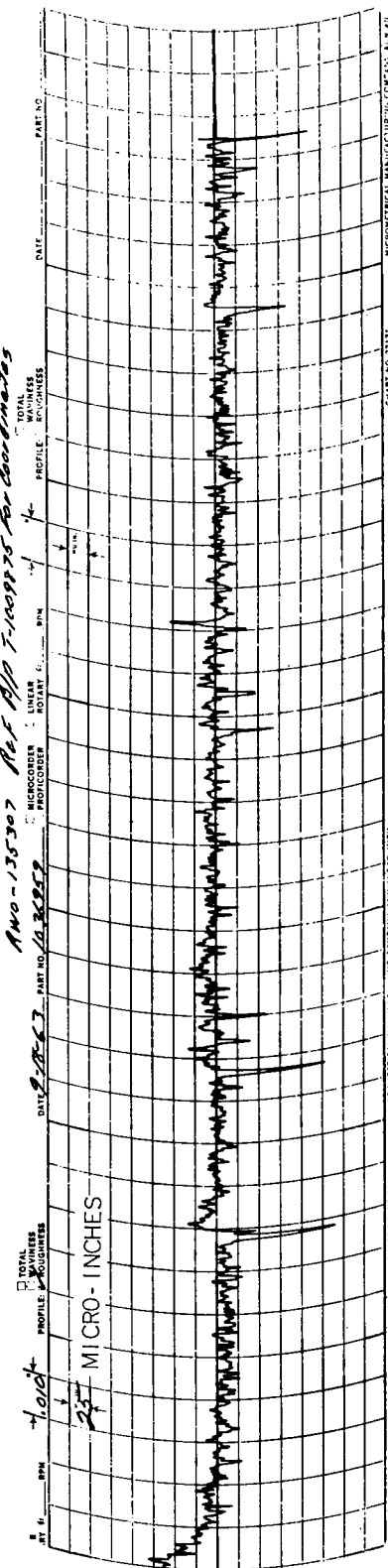


FIG 5

ZYGLO INDICATIONS ON THE RI-7C3 IMPELLER BEFORE TEST



CLOSE-UP VIEW RI-7C3 IMPELLER VANE 2 SURFACE BEFORE TEST

FIG 6



FIG 7

TYPICAL RUBBER MOLD OF RI-7C3 IMPELLER VANE SURFACE
BEFORE TEST



FIG 8
TURBOPUMP FOR LIQUID METAL TEST

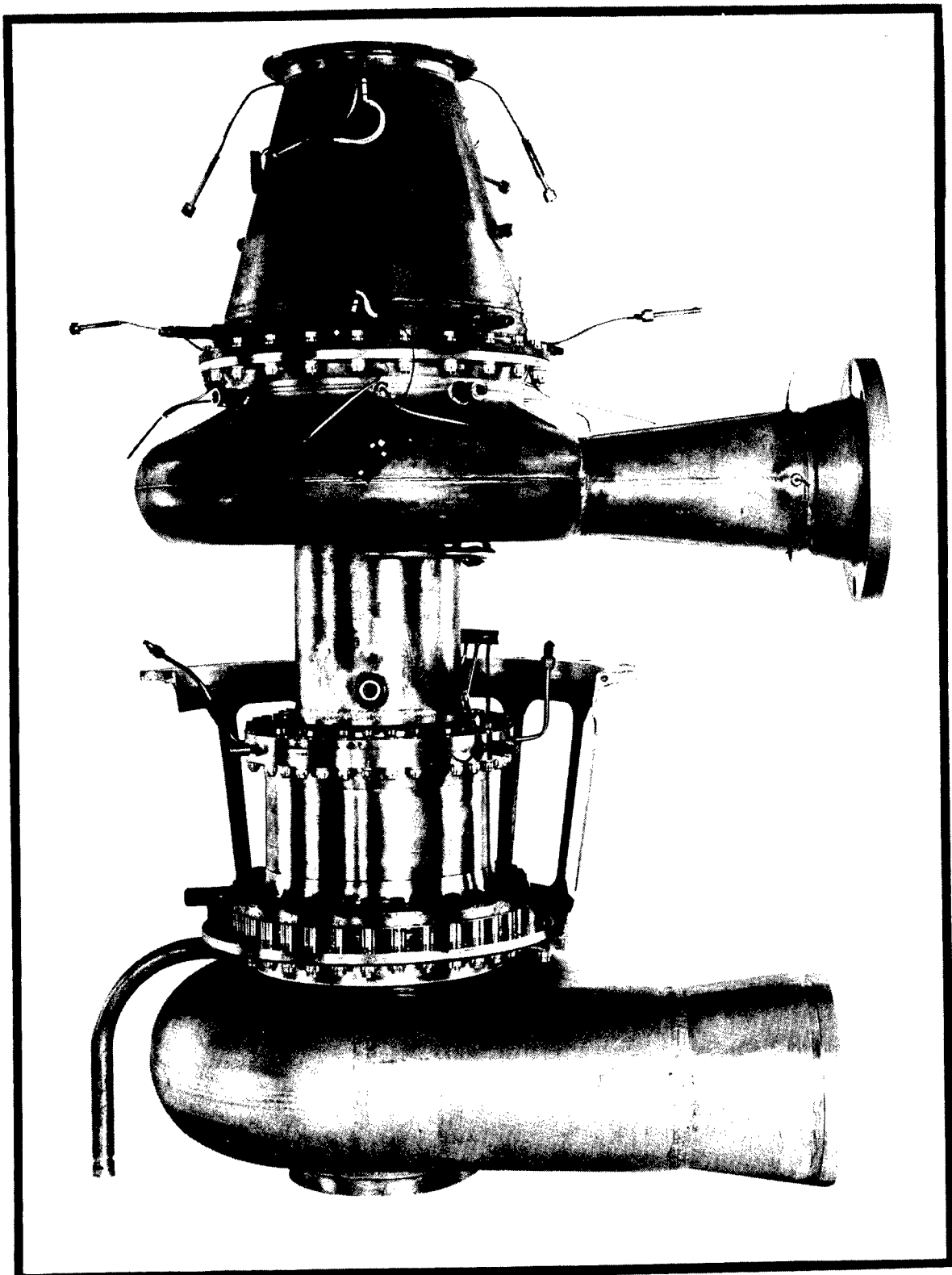


FIG 9
INTERNAL MODIFICATIONS TO TURBOPUMP

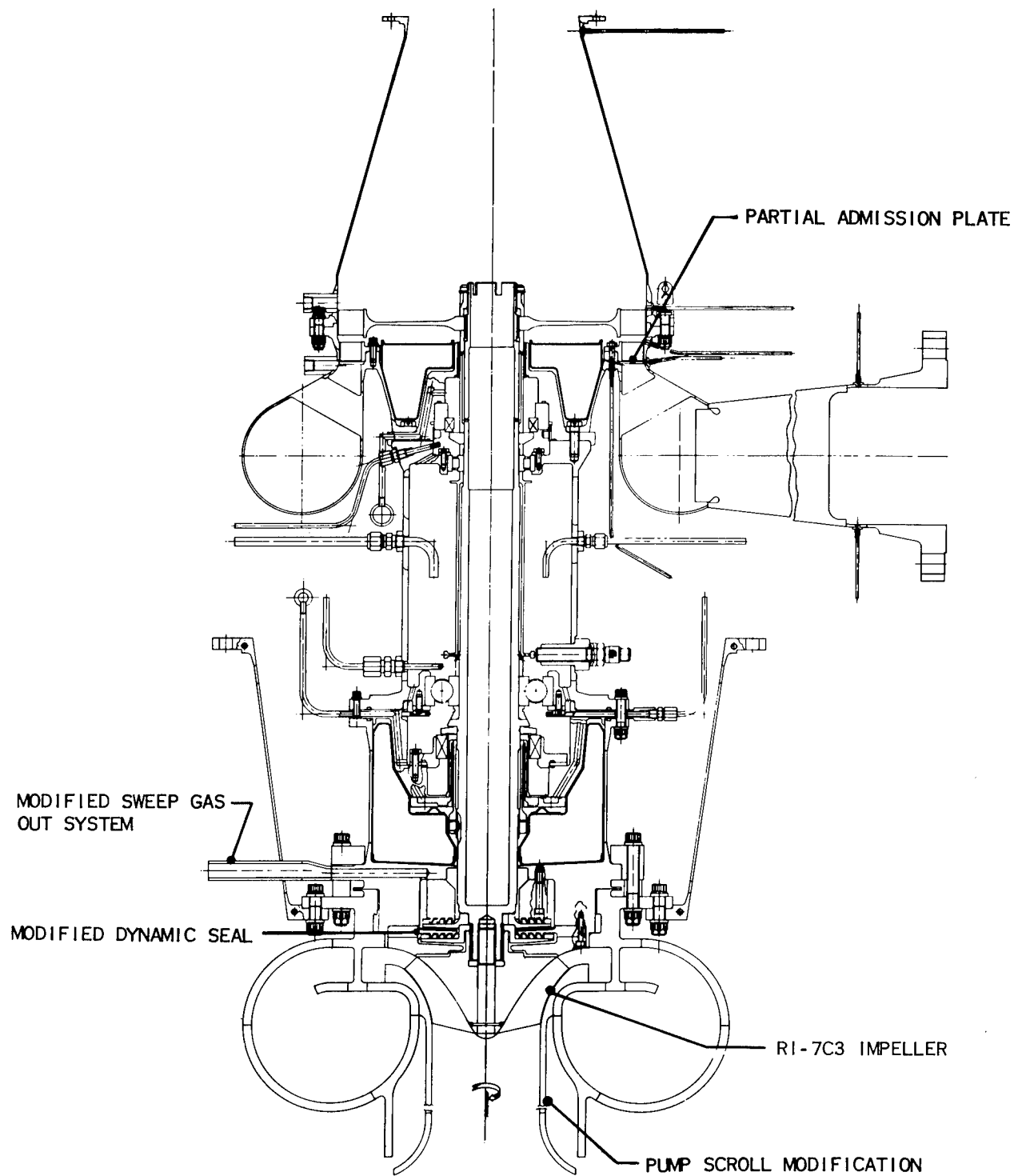
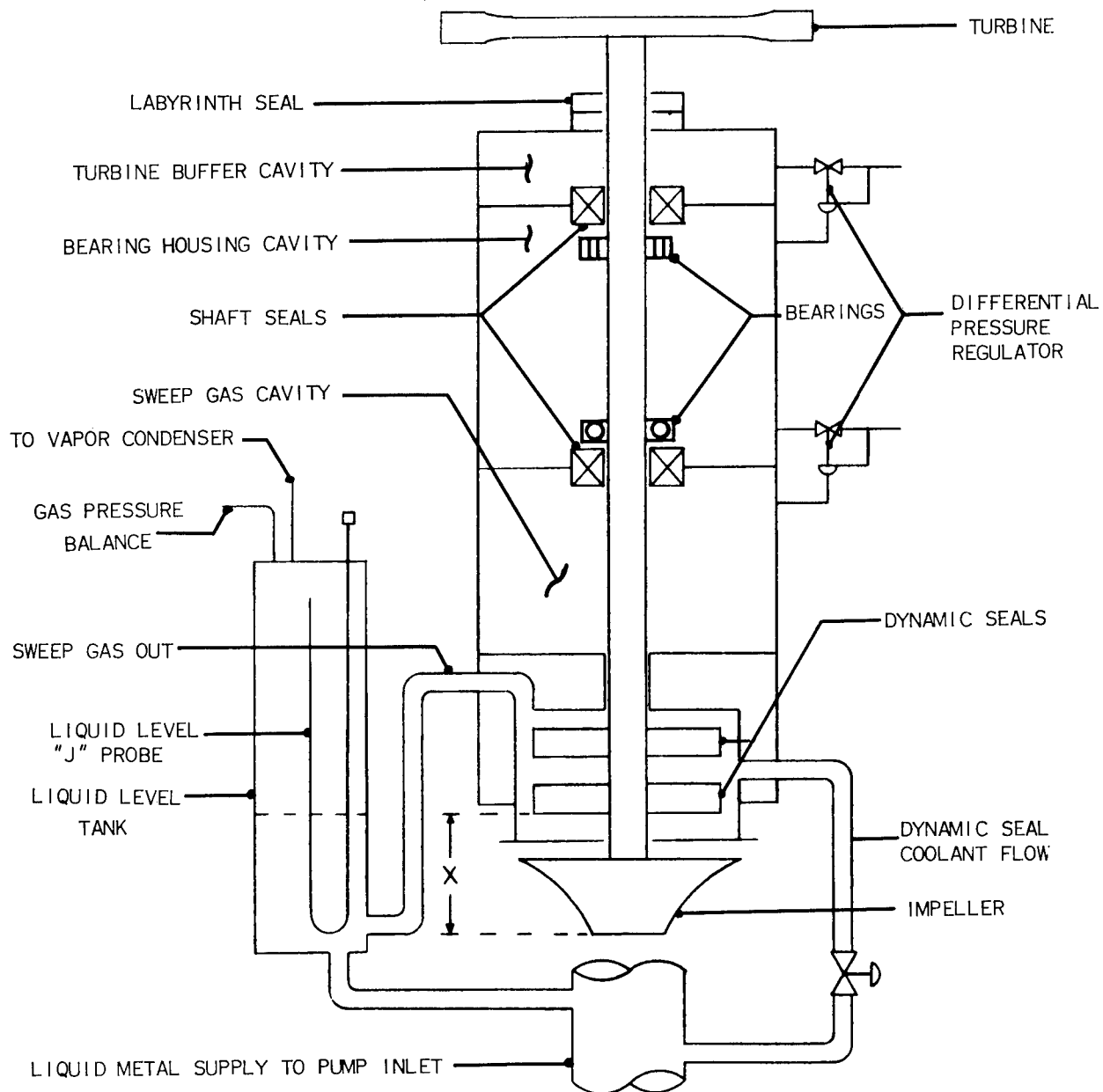


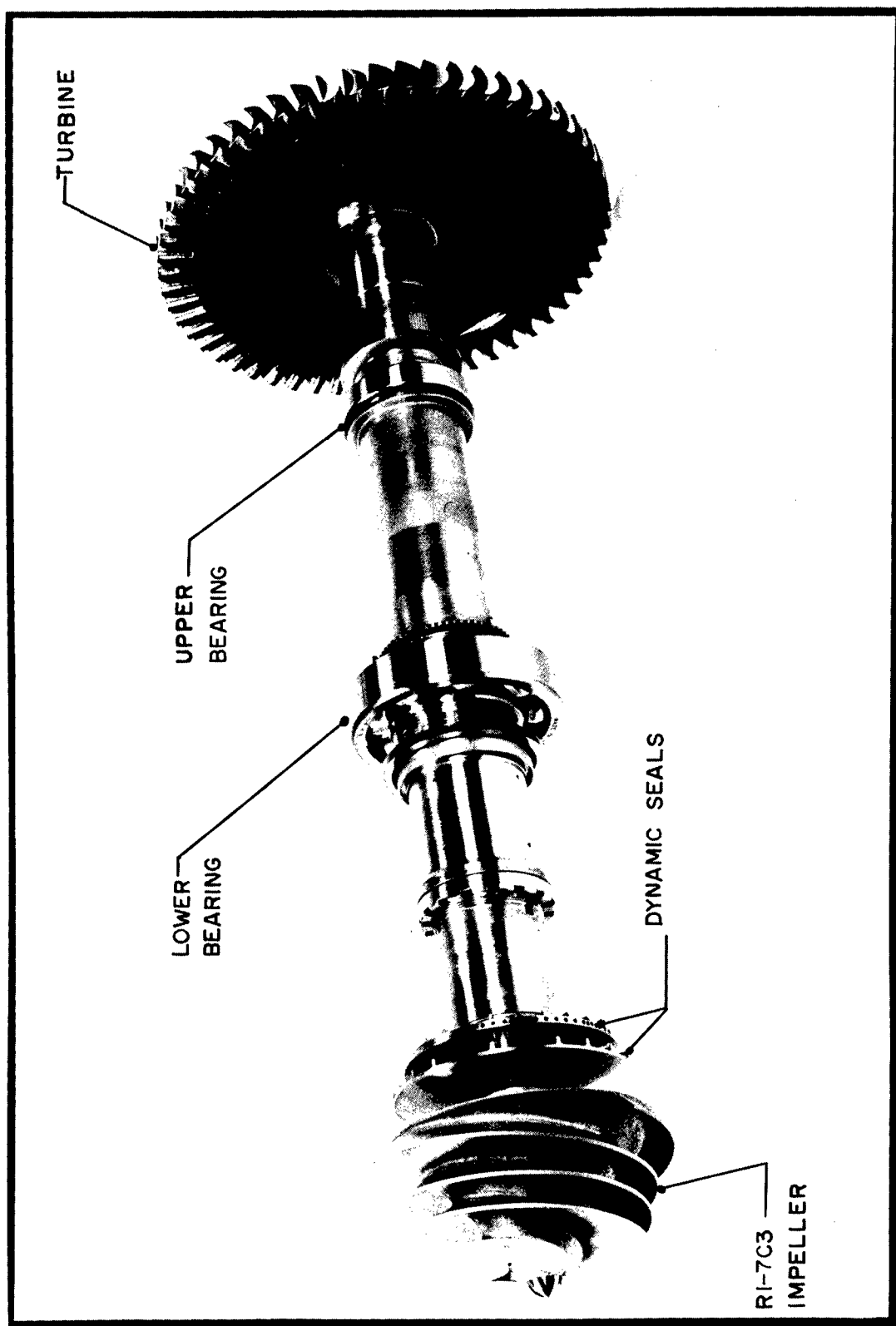
FIG 10

SEALING AND GAS CONTROL SCHEMATIC FOR TURBOPUMP



TURBOPUMP SHAFT ASSEMBLY

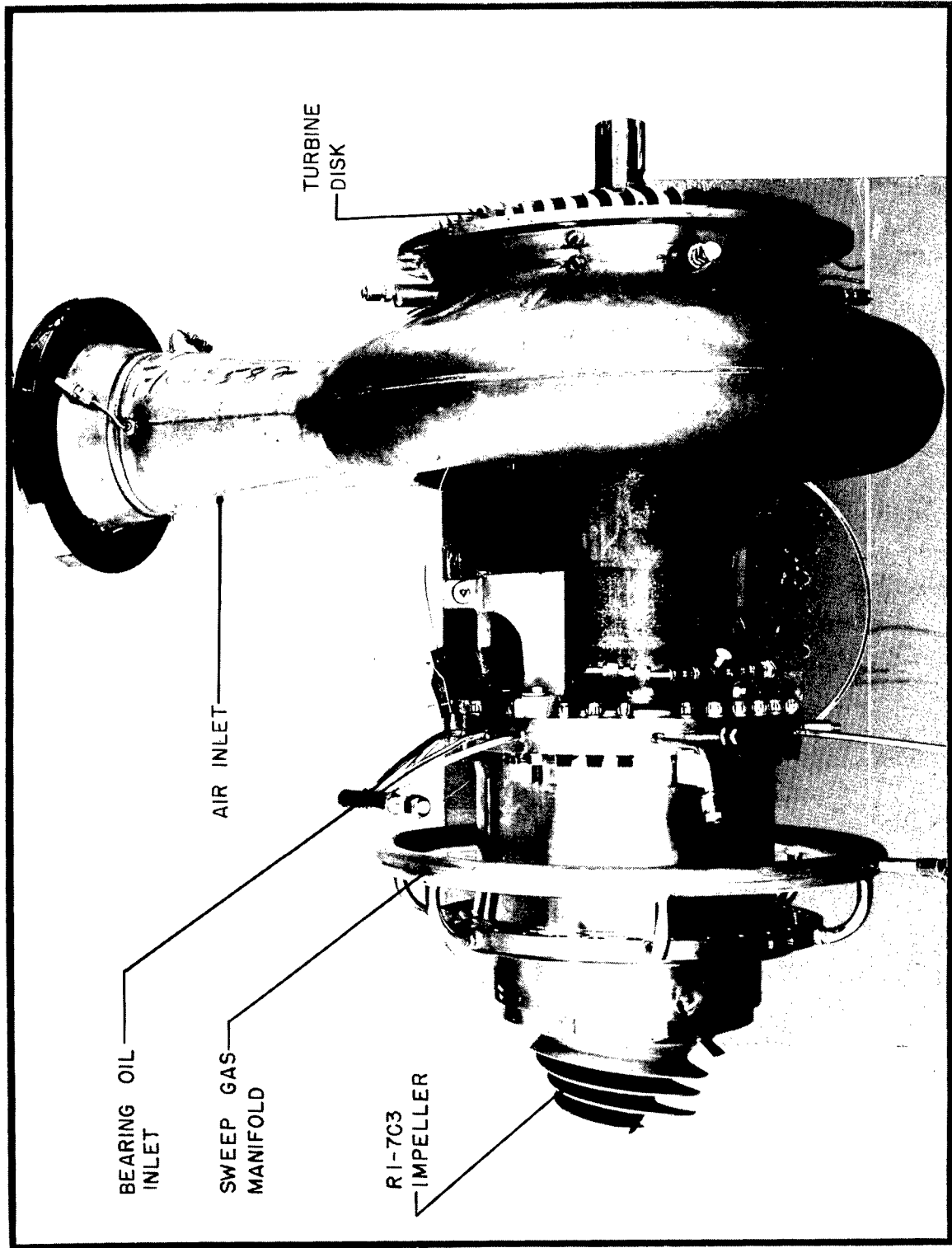
FIG 11



TURBOPUMP ASSEMBLY

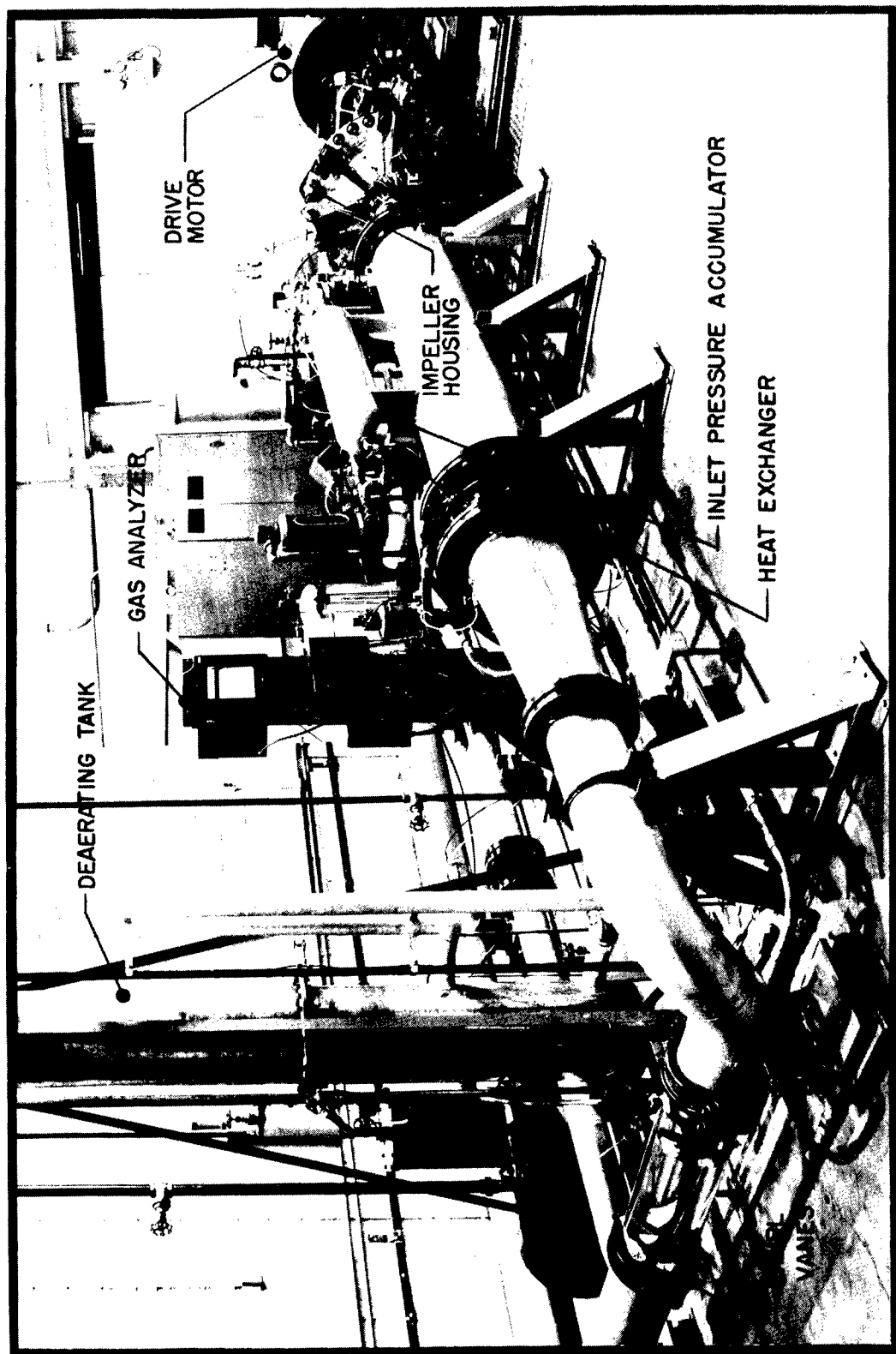
LESS PUMP SCROLL AND TURBINE EXHAUST CONE

FIG 12

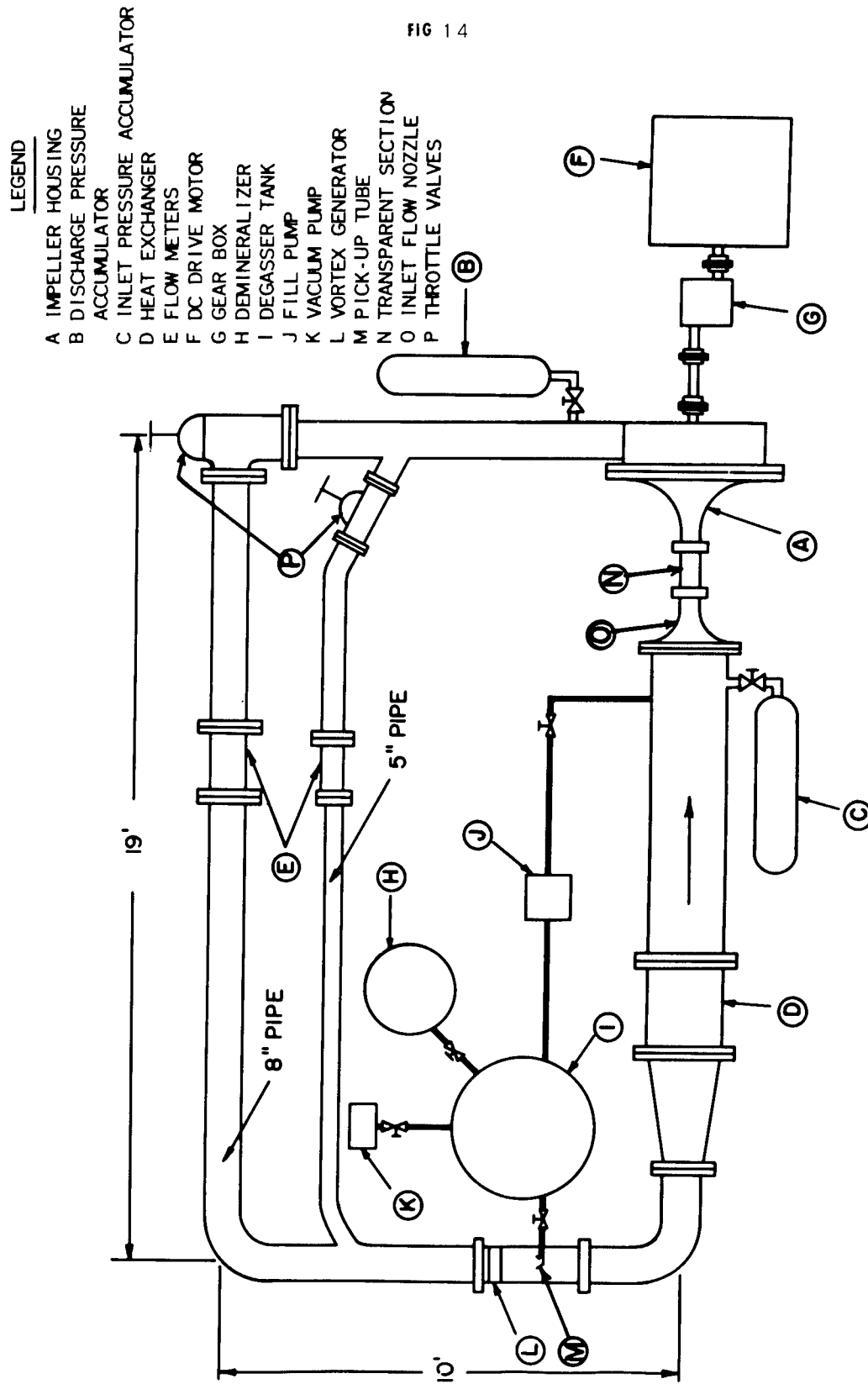


WATER IMPELLER TEST STAND

FIG 13



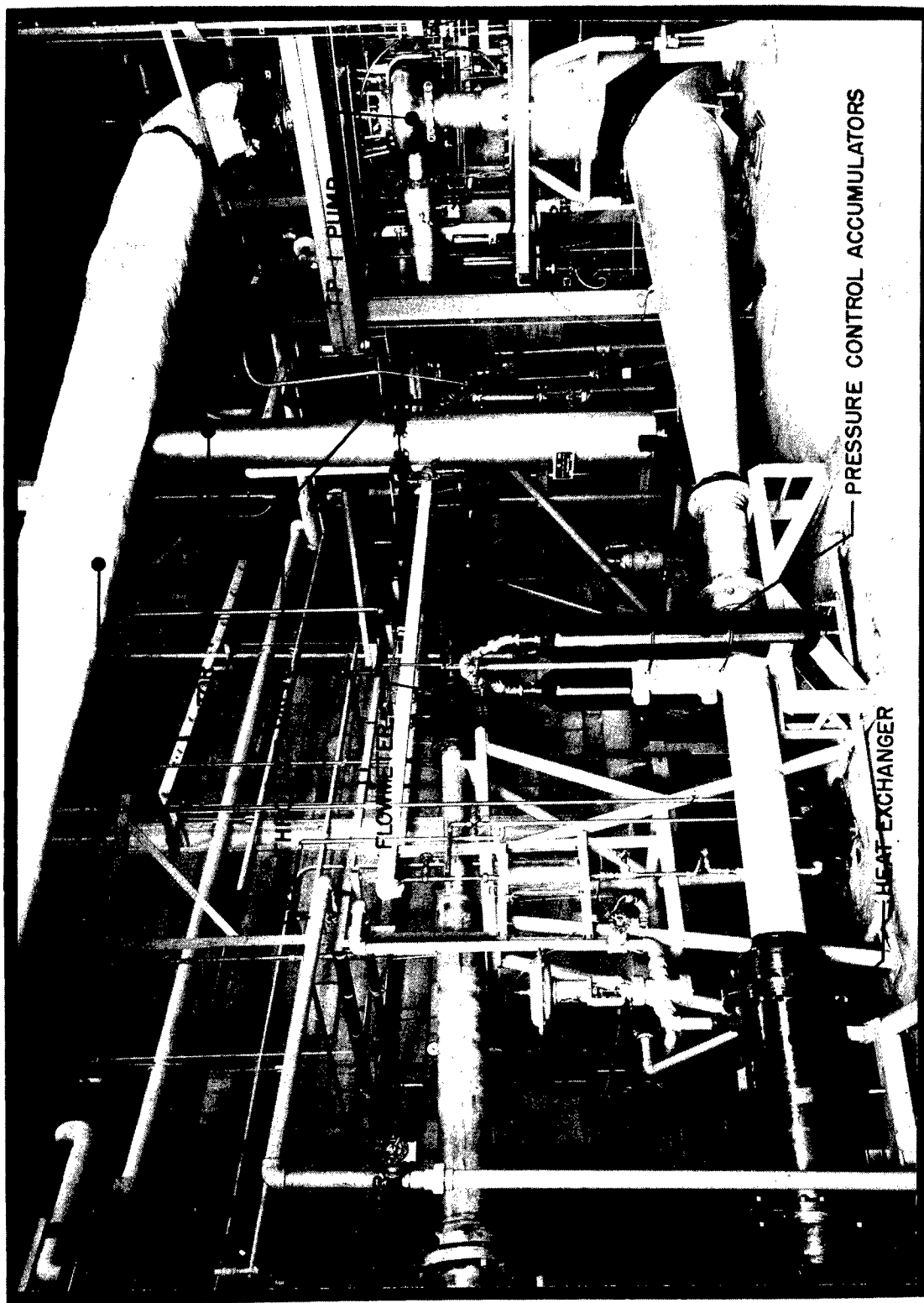
SCHEMATIC OF WATER IMPELLER TEST STAND



WATER PUMP TEST STAND

SHOWING LOOP AND INSTALLED TURBOPUMP

FIG 15



SCHEMATIC OF WATER PUMP TEST STAND

LEGEND

- A THROTTLE VALVE WITH PNEUMATIC OPERATOR
- B GENTILE FLOW MEASURING TUBE
- C SWIRL VANES AND DEGASSING PICKUP TUBE
- D SUCTION PUMP
- E DEGASSING COLUMN
- F DISCHARGE PUMP
- G VACUUM PUMP
- H ACCUMULATOR BOTTLES, INLET
- I STILLING CHAMBER WITH TURNING VANES
- J TURBOPUMP
- K ACCUMULATOR BOTTLES, DISCHARGE
- L HEAT EXCHANGER
- M SWEET GAS OUT OBSERVATION TANK
- N TURBINE EXHAUST
- O SWING CHECK VALVE
- P AIR THROTTLE VALVE
- Q AIR FLOWMETER

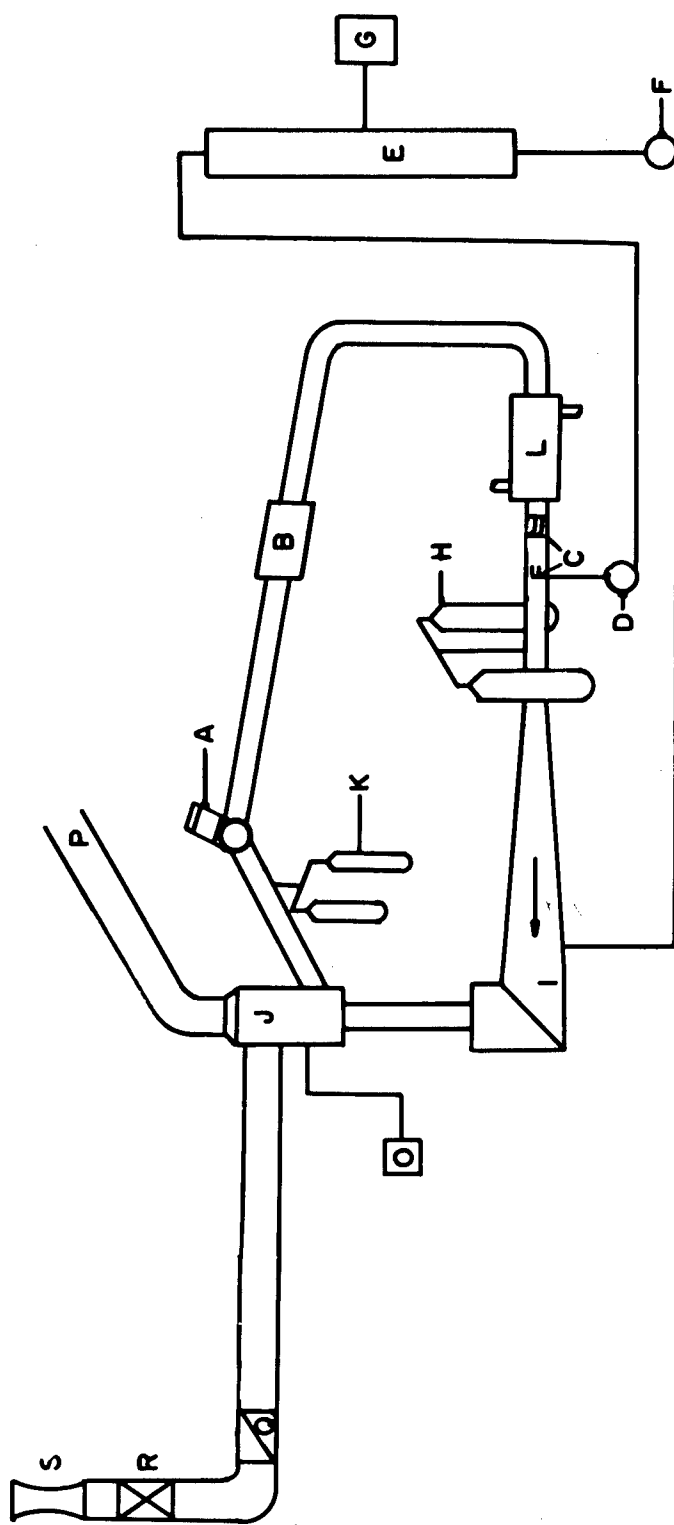
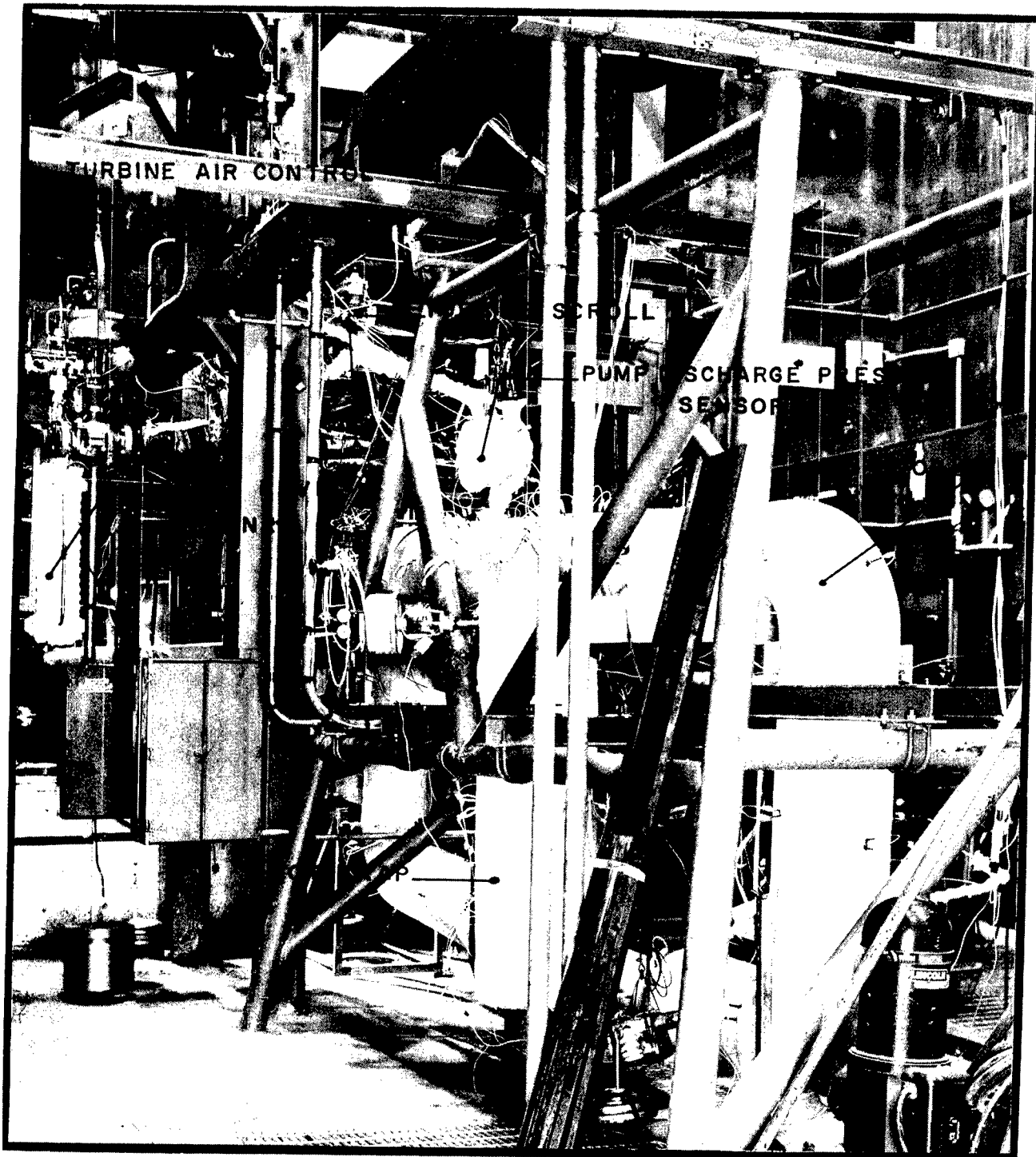


FIG 16

FIG 17

LIQUID METAL PUMP TEST STAND



SCHEMATIC OF LIQUID METAL PUMP TEST STAND

FIG 18

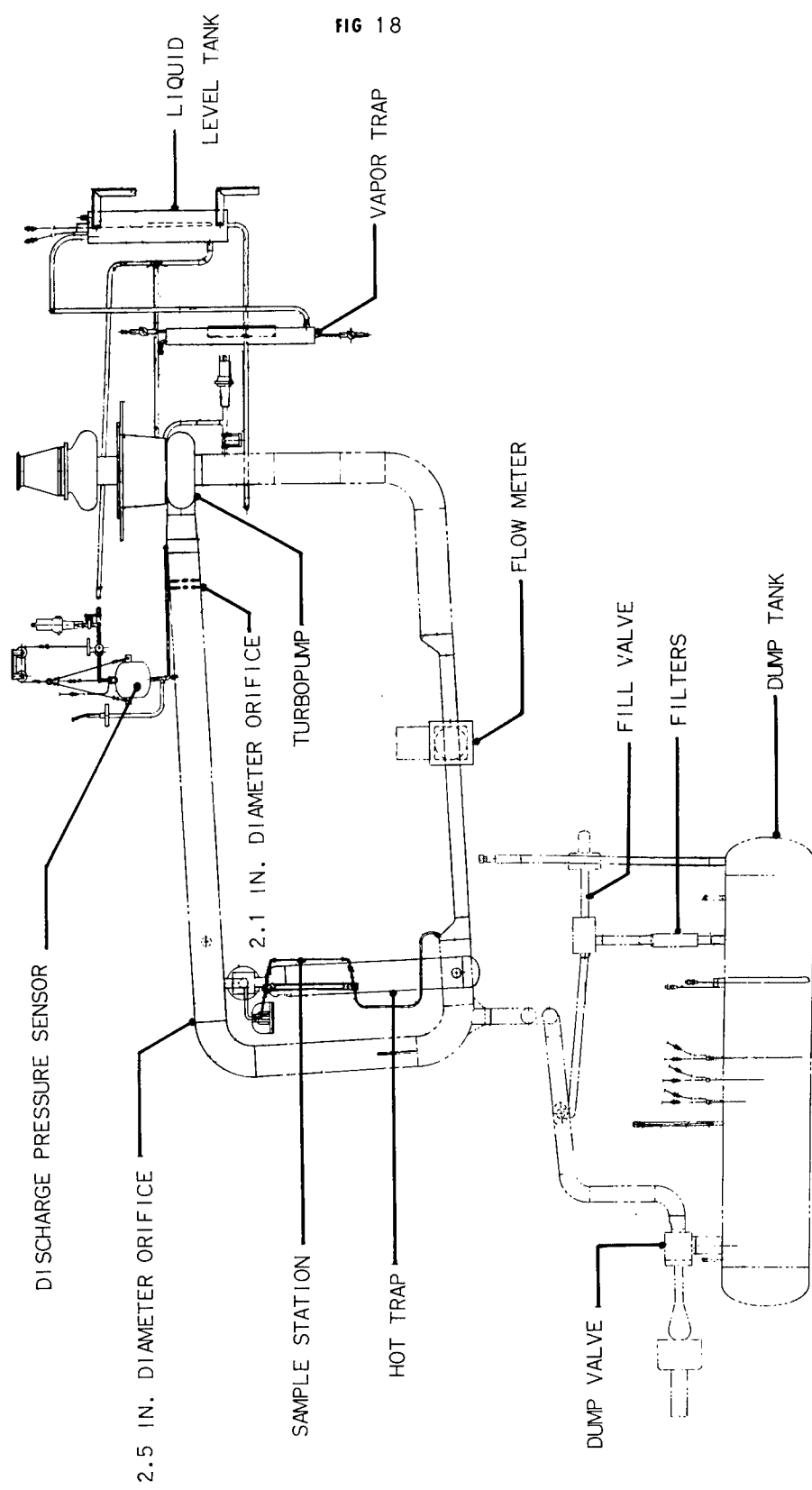


FIG 19

VIEW OF LIQUID METAL PUMP TEST STAND

BEFORE REWORKING FOR THIS INVESTIGATION

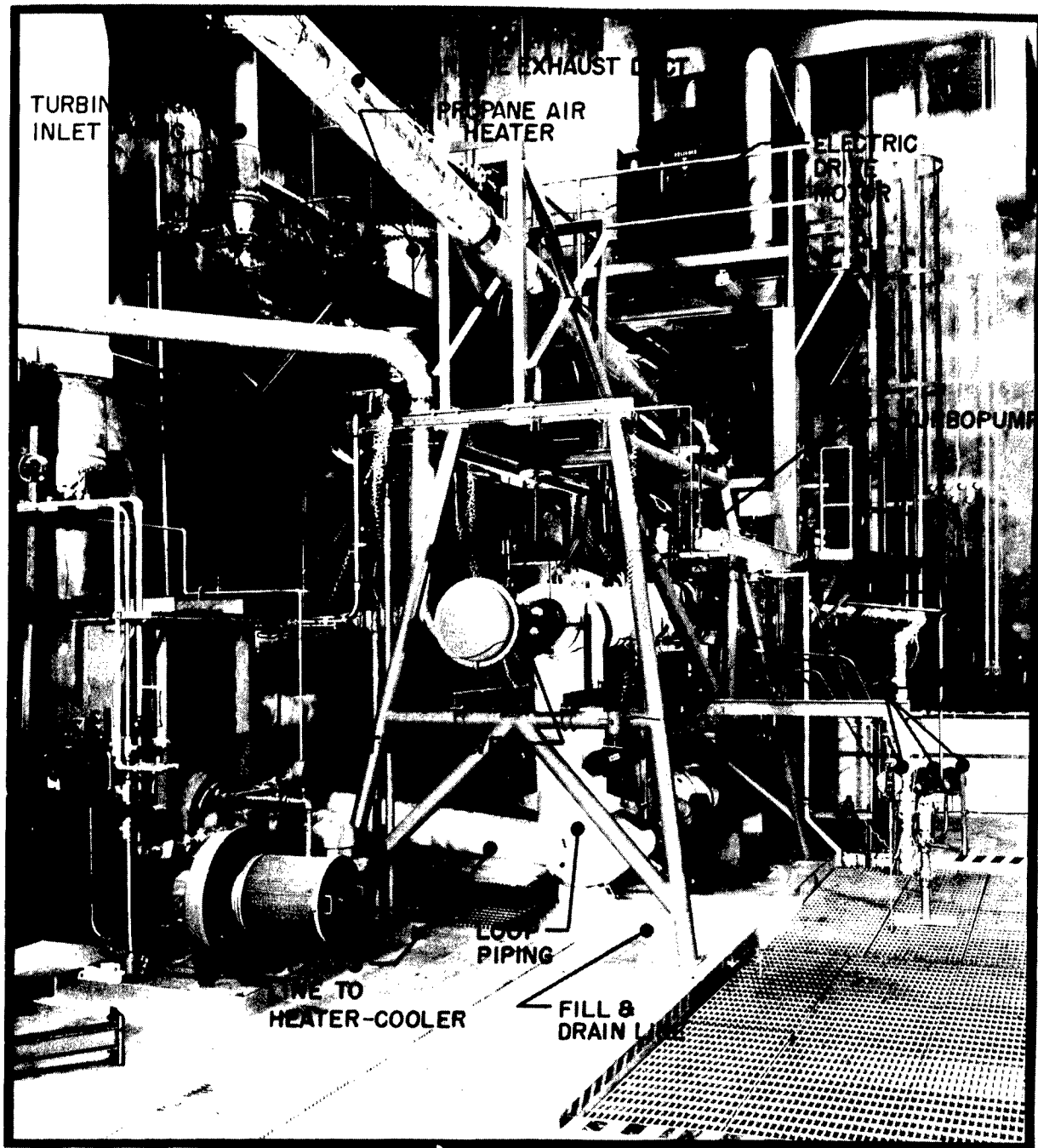
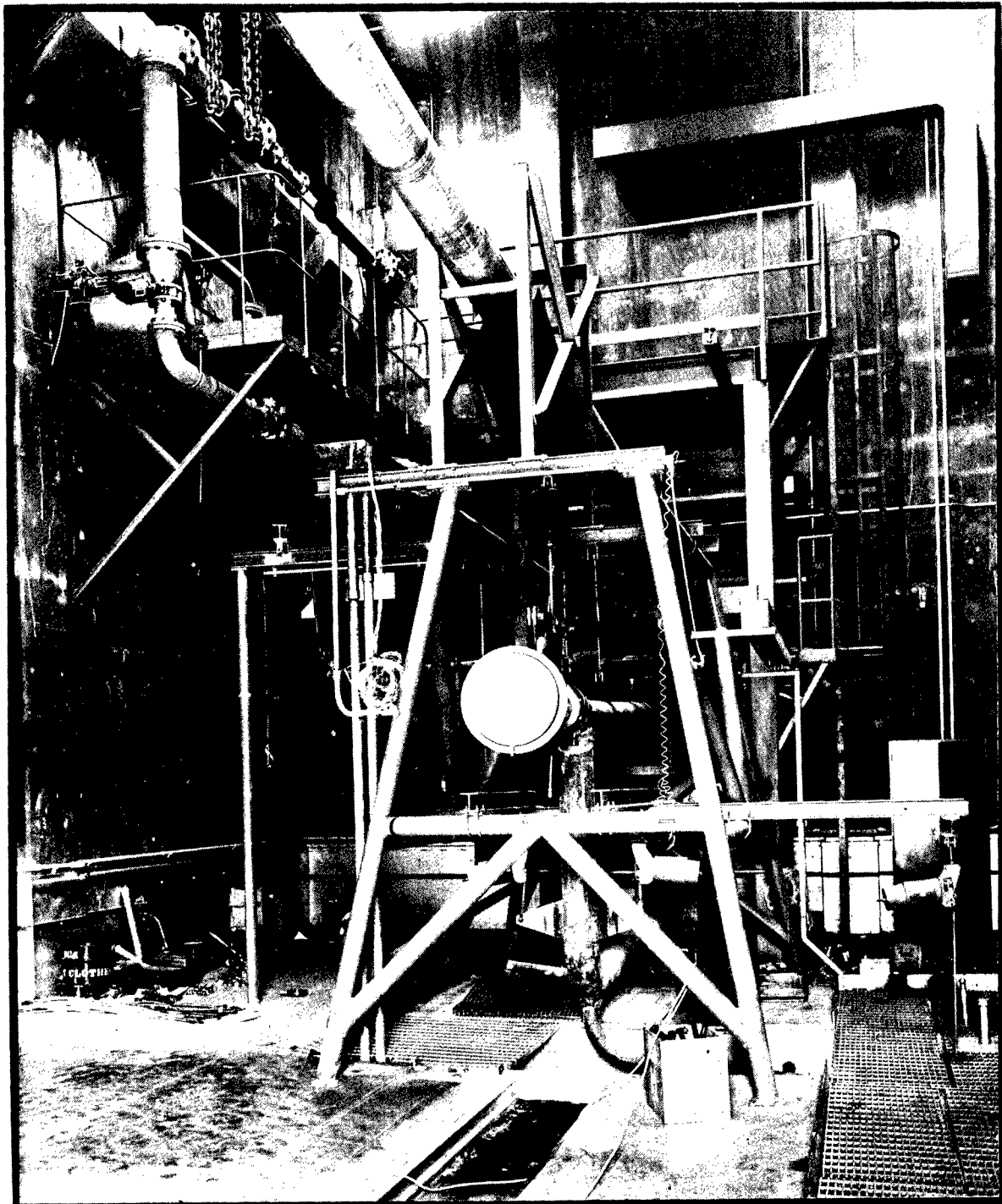


FIG 20

VIEW OF LIQUID METAL PUMP TEST STAND DURING CONSTRUCTION



LIQUID METAL PUMP TEST STAND CONTROL PANELS

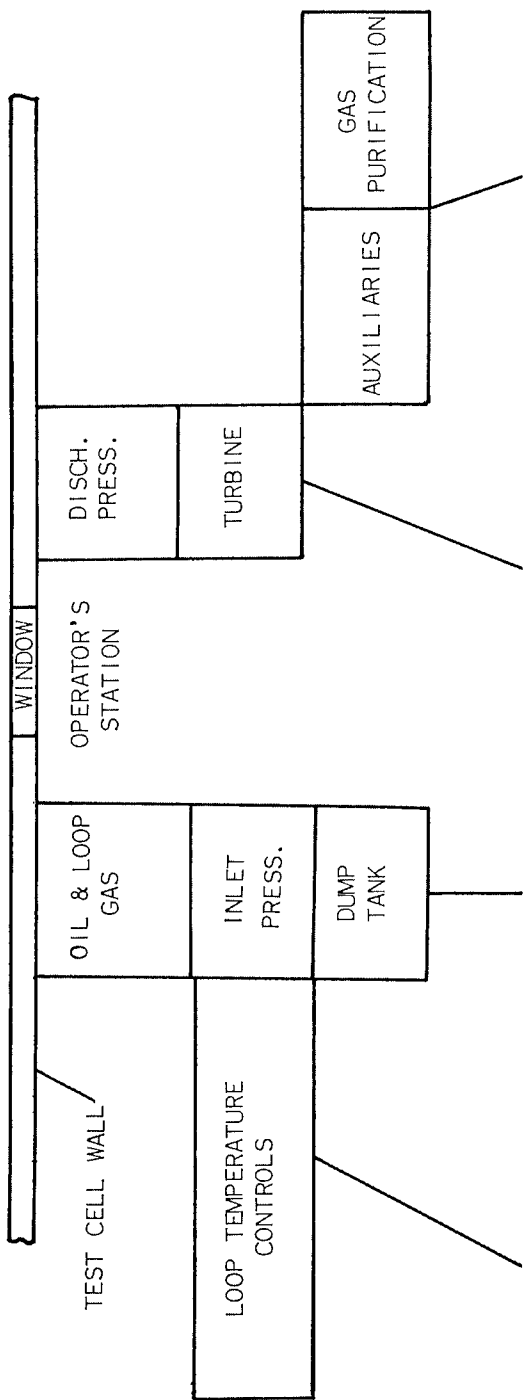


FIG 21

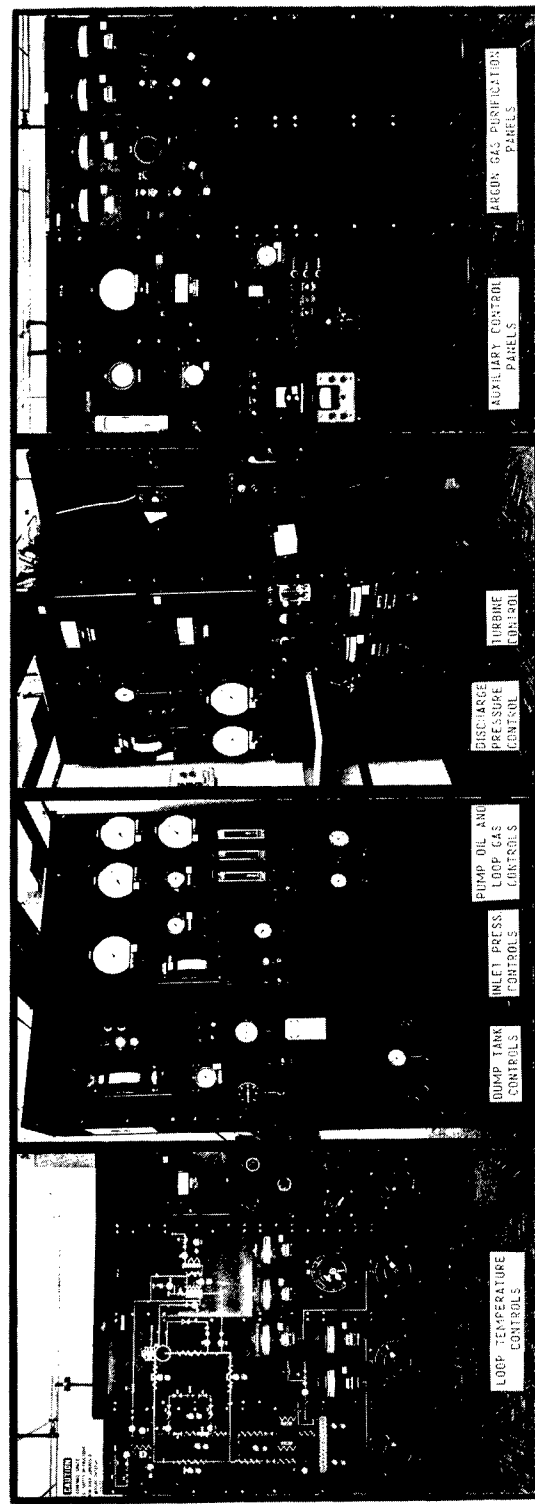


FIG 22

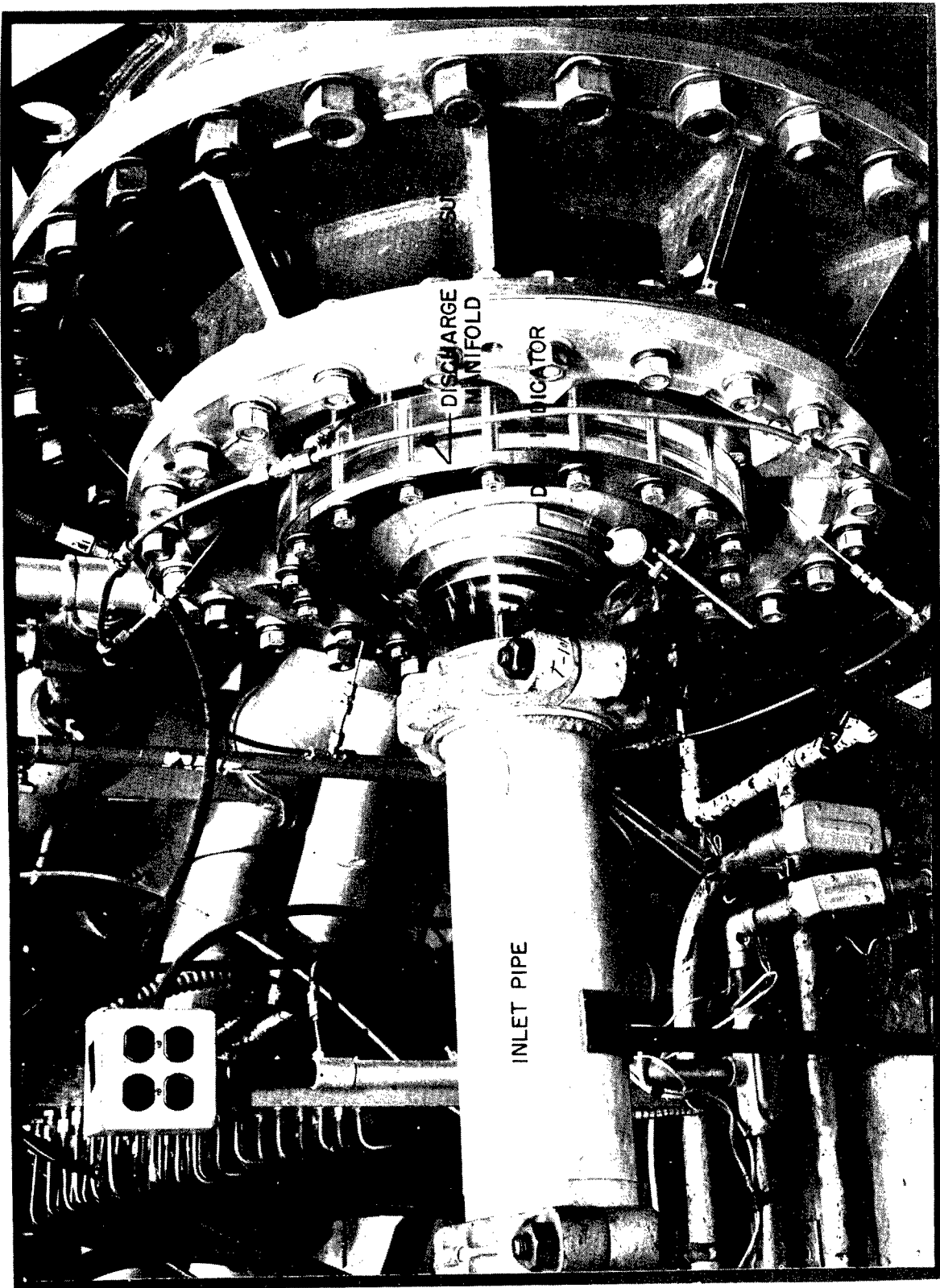


FIG 23

HYDRAULIC PERFORMANCE FOR THE RI-7C3 IMPELLER

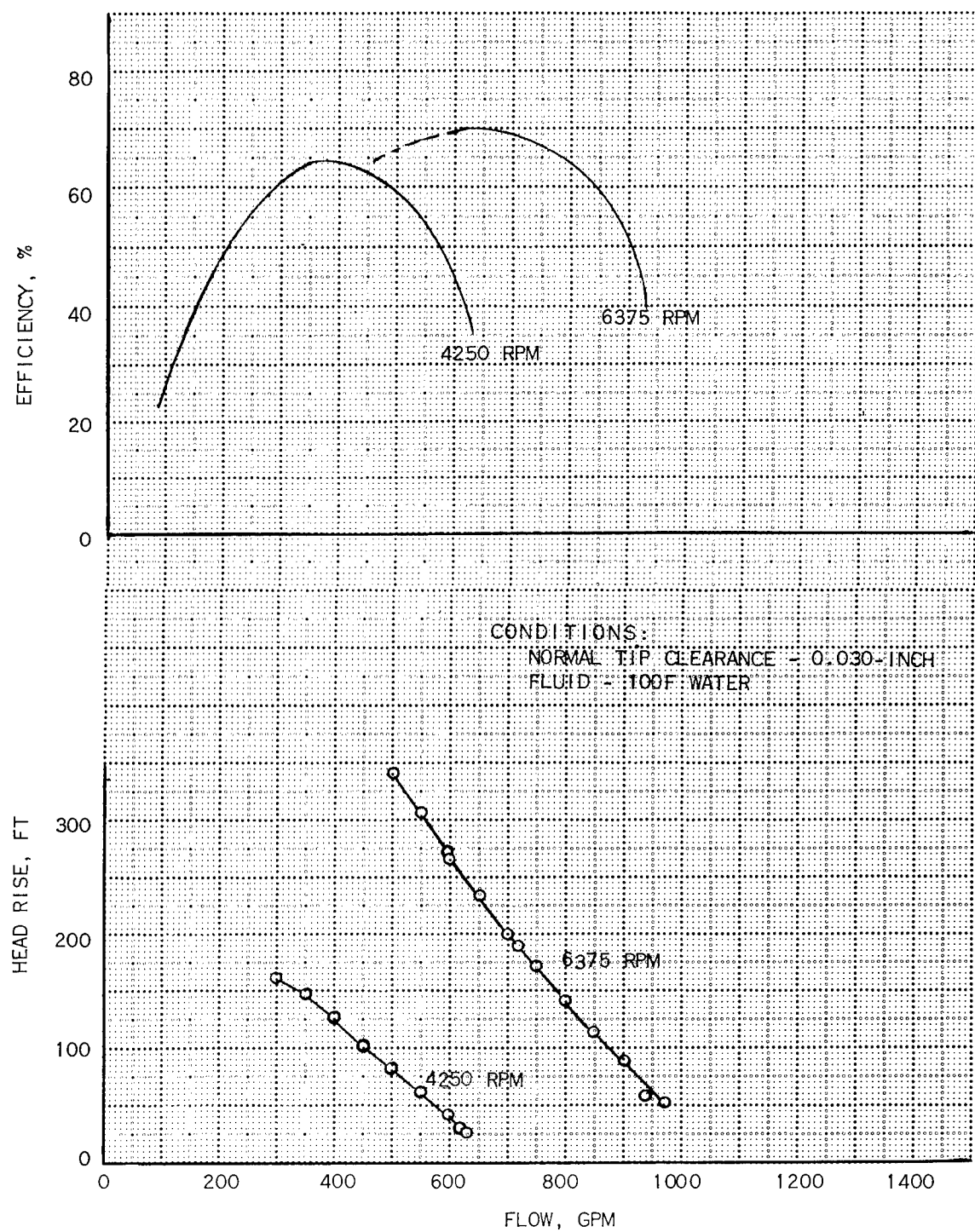
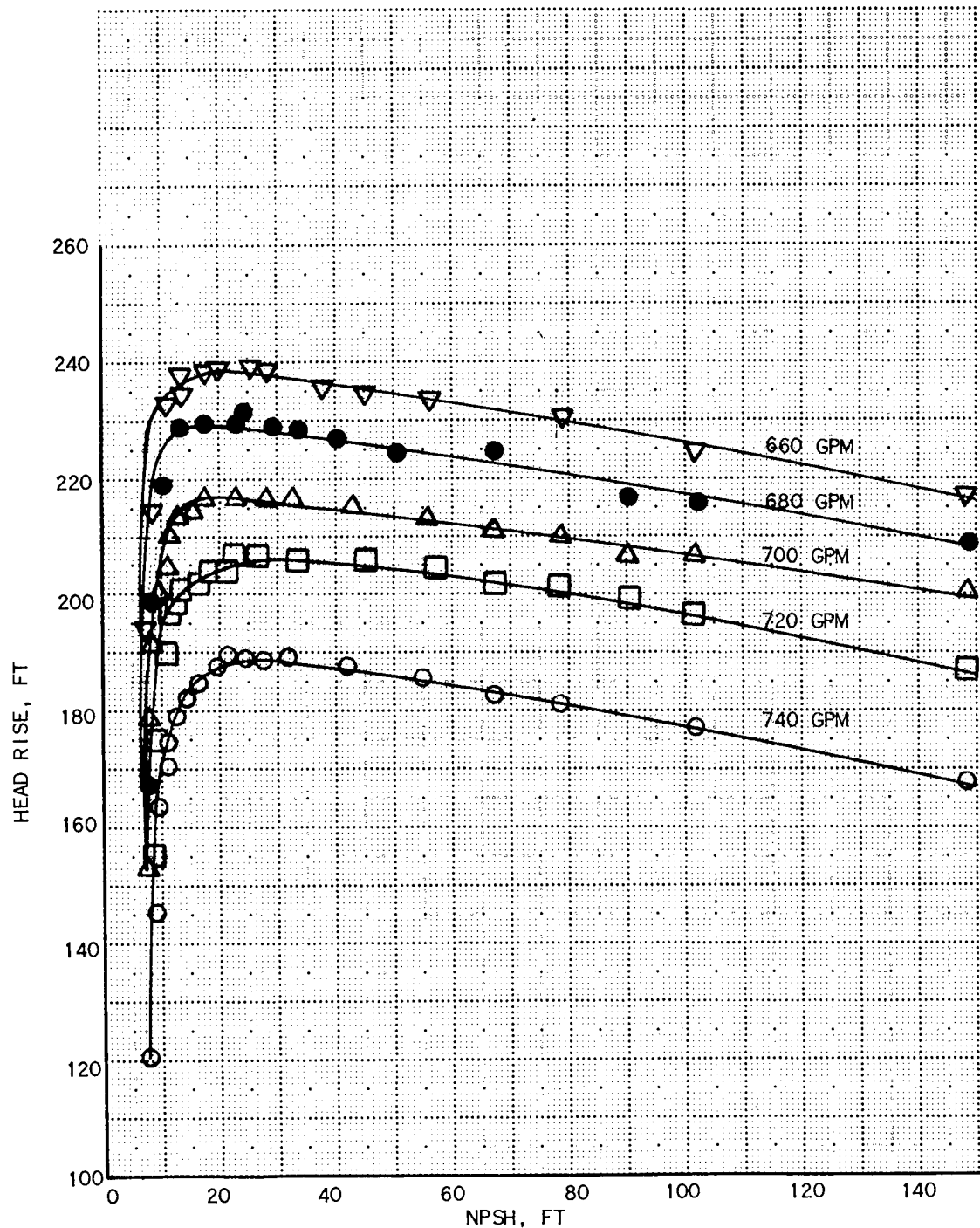


FIG 24
CAVITATION PERFORMANCE FOR RI - 7C3 IMPELLER

CONDITIONS:
NOMINAL TIP CLEARANCE: 0.030 INCH
FLUID: 100F WATER
SHAFT SPEED: 6375 RPM



PHOTOGRAPHIC SET UP FOR HIGH SPEED MOTION PICTURES

FIG 25

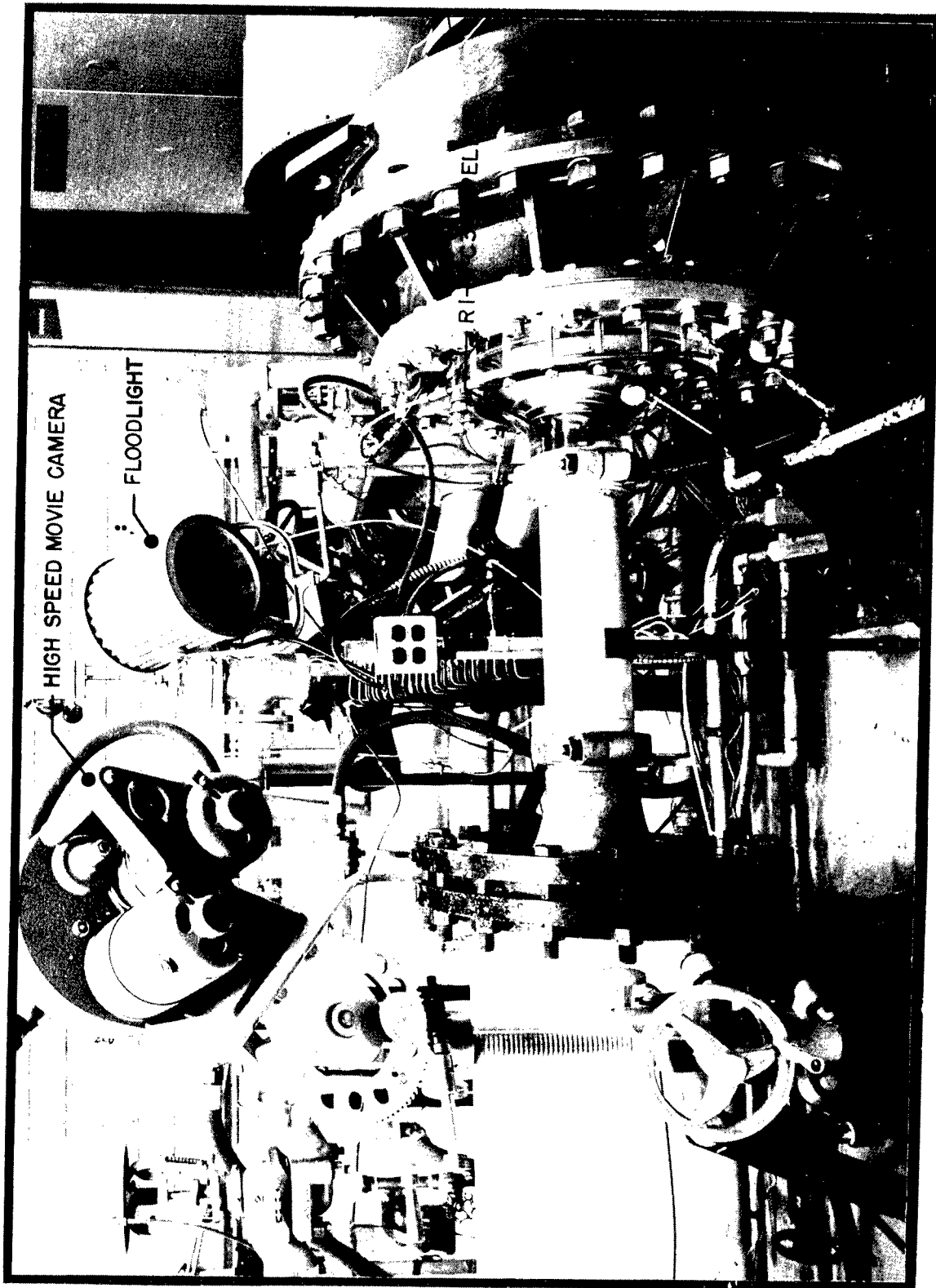


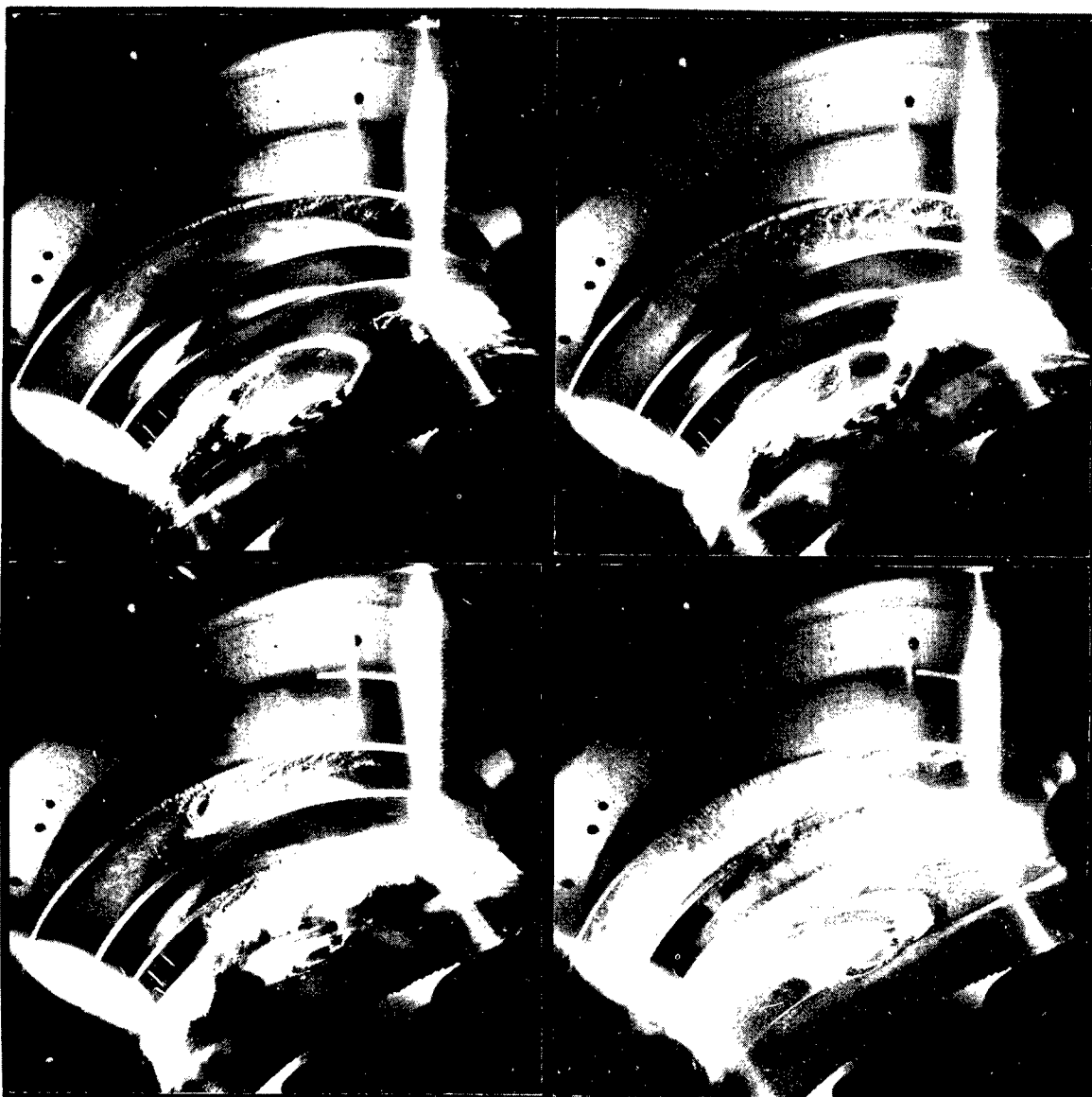
FIG 26

VISUAL CAVITATION PATTERNS AT 660 GPM AS FUNCTIONS OF NPSH

SPEED: 6375 RPM

NPSH - 35 FT
 N_{SV} - 11,380

NPSH - 24 FT
 N_{SV} - 15,110



NPSH - 15 FT
 N_{SV} - 21,500

NPSH - 8 FT
 N_{SV} - 34,400

FIG 27

VISUAL CAVITATION PATTERNS AT 680 GPM AS FUNCTIONS OF NPSH

SPEED: 6375 RPM

NPSH - 35 FT
 N_{SV} - 11,550

NPSH - 19 FT
 N_{SV} - 18,500

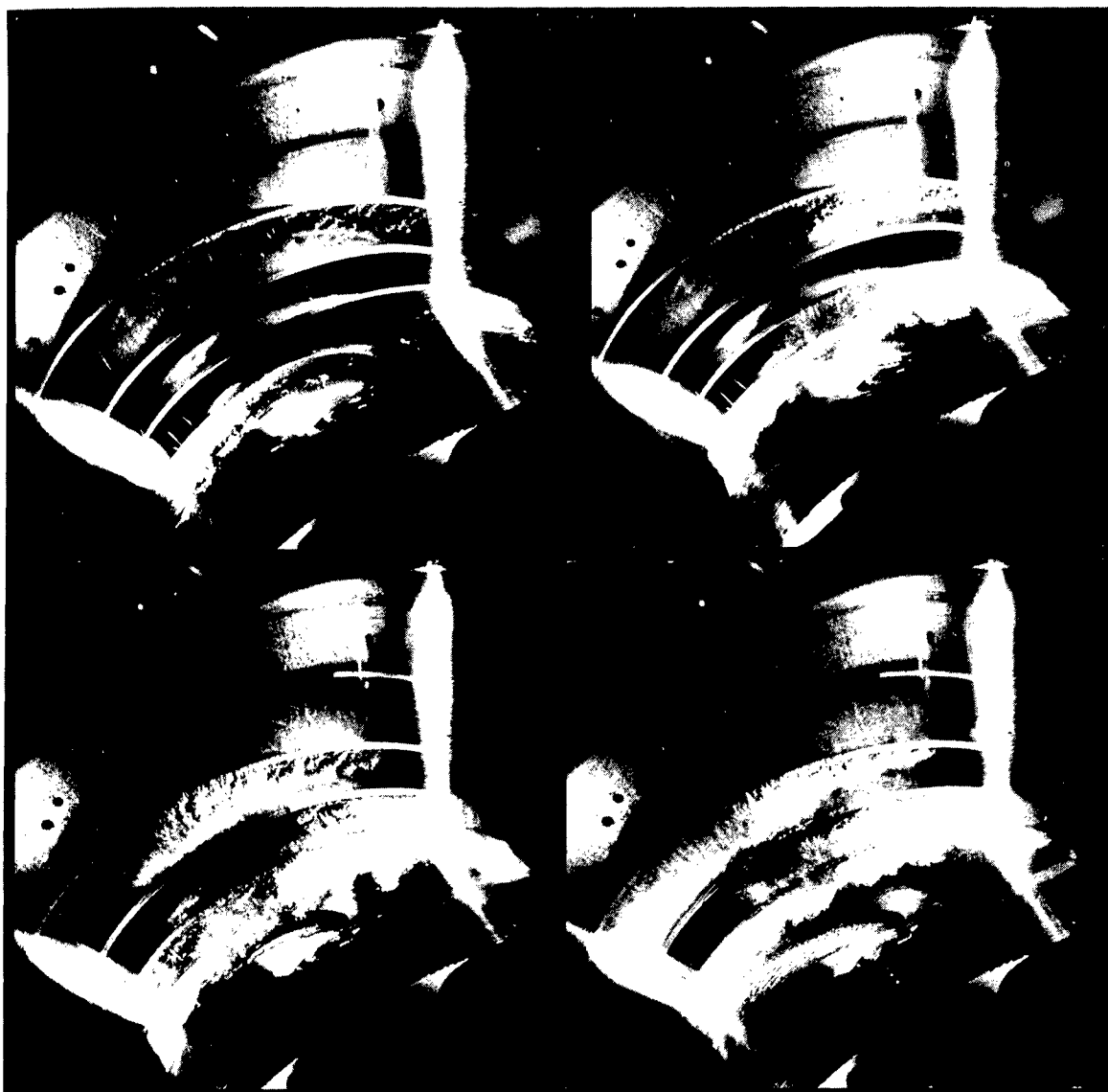
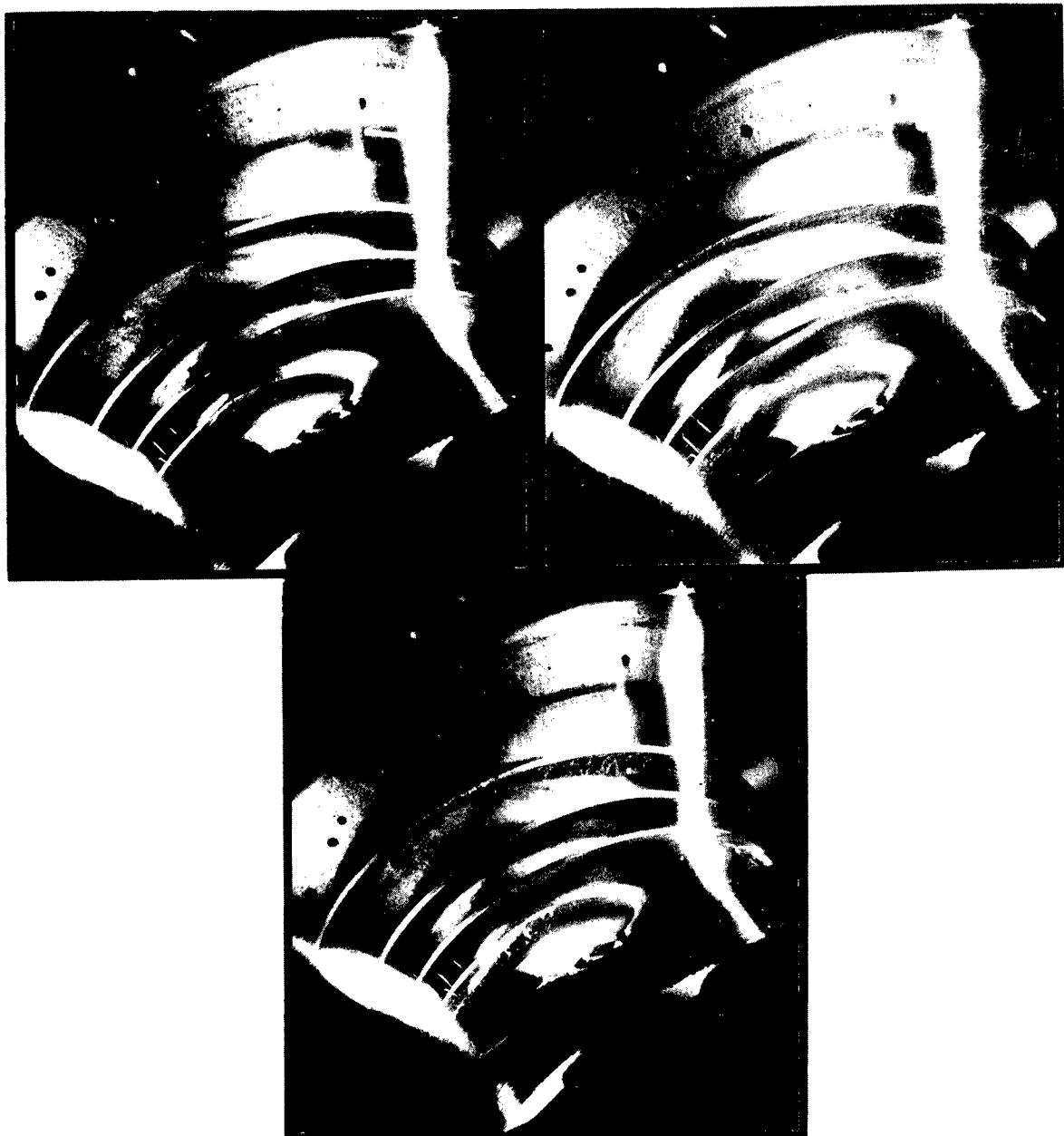


FIG 28

VISUAL CAVITATION PATTERNS AT 700 GPM AS FUNCTIONS OF NPSH

NPSH=150 FT
 $N_{SV} = 3930$

NPSH=100FT
 $N_{SV} = 5480$



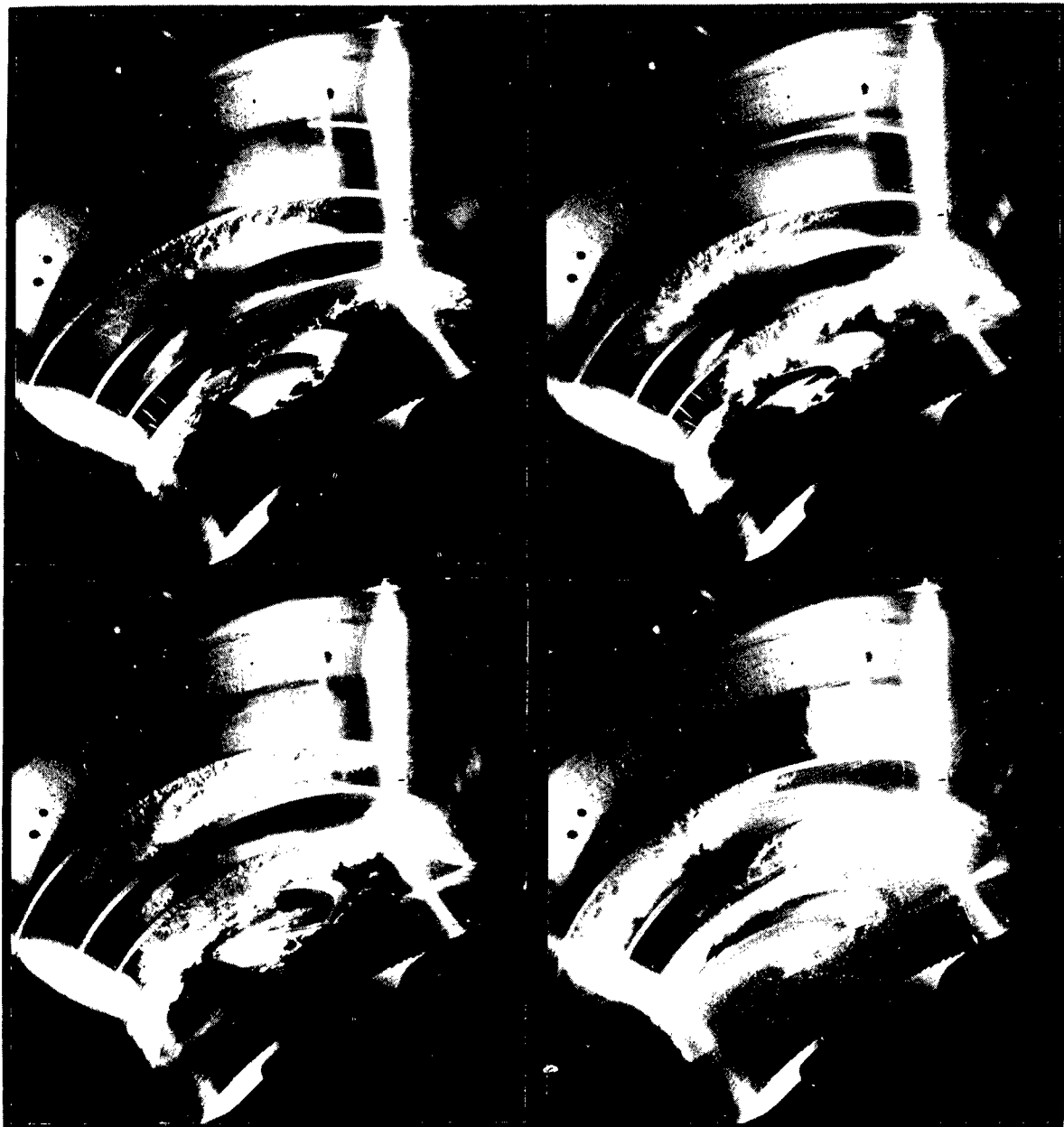
NPSH=60FT
 $N_{SV} = 7790$

FIG 28

VISUAL CAVITATION PATTERNS AT 700 GPM AS FUNCTIONS OF NPSH
(CONTINUED)

NPSH=35FT
 $N_{SV}=11,690$

NPSH=17.7 FT
 $N_{SV}=19,500$



NPSH=15FT
 $N_{SV}=22,100$

NPSH=8 FT
 $N_{SV}=35,400$

FIG 29

VISUAL CAVITATION PATTERNS AT 720 GPM AS FUNCTIONS OF NPSH

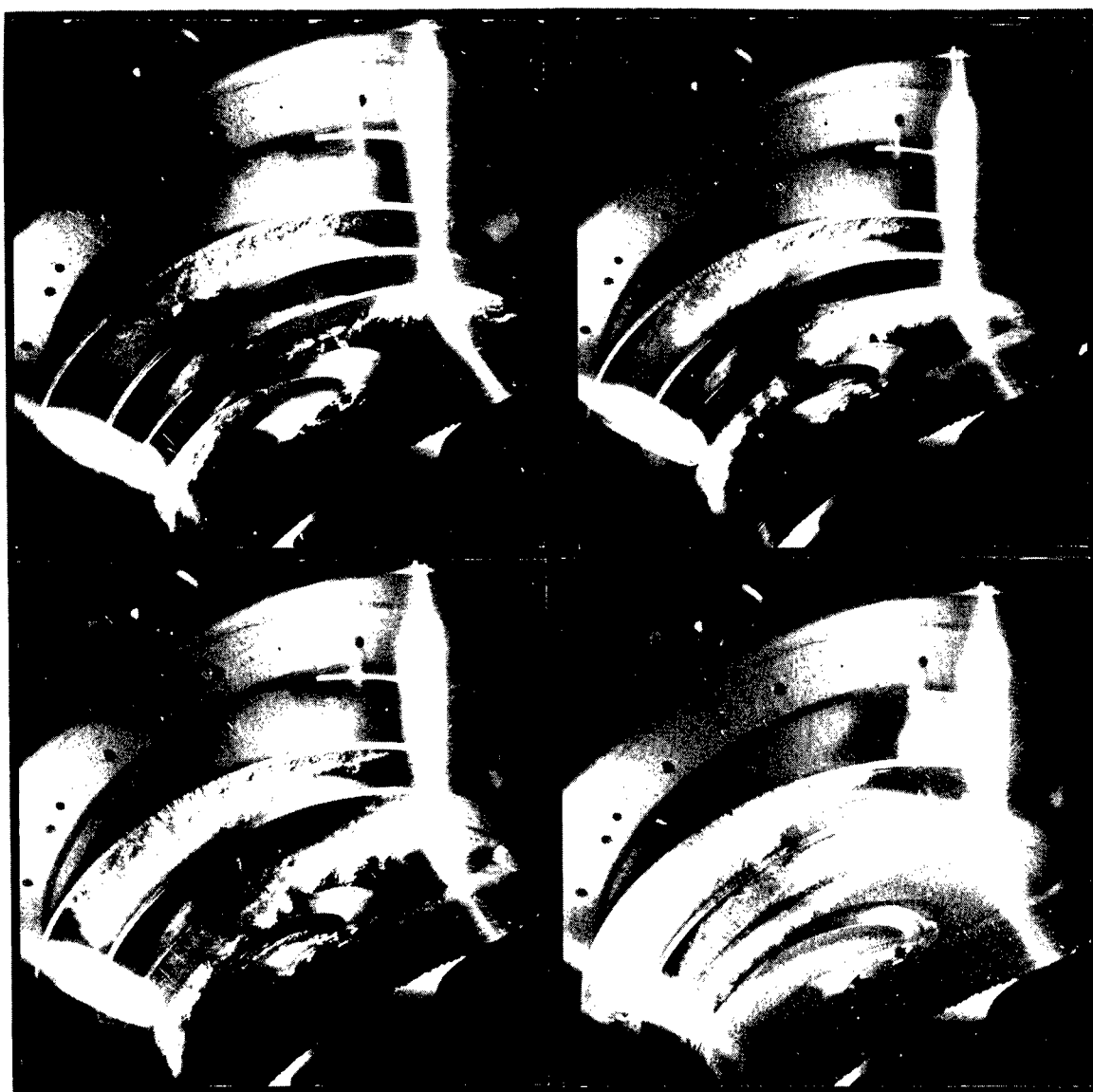
SPEED: 6375 RPM

NPSH - 35 FT

N_{SV} - 11,860

NPSH - 21 FT

N_{SV} - 17,420



NPSH - 15 FT

N_{SV} - 22,610

NPSH - 8 FT

N_{SV} - 36,200

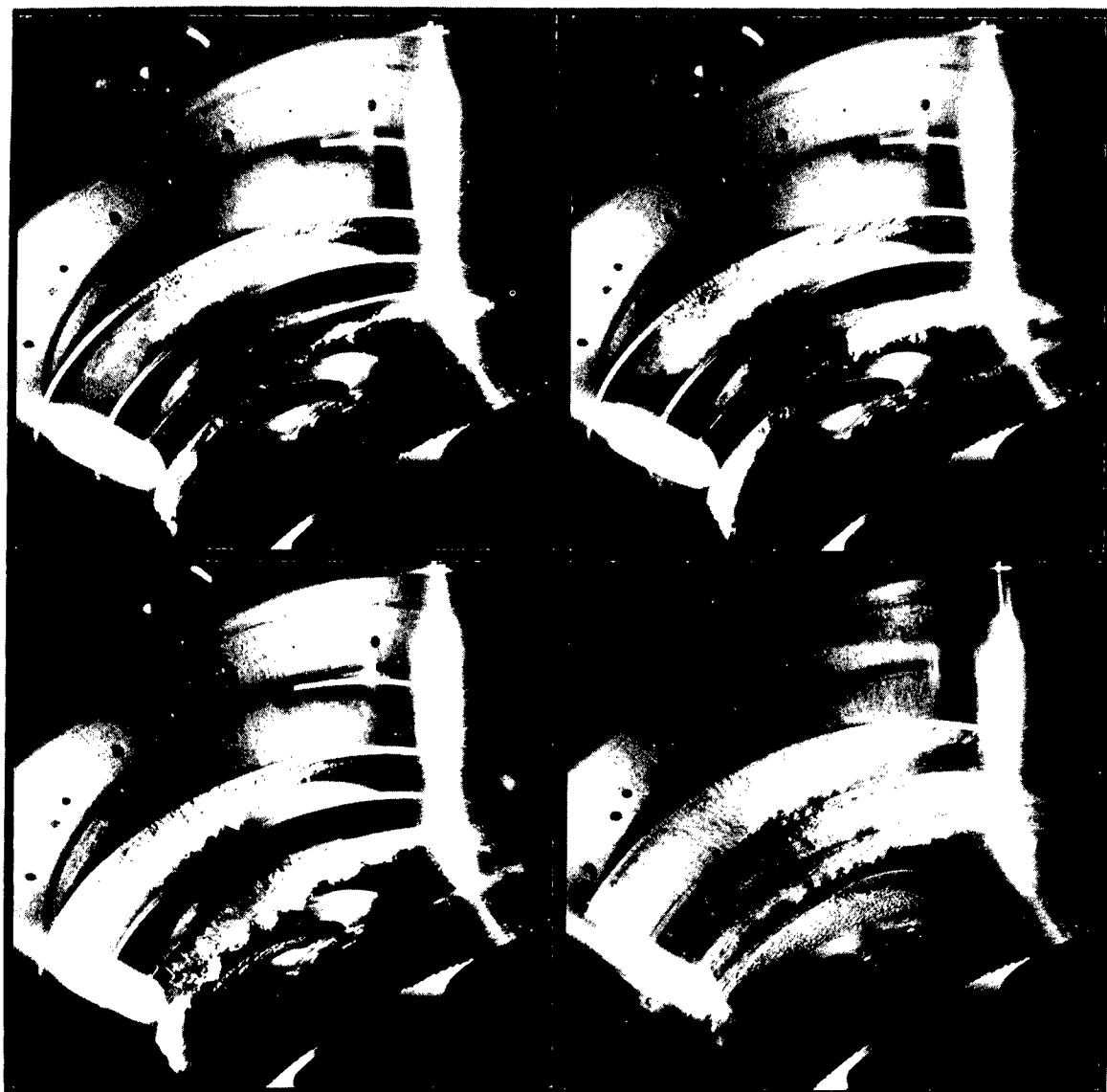
FIG 30

VISUAL CAVITATION PATTERNS AT 740 GPM AS FUNCTIONS OF NPSH

SPEED: 6375 RPM

NPSH - 35 FT
 N_{SV} - 12,020

NPSH - 26 FT
 N_{SV} - 15,020



NPSH - 15 FT
 N_{SV} - 22,760

NPSH - 8 FT
 N_{SV} - 36,400

FIG 31

NOISE AS FUNCTIONS OF NPSH FOR VARIOUS FLOW RATES

CONDITIONS:

NOMINAL TIP CLEARANCE: 0.030 INCH

FLUID: 100F WATER

SHAFT SPEED: 6375 RPM

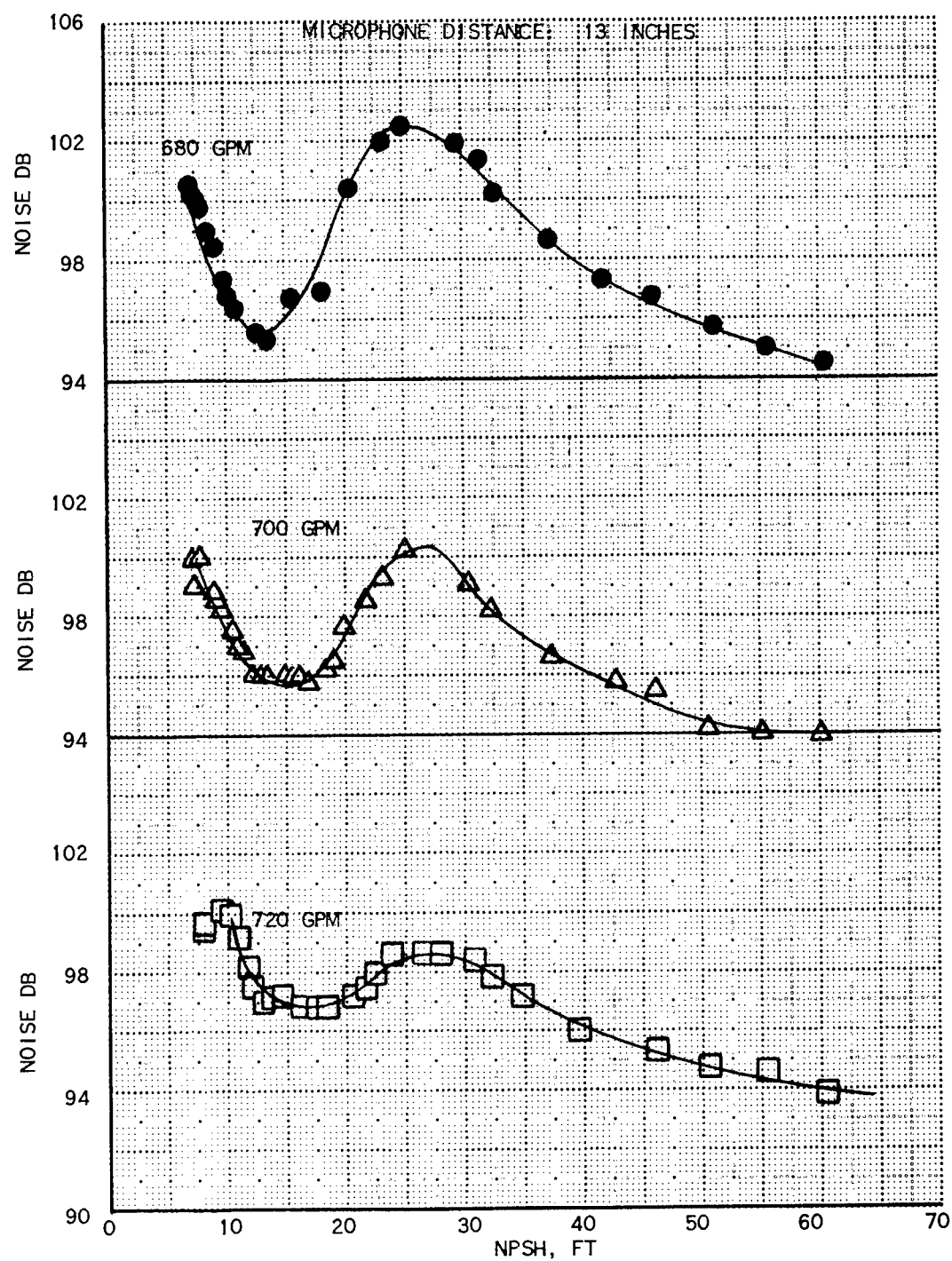


FIG 32

CROSSPLOT OF NOISE AND CAVITATION PERFORMANCE FOR 21 INCH MICROPHONE DISTANCE

CONDITIONS:

NOMINAL TIP CLEARANCE: 0.030 INCH

FLUID: 100% WATER

TESTD. 1001 WATER

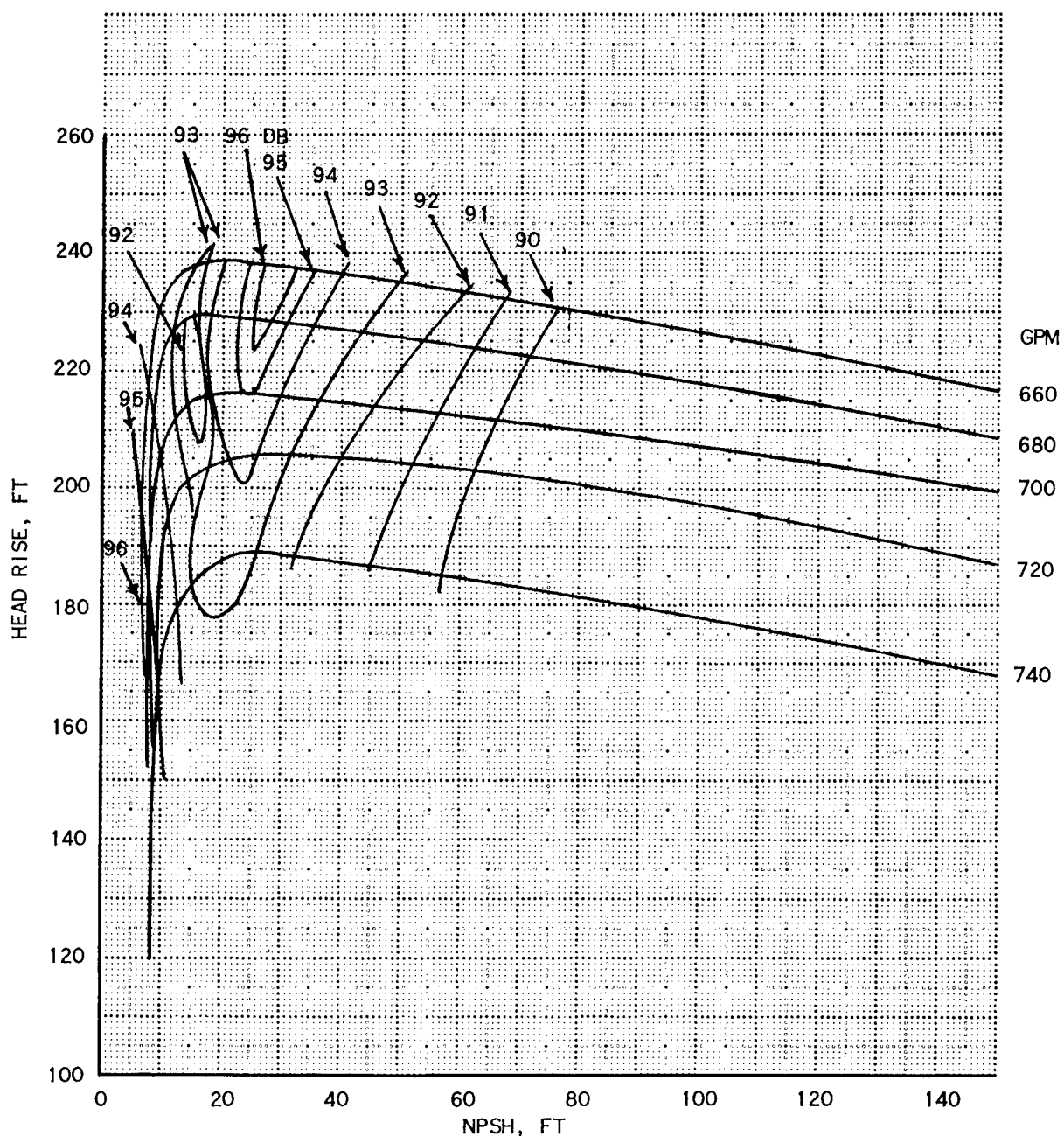


FIG 33

CROSSPLOT OF NOISE AND CAVITATION PERFORMANCE
FOR 13 INCH MICROPHONE DISTANCE

CONDITIONS:

NOMINAL TIP CLEARANCE: 0.030 INCH

FLUID: 100F WATER

SHAFT SPEED: 6375 RPM

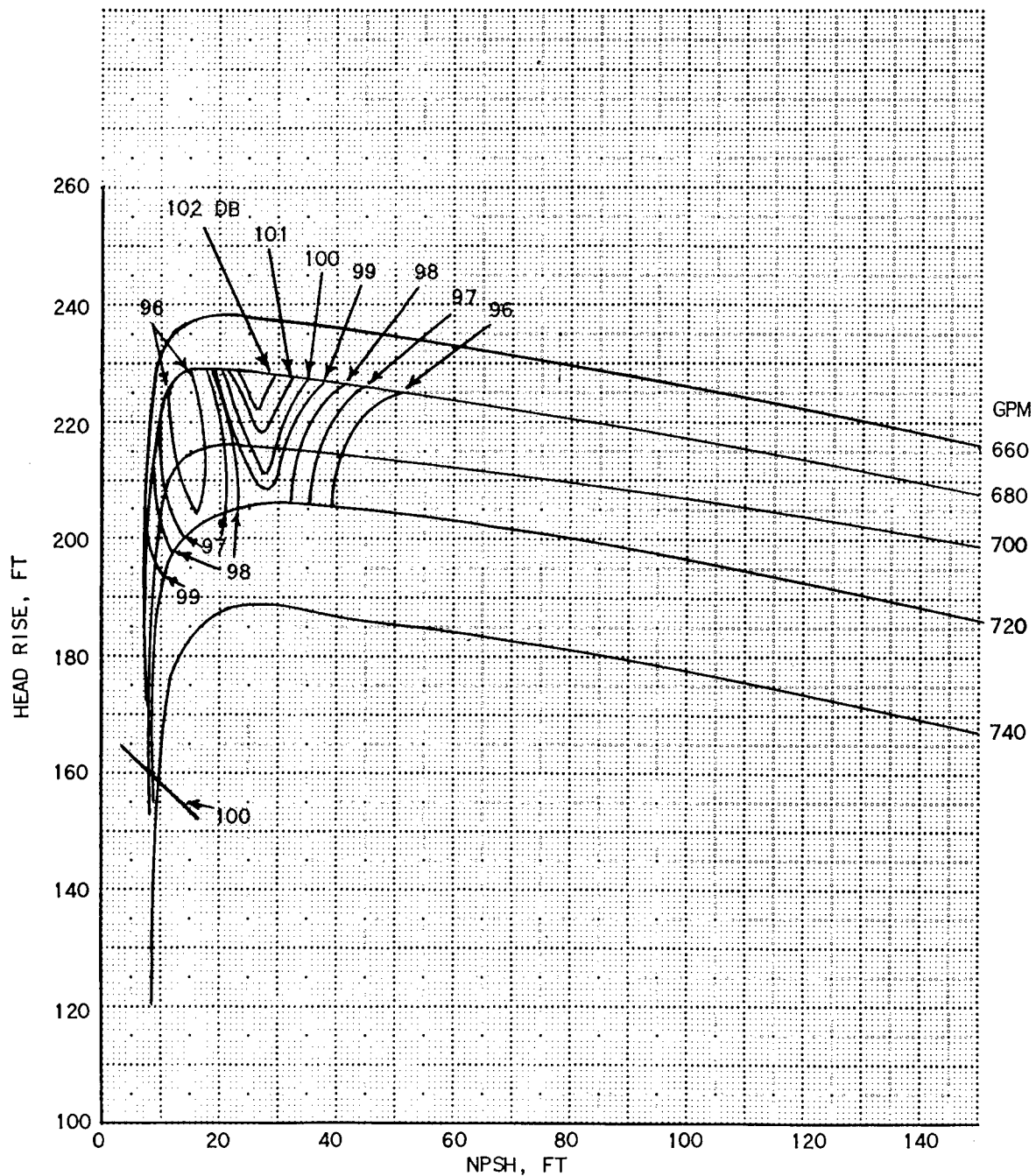


FIG 34

CALIBRATION OF HORIZONTAL AXIS ON THE 512 CHANNEL ANALYZER
DISPLAY

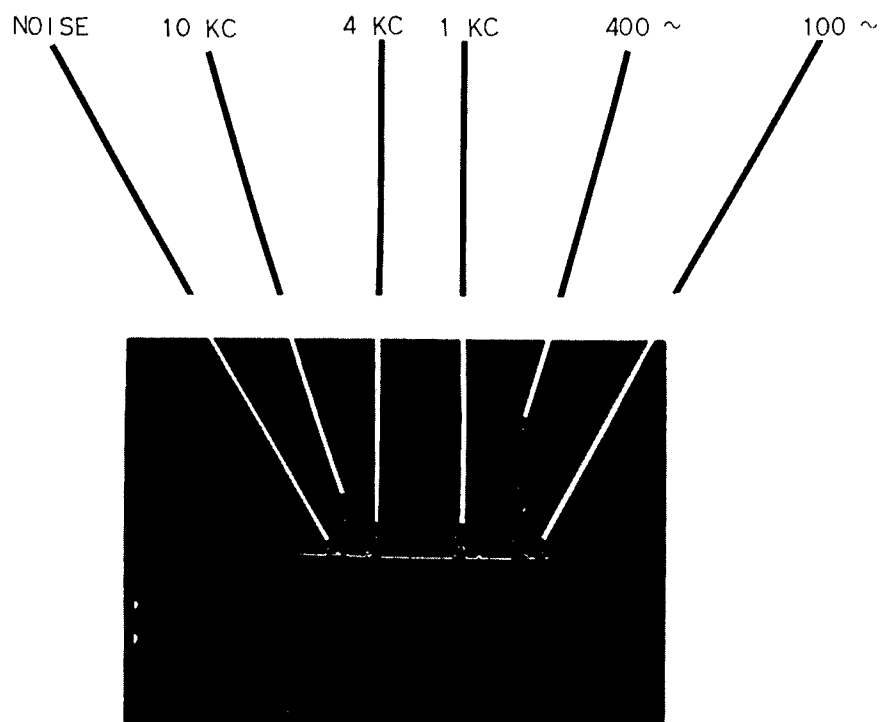


FIG 35

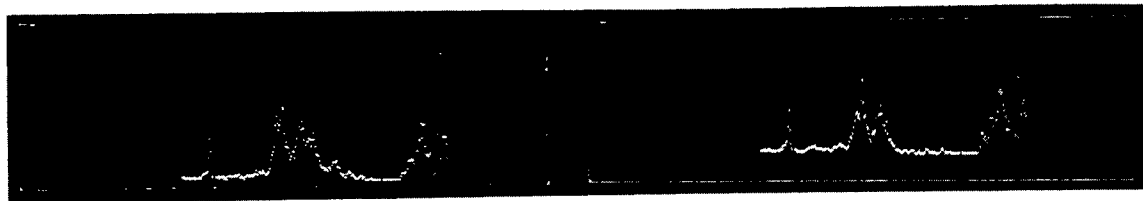
ACOUSTIC NOISE SPECTRA OF CAVITATING IMPELLER

CONDITIONS:

SPEED: 6375 RPM

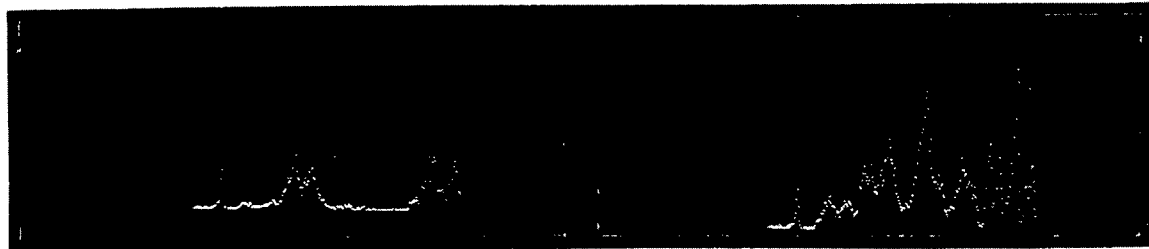
FLOW RATE: 700 GPM

DISCRIMINATOR AMPLITUDE: ~ 0.4



NPSH = 35 FT.

NPSH = 17.7 FT.

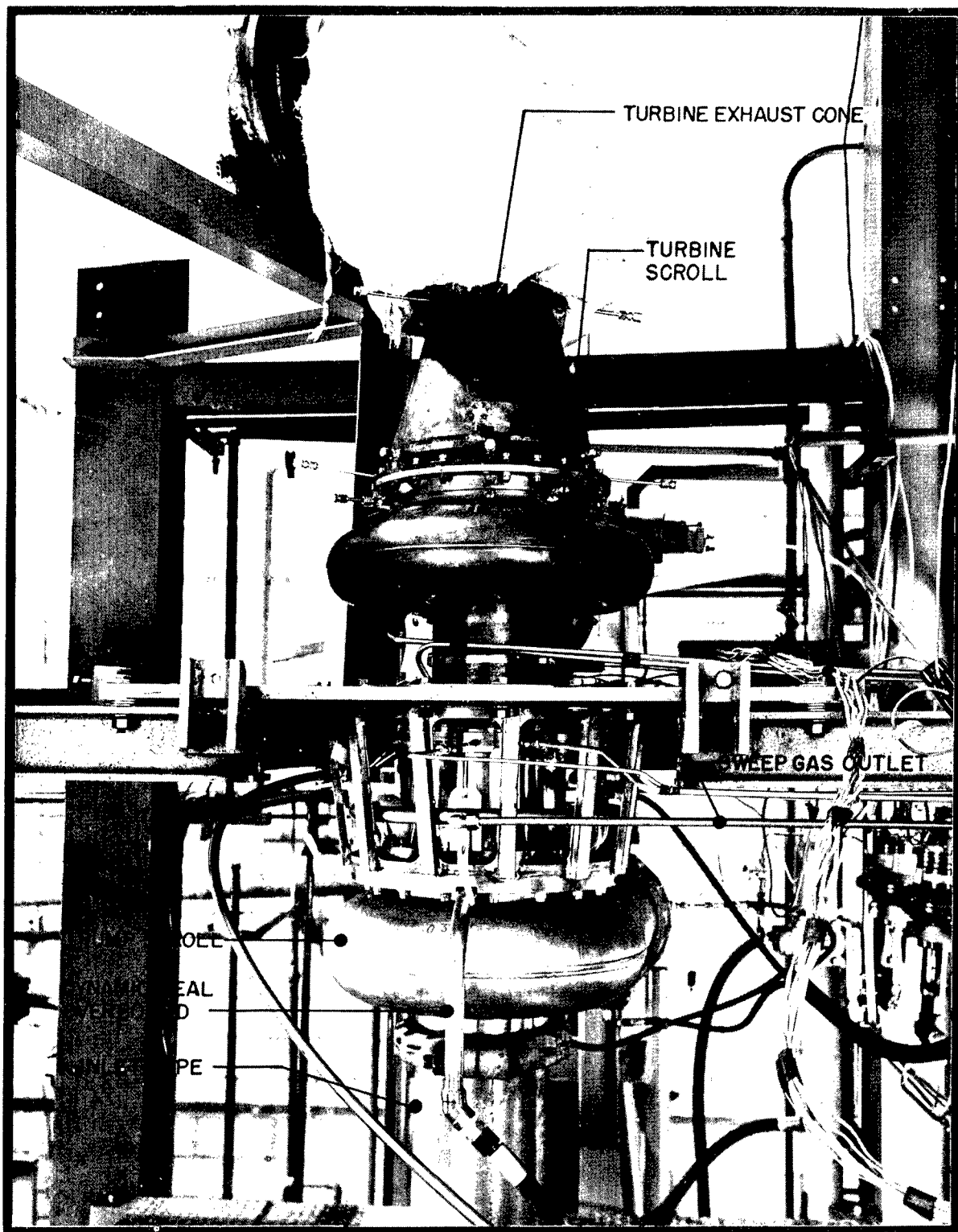


NPSH = 15 FT.

NPSH = 8 FT.

FIG 36

TURBOPUMP INSTALLED IN WATER PUMP TEST STAND



HYDRAULIC PERFORMANCE OF THE TURBOPUMP WITH THE RI-7C3 IMPELLER
IN WATER TEST

FIG 37

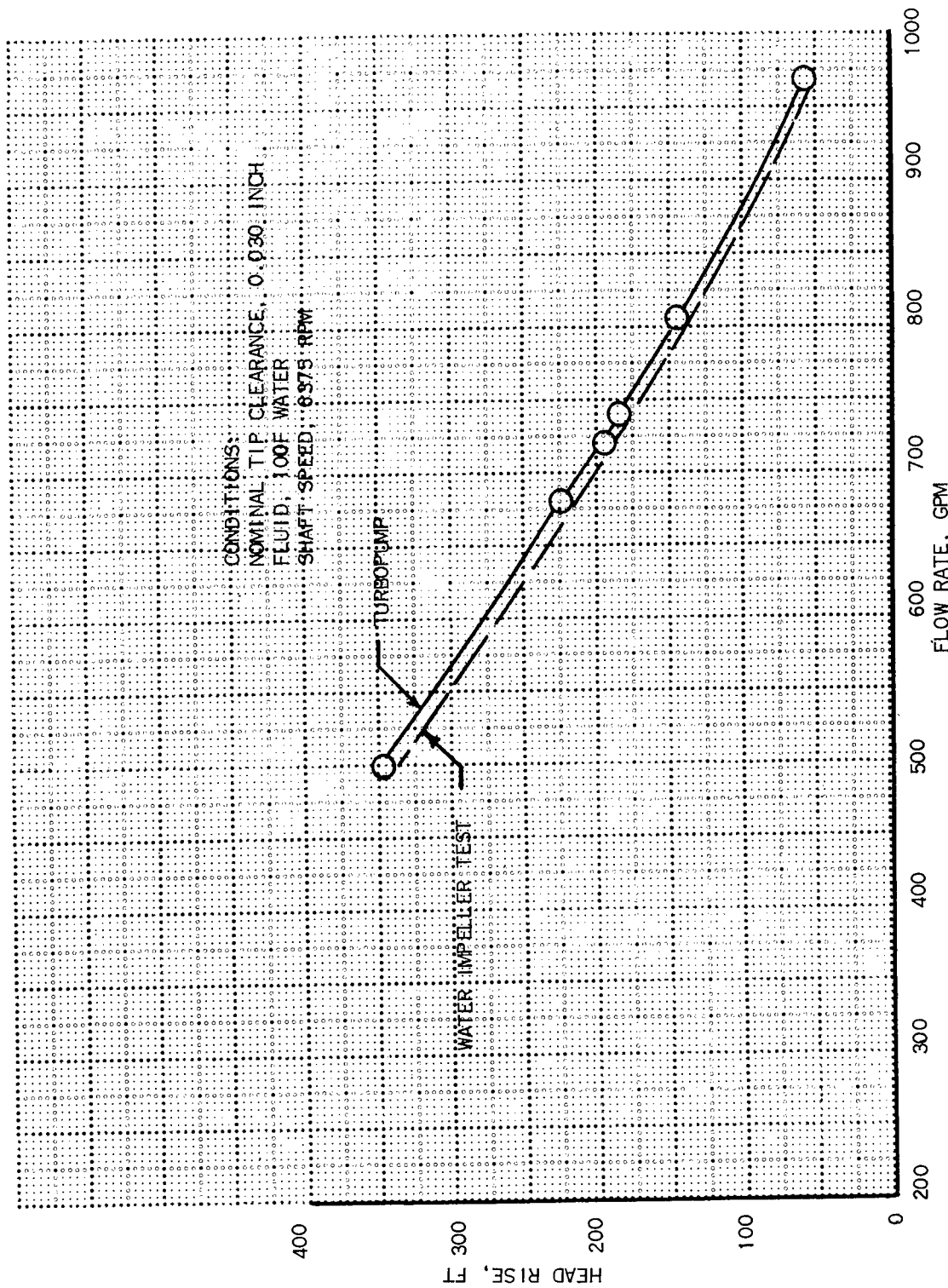


FIG 38
CAVITATION PERFORMANCE OF THE TURBOPUMP WITH THE
RI-7C3 IMPELLER IN WATER TEST

CONDITIONS:
NOMINAL TIP CLEARANCE, 0.030 INCH
FLUID, 100F WATER
SHAFT SPEED, 6375 RPM
- - - WATER IMPELLER TESTS
—○— TURBOPUMP

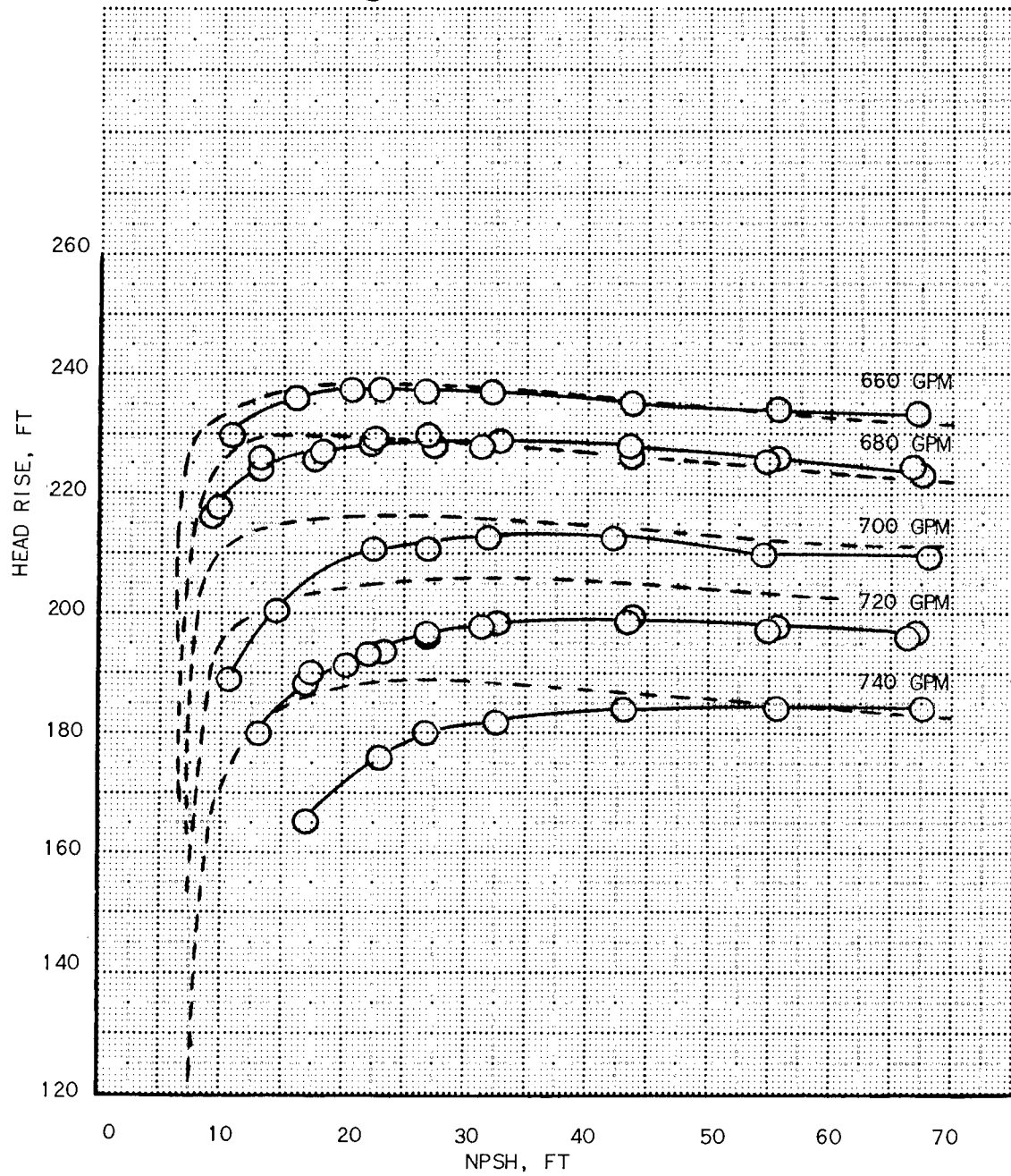


FIG 39

SETUP FOR SOUND READINGS IN WATER PUMP TEST STAND

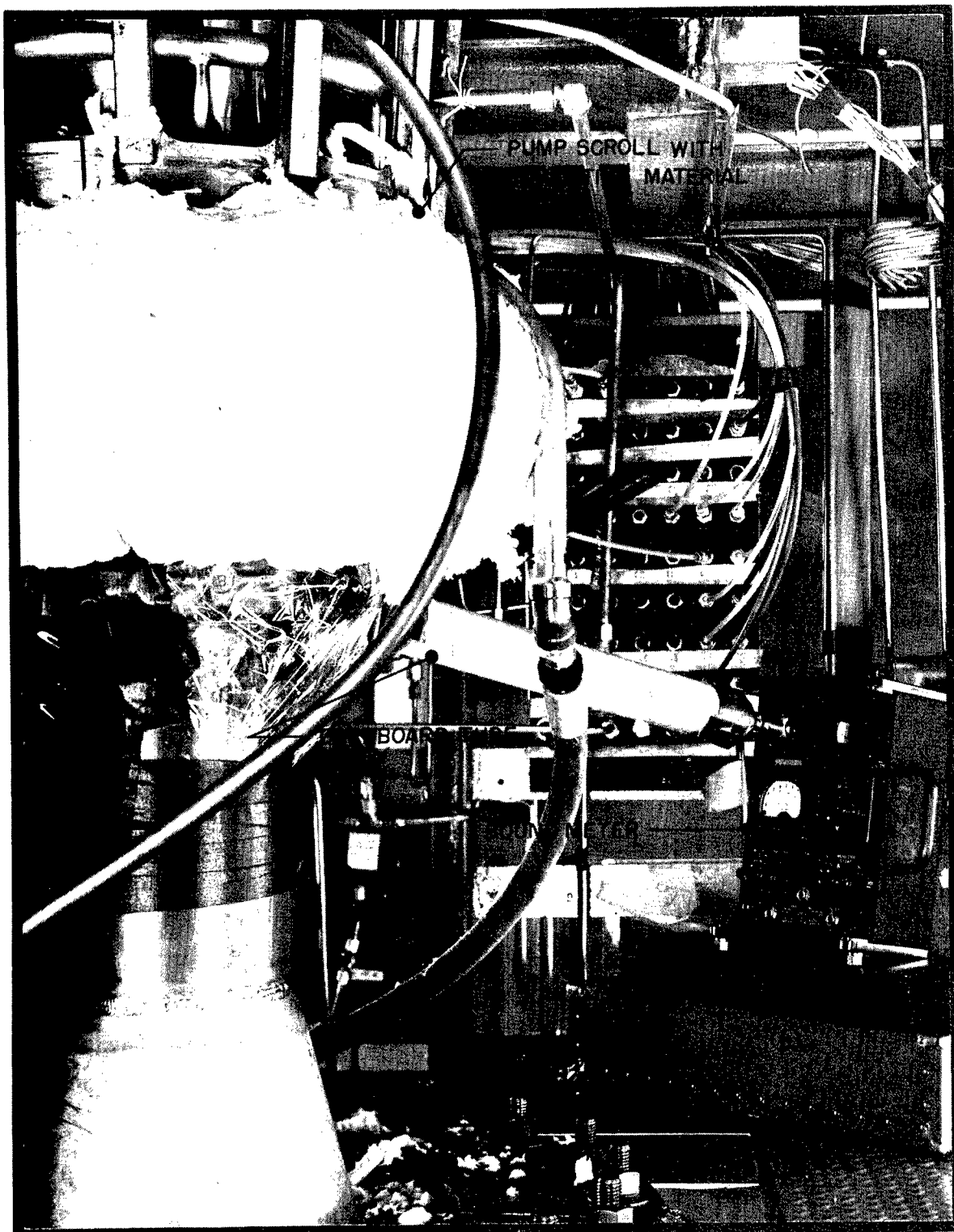


FIG 40
CROSS PLOT OF NOISE AND CAVITATION PERFORMANCE
FOR THE TURBOPUMP WATER TEST

CONDITIONS:
NOMINAL TIP CLEARANCE, 0.030 INCH
FLUID, 100F WATER
SHAFT SPEED, 6375 RPM

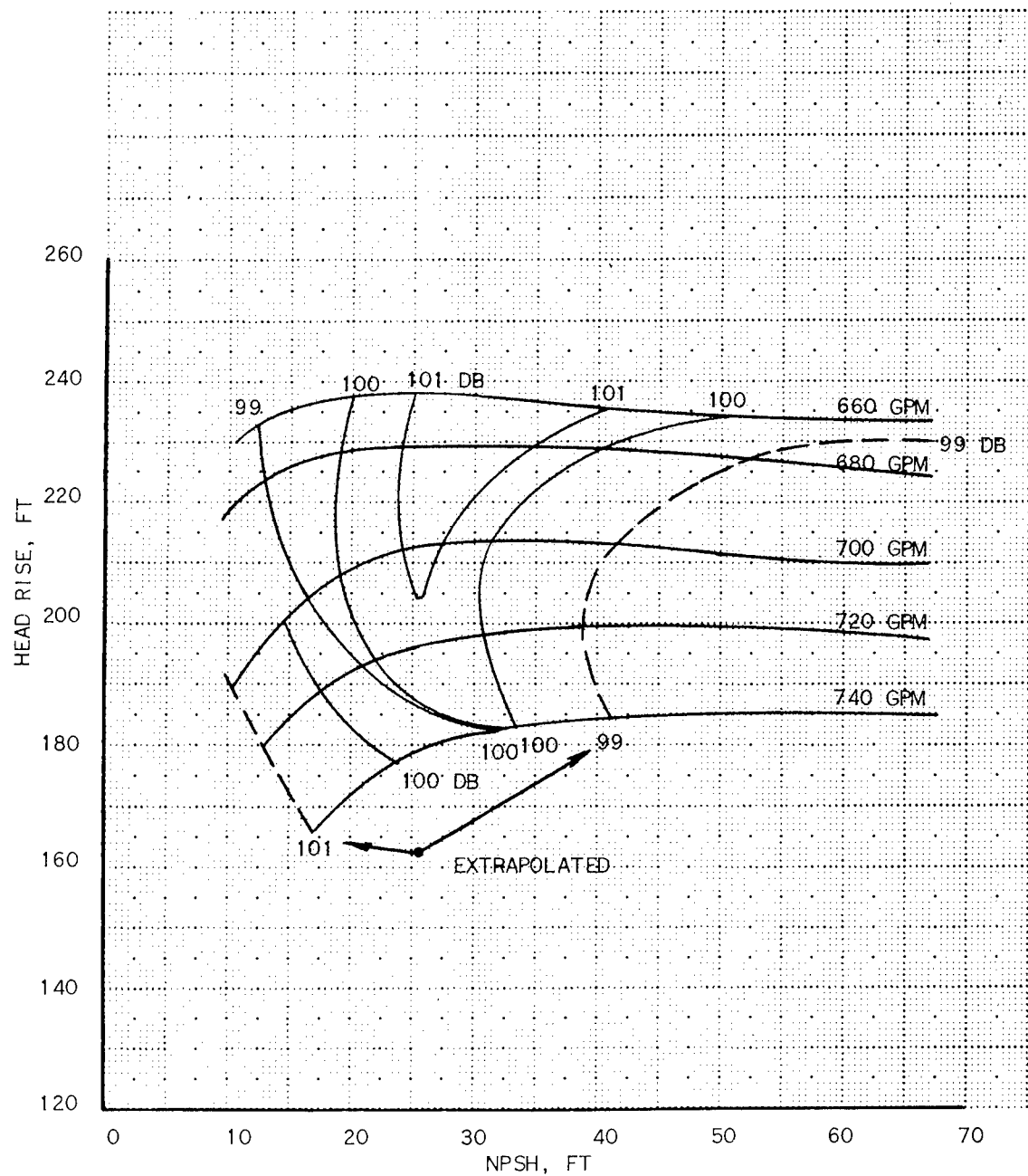


FIG 41

OVER-ALL VIEW OF LOCALIZED SCORING ON IMPELLER
AFTER WATER TEST IN TURBOPUMP

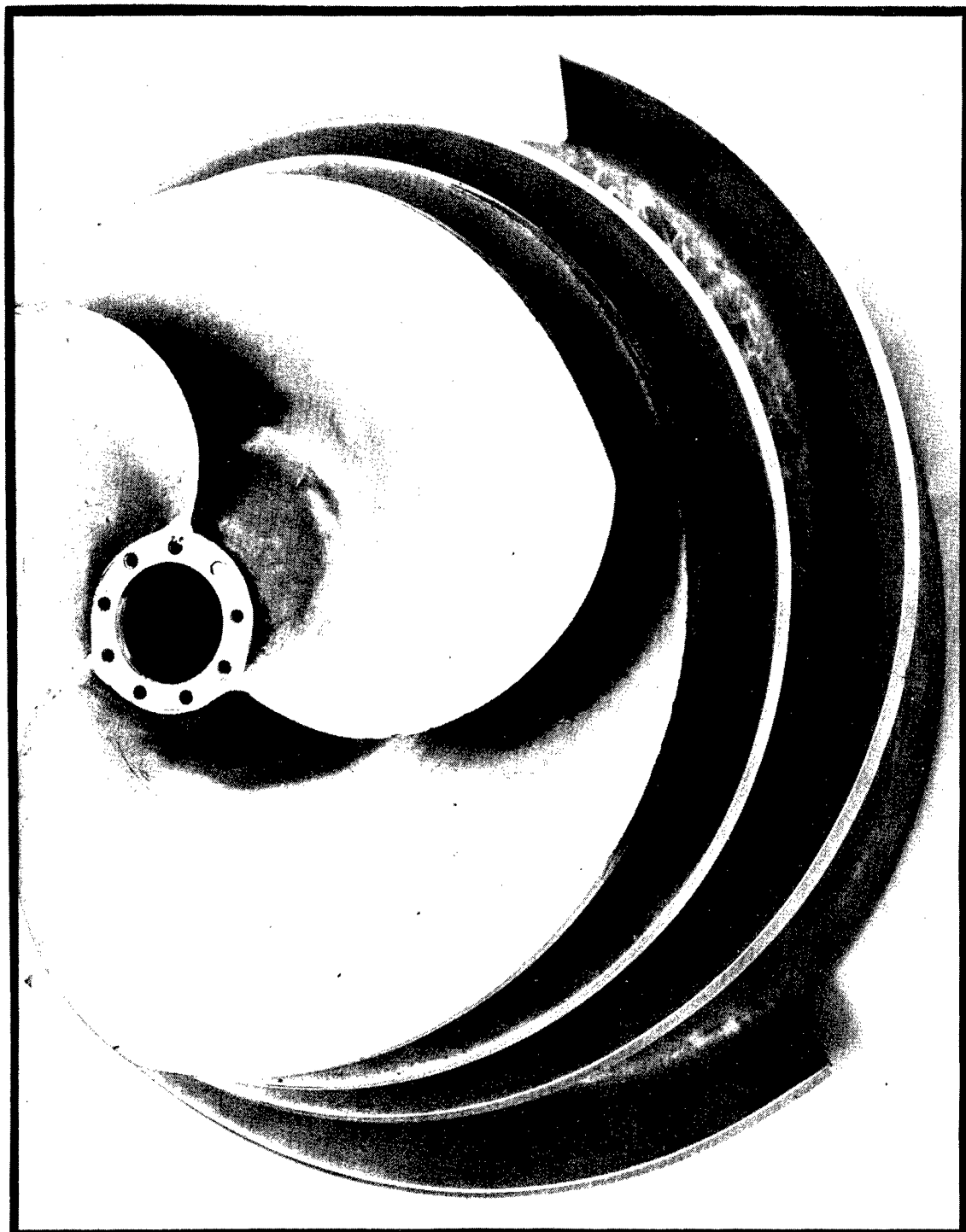


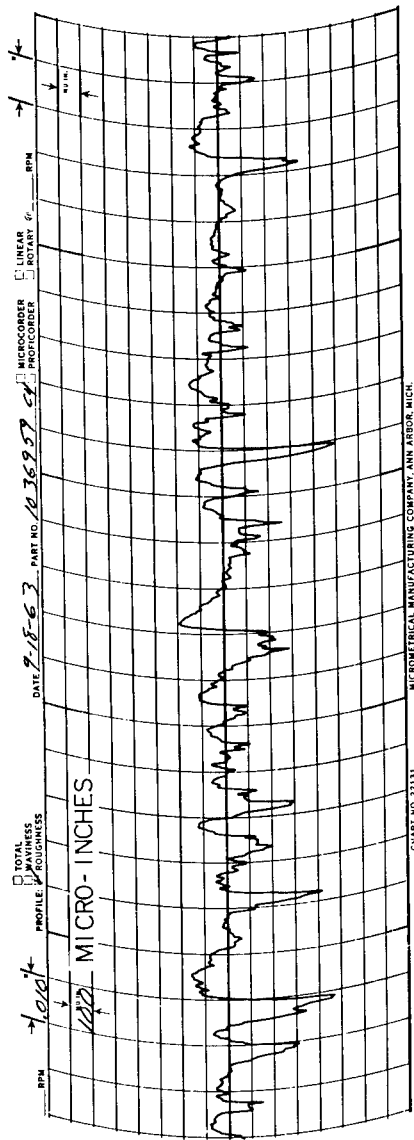
FIG 42
IMPELLER RUB MARKS IN TURBOPUMP SCROLL AFTER
WATER TEST



SURFACE ROUGHNESS MEASUREMENTS COMPARED AFTER

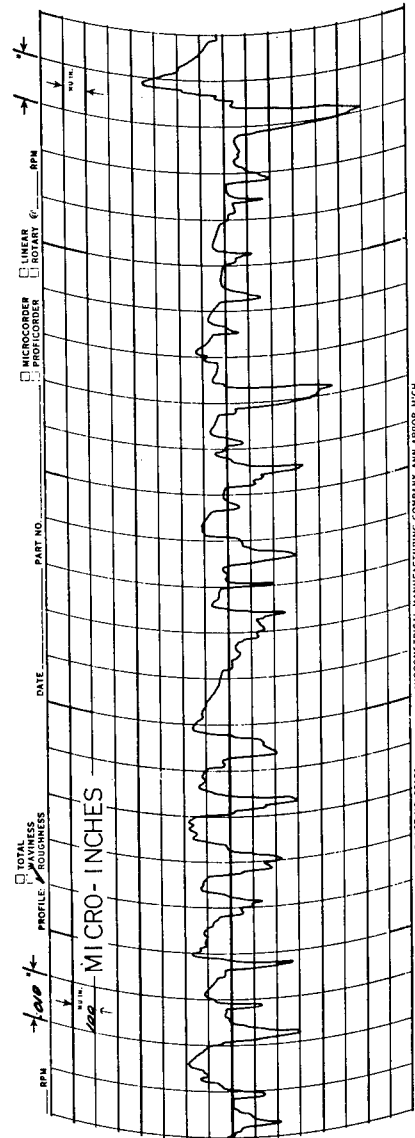
WATER TEST

BLADE 2, STATION 6, PRESSURE SIDE



BEFORE WATER TEST

FIG 43



AFTER WATER TEST

FIG 44

TURBOPUMP INSTALLED IN LIQUID METAL PUMP TEST STAND

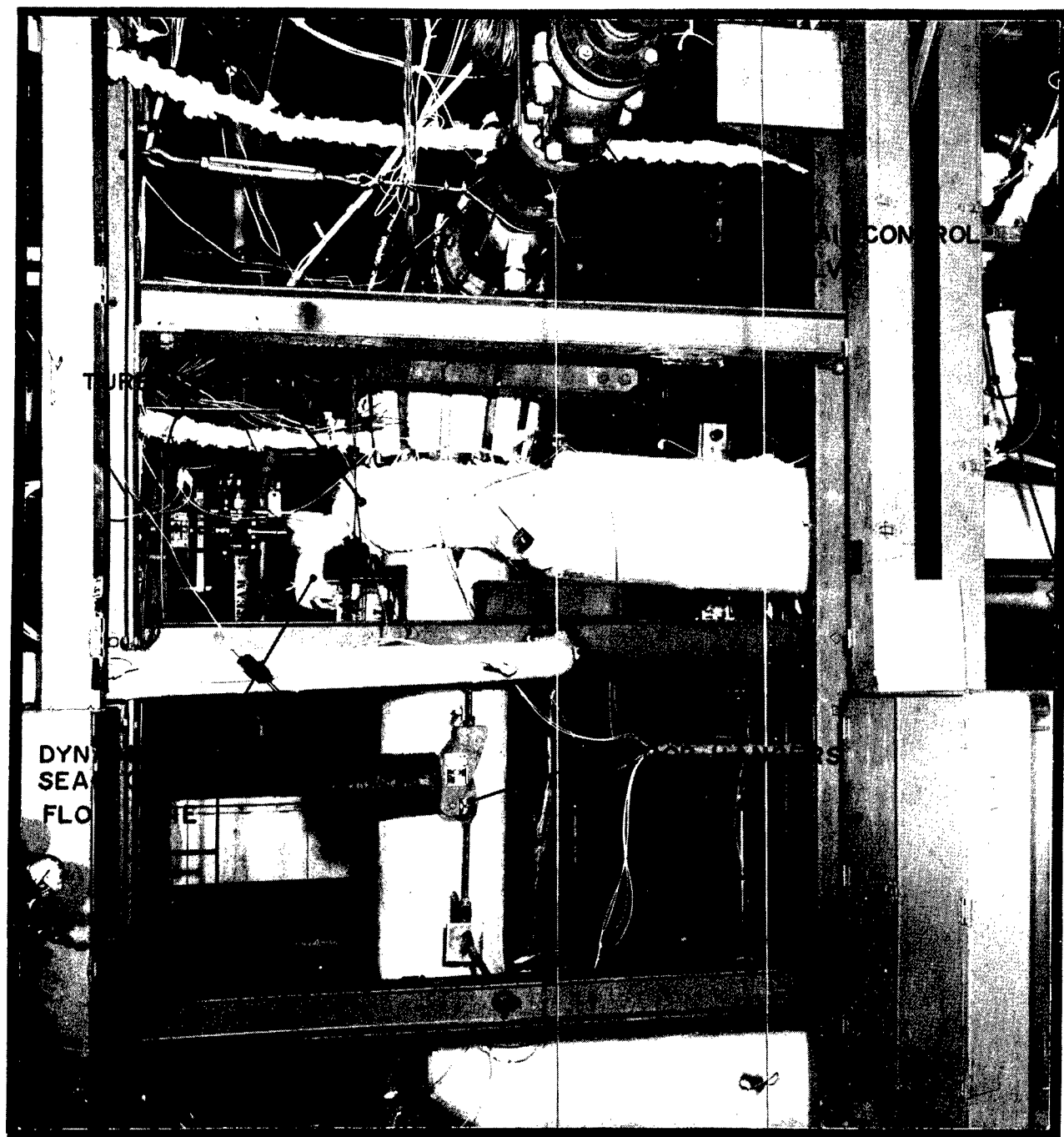


FIG 45

HYDRAULIC PERFORMANCE OF THE TURBOPUMP
WITH IMPELLER WATER TEST

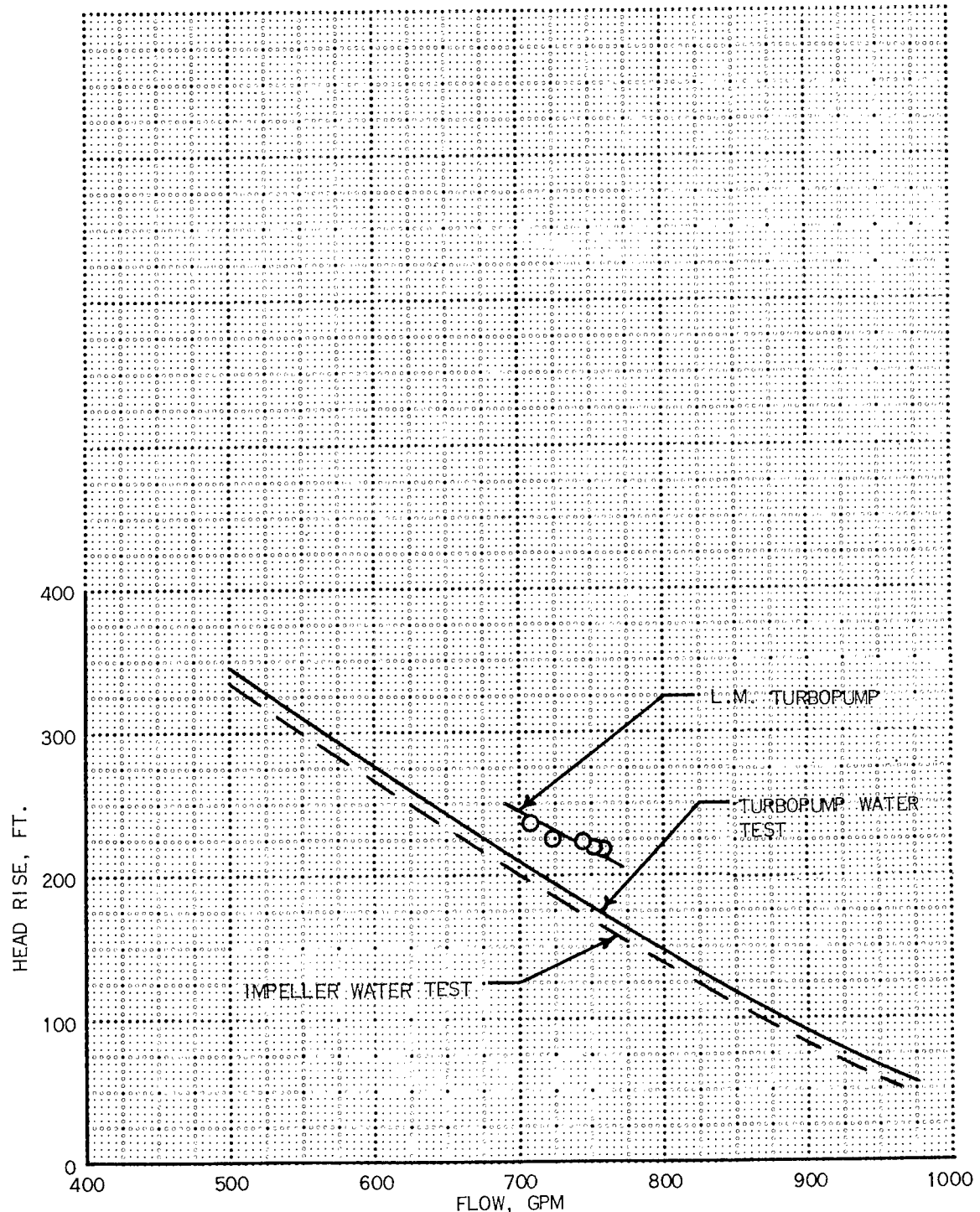


FIG 46

TURBOPUMP CAVITATION PERFORMANCE AND SOUND INTENSITY
IN 1400F POTASSIUM AT CONSTANT THROTTLE

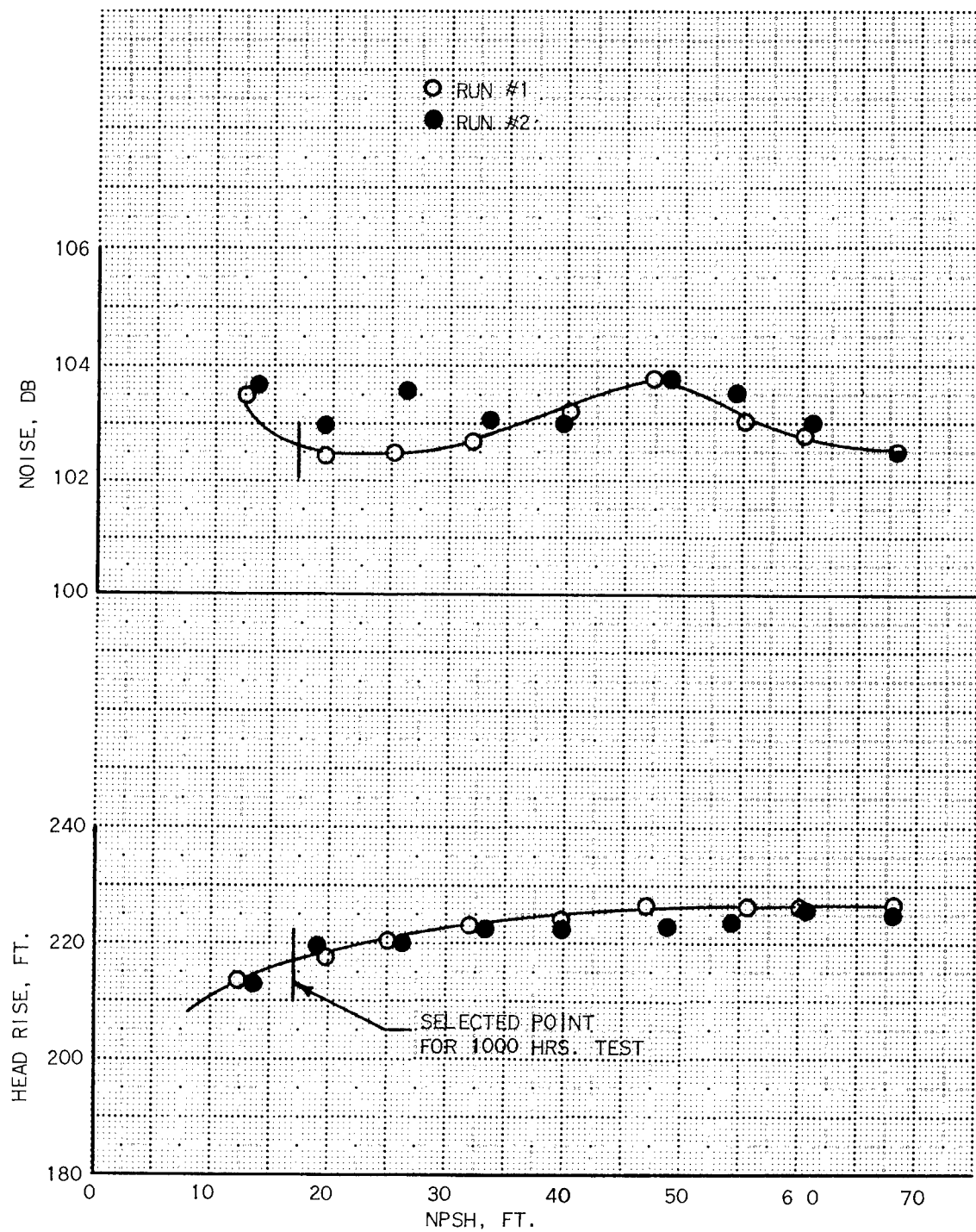
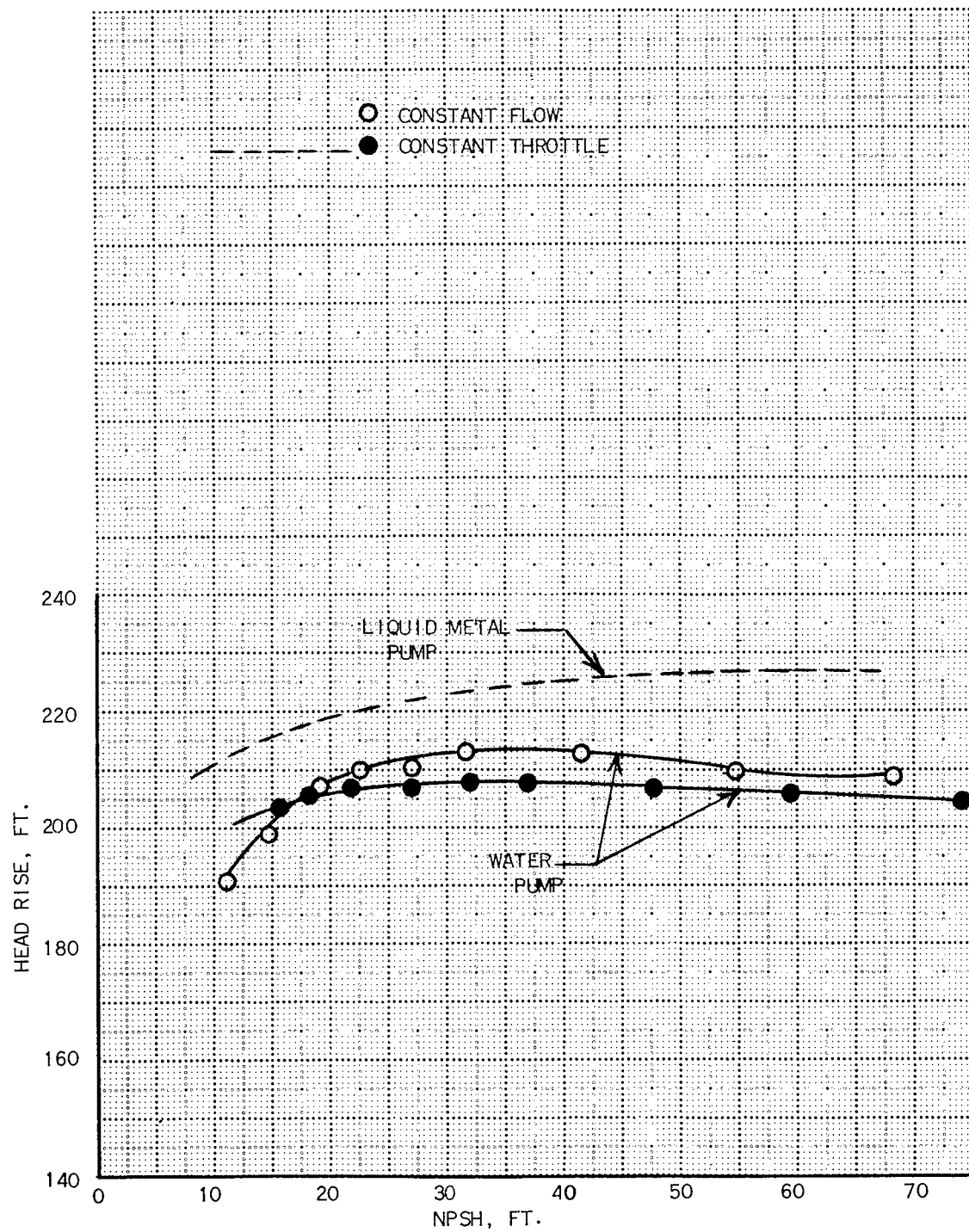


FIG 47

TURBOPUMP CAVITATION PERFORMANCE COMPARED AT CONSTANT
FLOW AND CONSTANT THROTTLE



PLLOT OF HOURLY READINGS FOR LIQUID METAL TEST OF TURBOPUMP

TEMPERATURE: 1400F SPEED: 6375 RPM

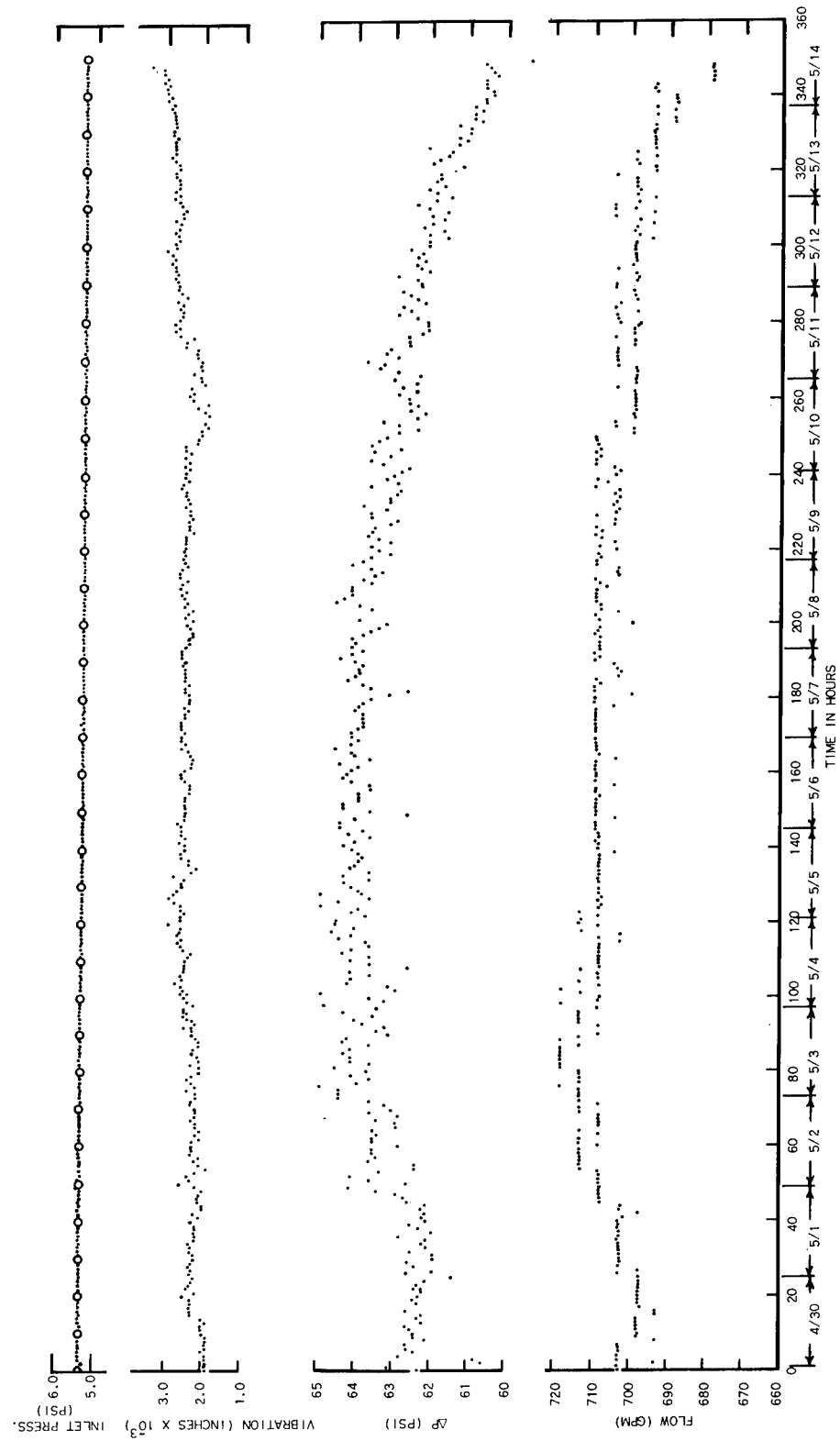


FIG 49

IMPELLER DAMAGE AS SEEN AFTER LIQUID METAL TEST

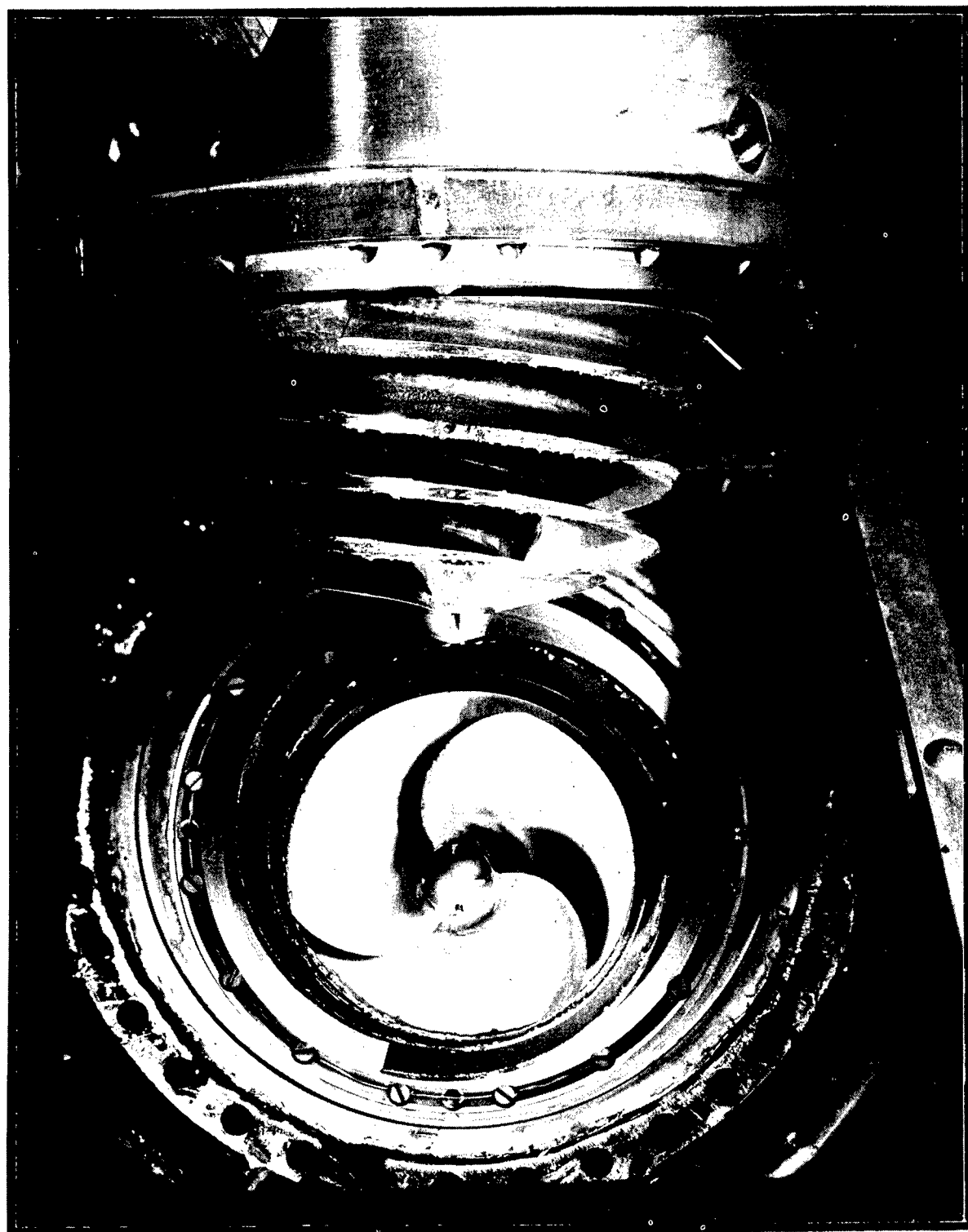


FIG 50

OVER-ALL VIEW OF IMPELLER INLET

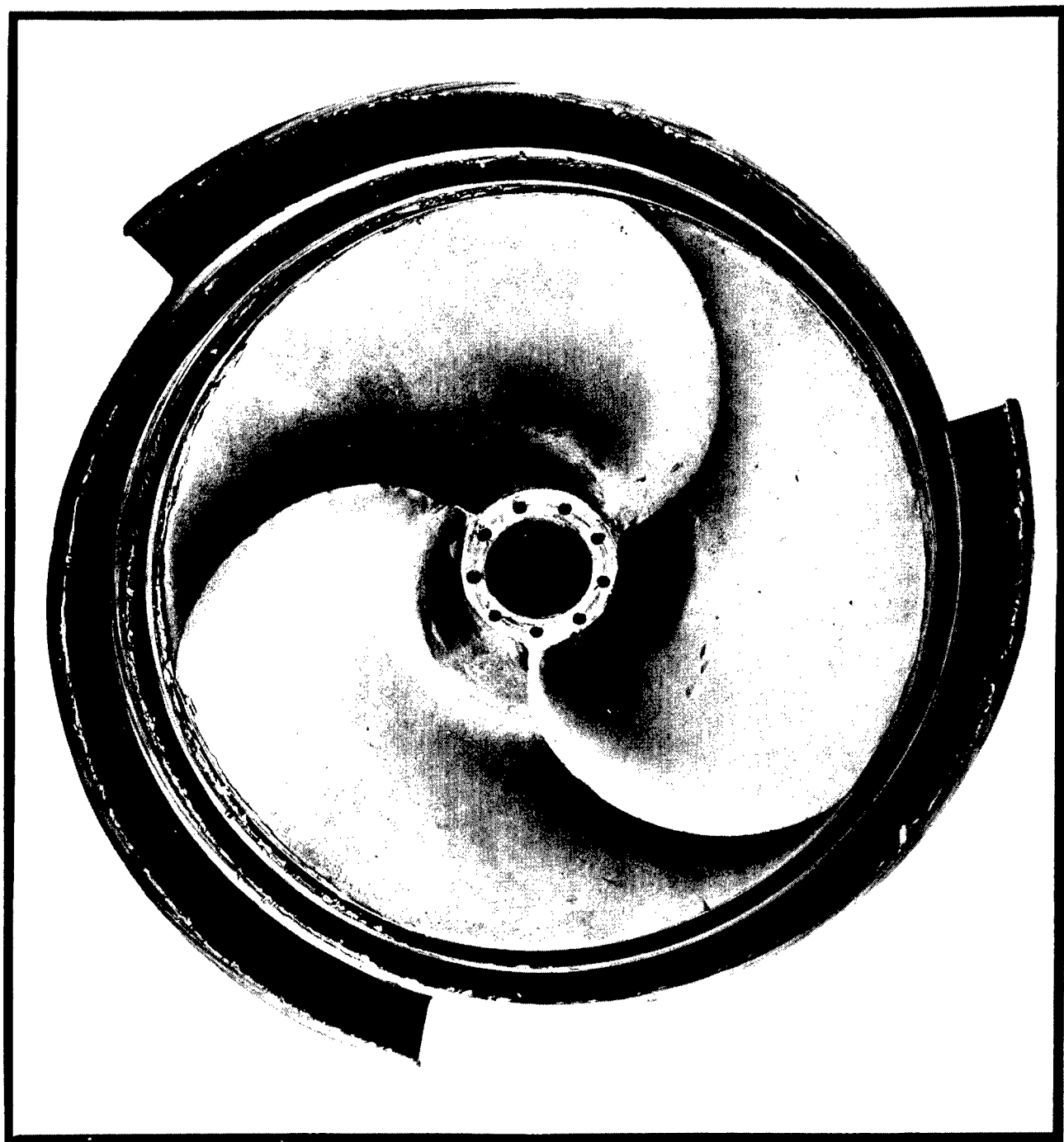


FIG 51

RUB MARKS ON SCROLL ADAPTER



FIG 52

LOWER DYNAMIC SEAL (POSTTEST)

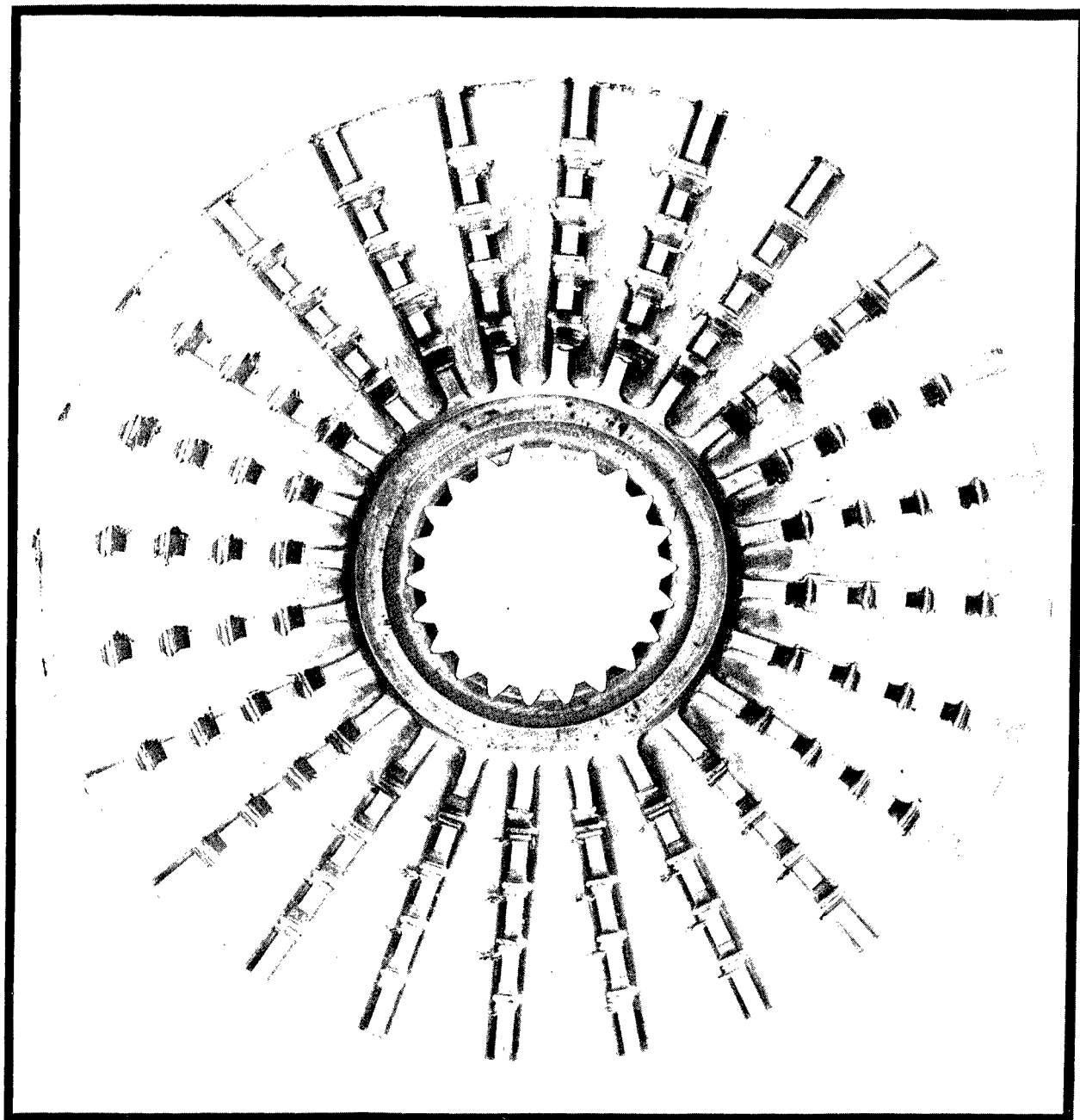
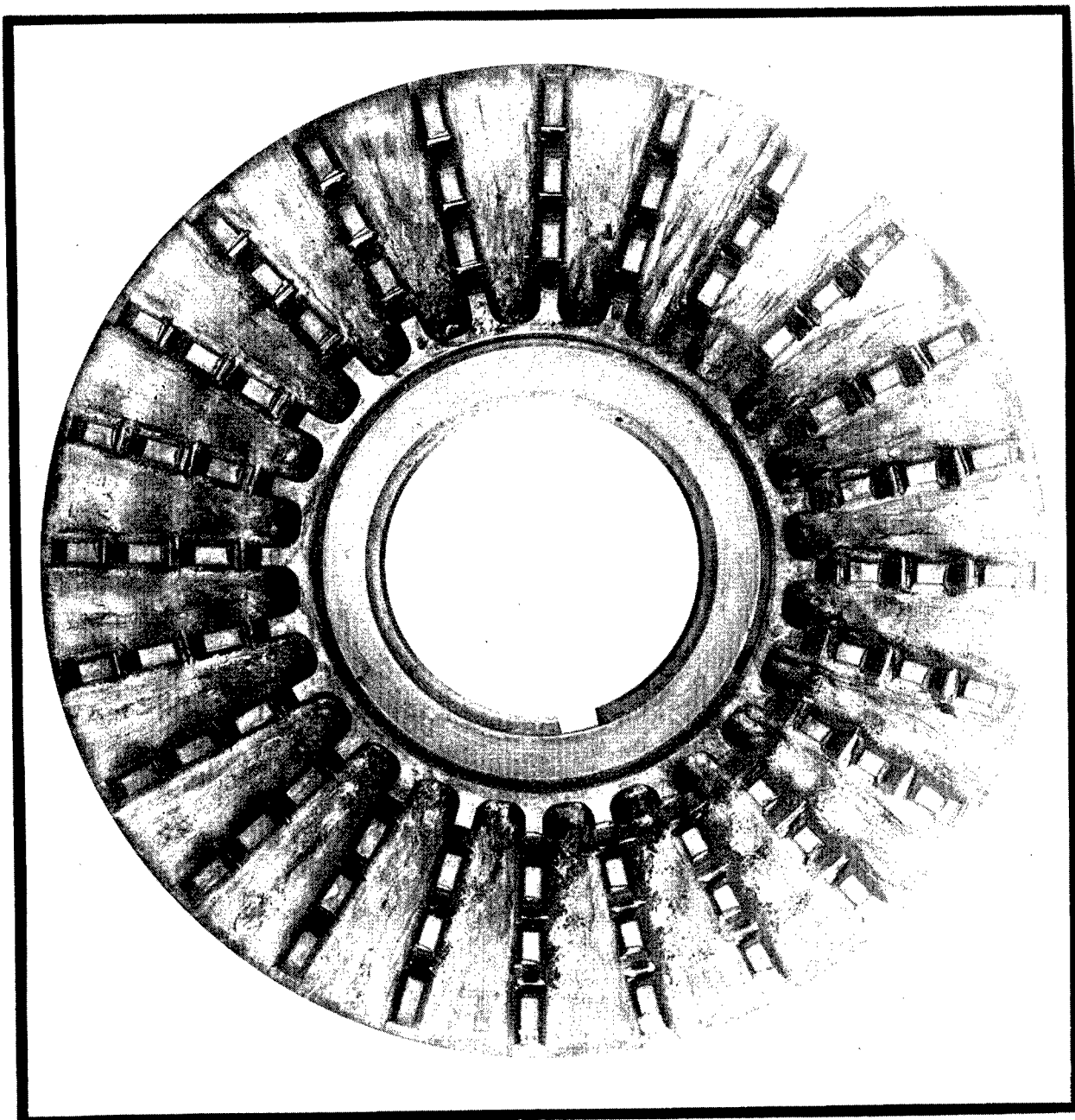


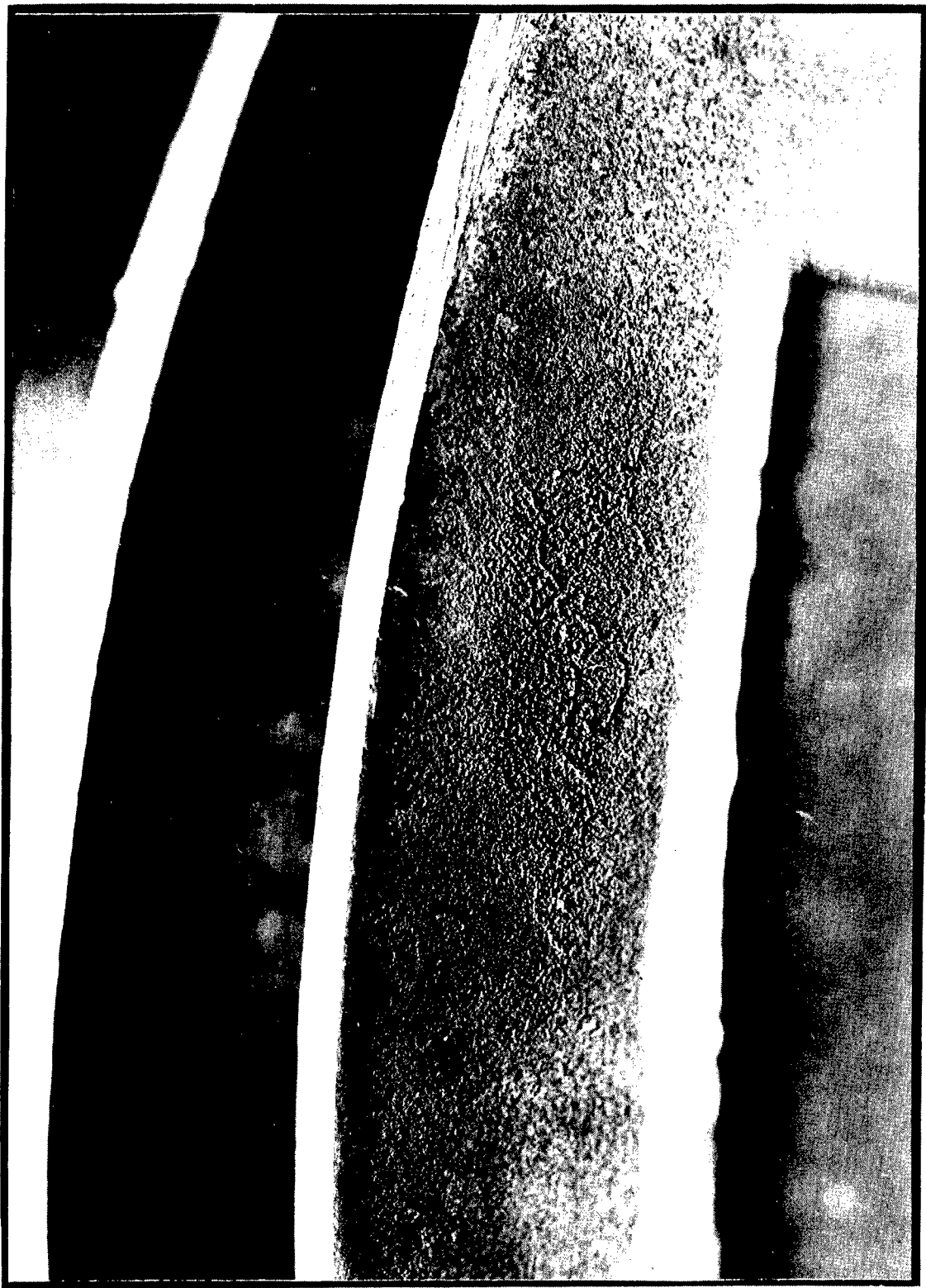
FIG 53

UPPER DYNAMIC SEAL (POSTTEST)



CAVITATION DAMAGE ON VANE 1

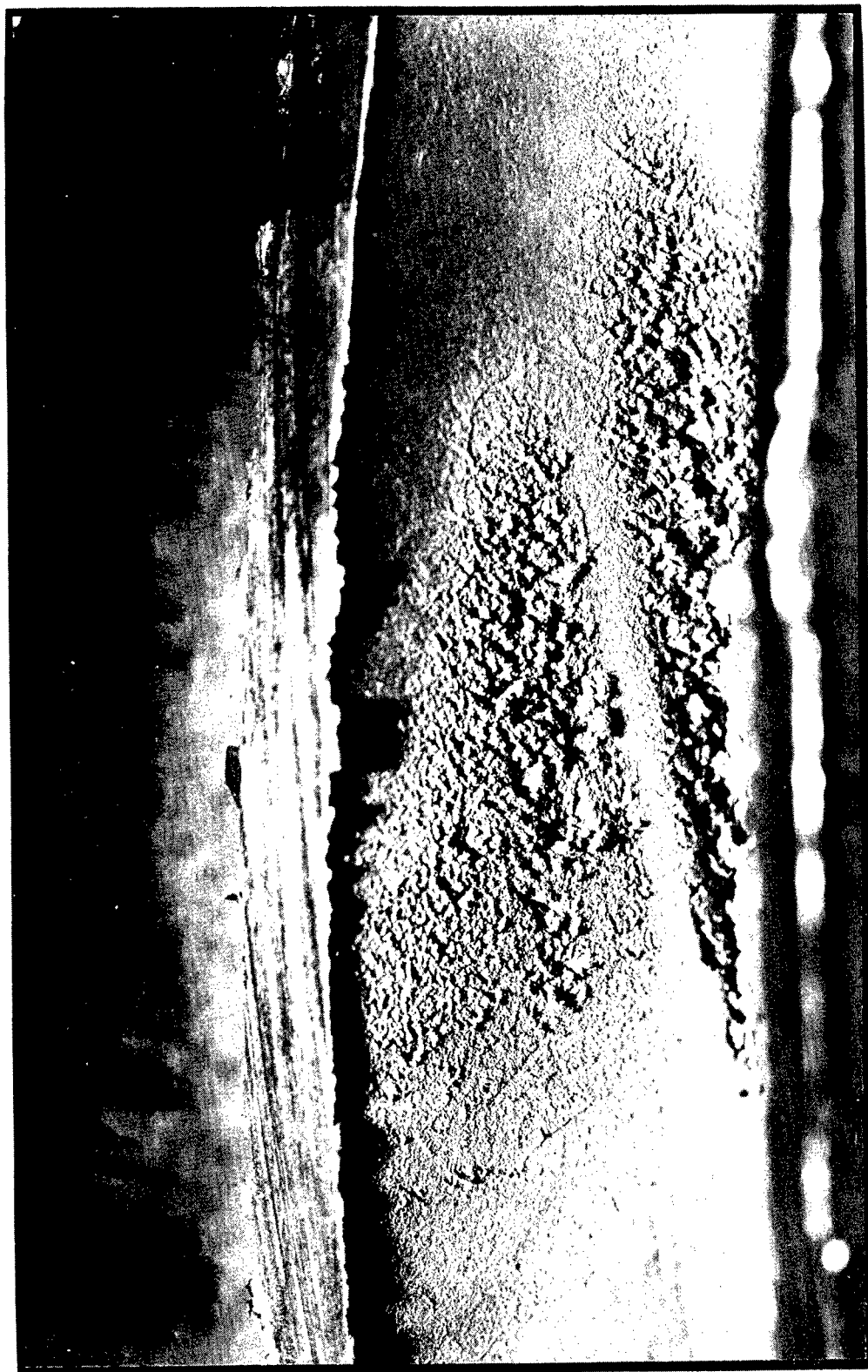
FIG 54



SURFACE AT $\sim 6\times$

CAVITATION DAMAGE ON VANE 2

FIG 55



SURFACE AT $\sim 6\times$

CAVITATION DAMAGE ON VANE 3

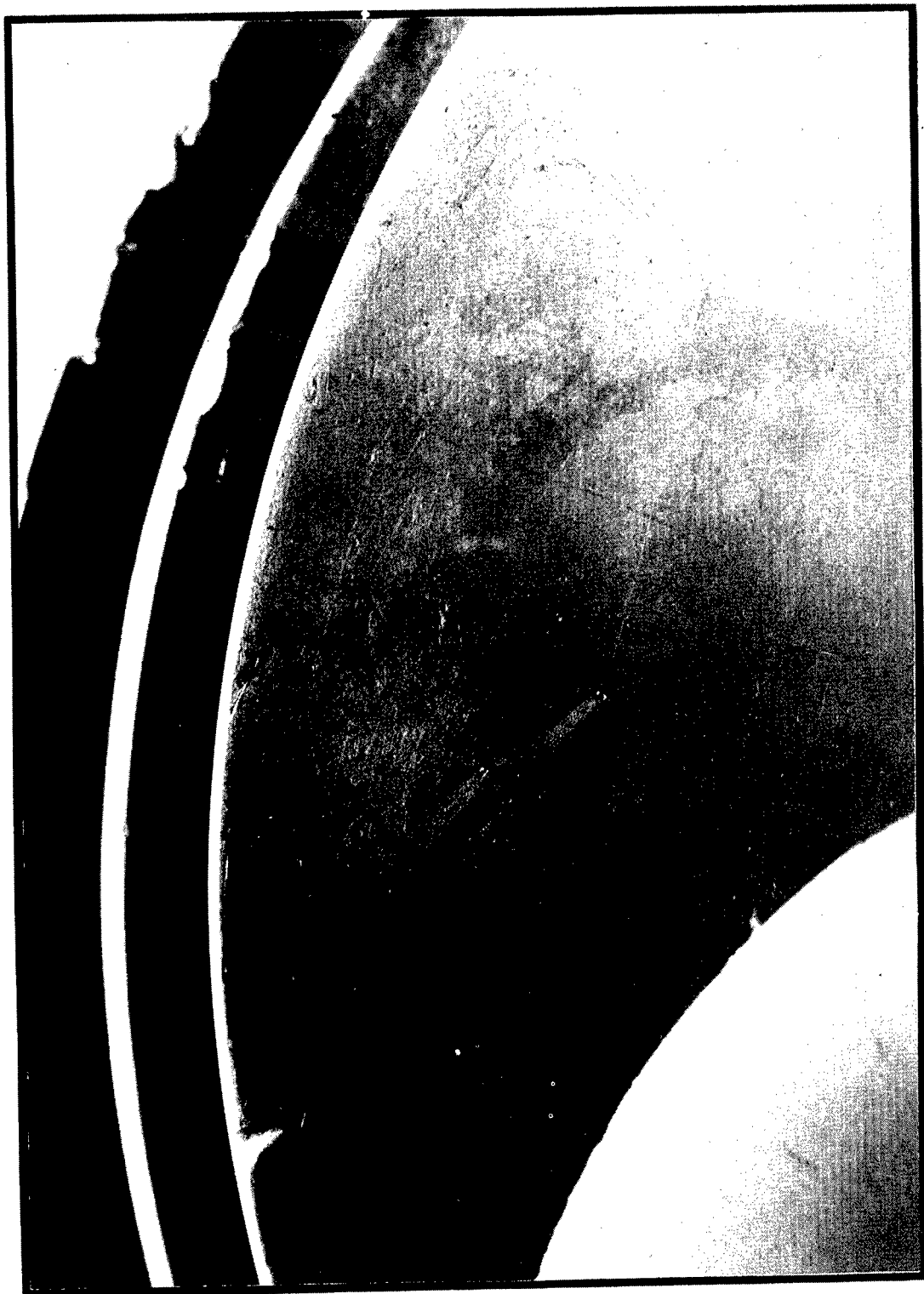
FIG 56



SURFACE A1 6X

SECONDARY CAVITATION DAMAGE ON VANE 2

FIG 57

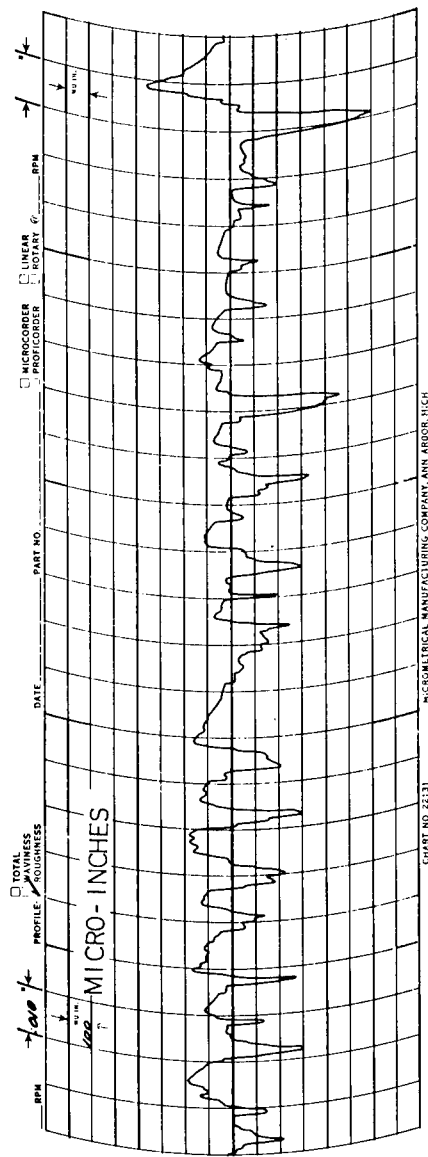


SURFACE AT 4X

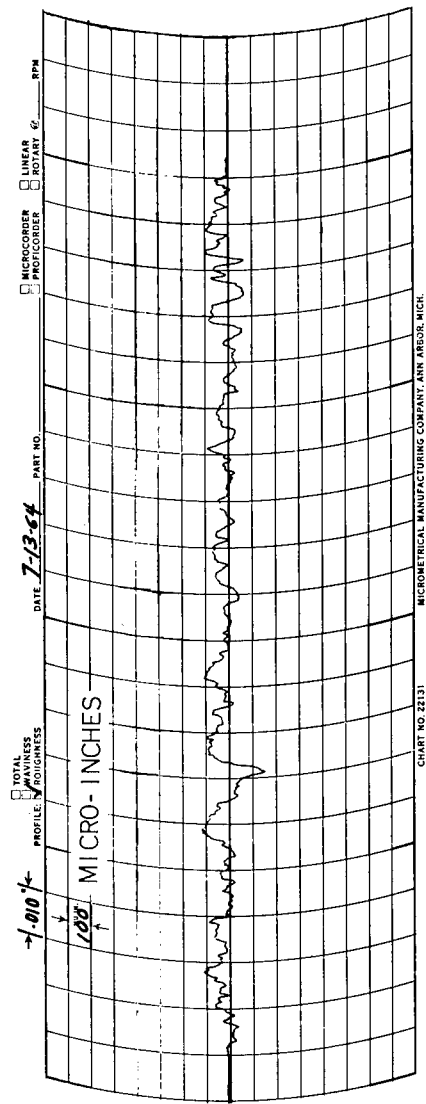
SURFACE ROUGHNESS MEASUREMENTS COMPARED AFTER

LIQUID METAL TEST

BLADE 2, STATION 6, PRESSURE SIDE



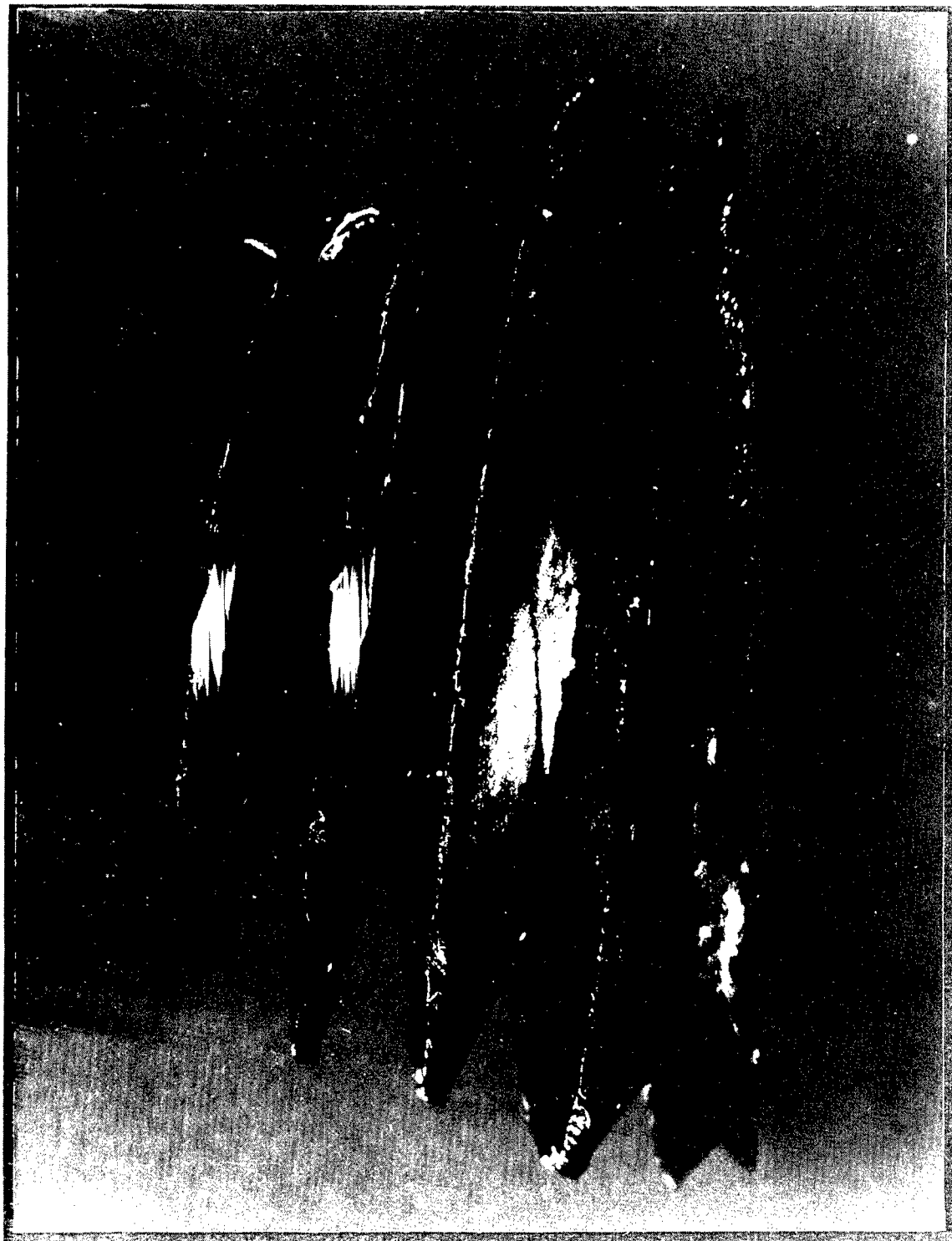
PRETEST



POSTTEST

FIG 58

FIG 59



ZYGLO INSPECTION OF POSTTEST IMPELLER (PRESSURE SIDE)

FIG 60

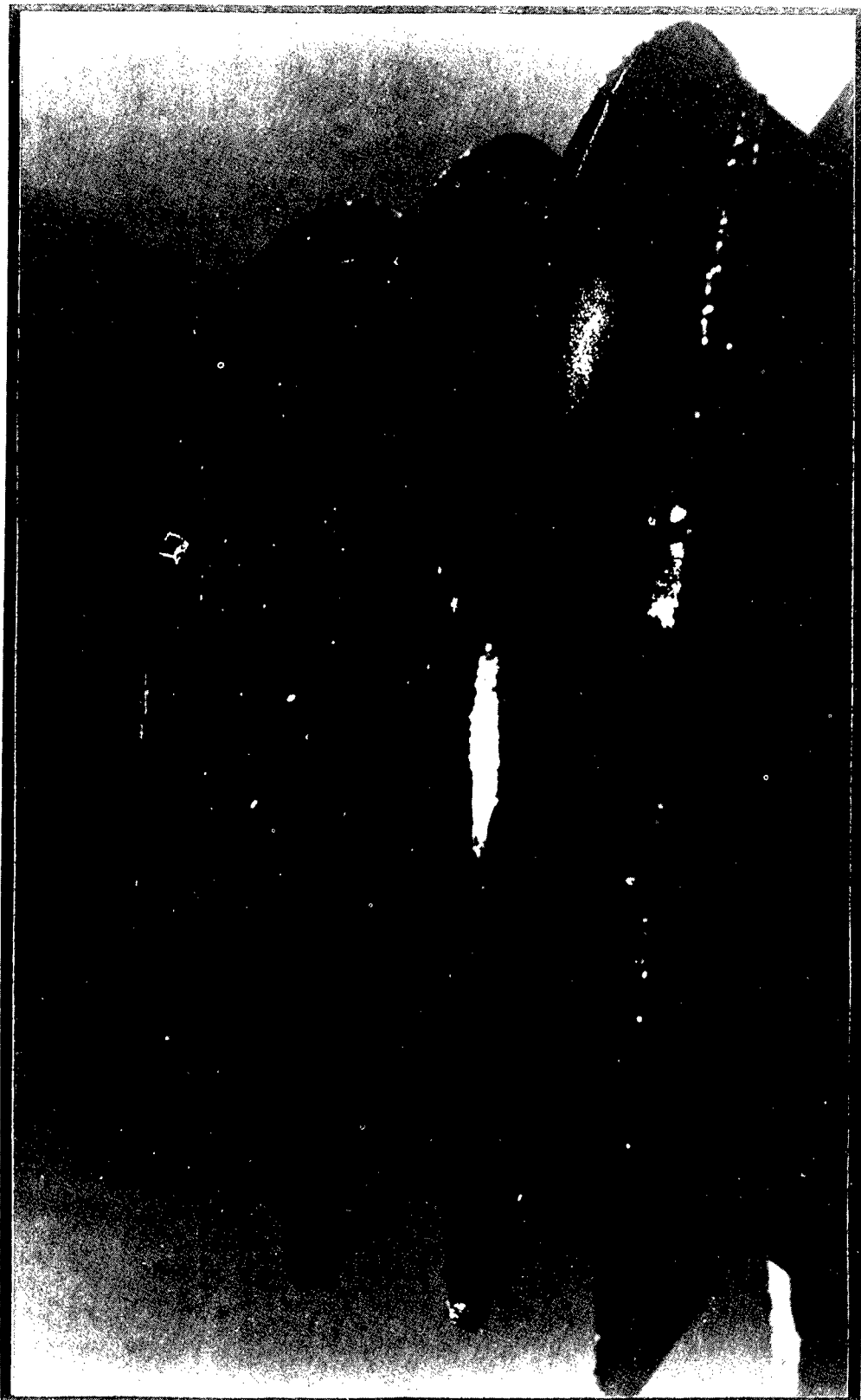
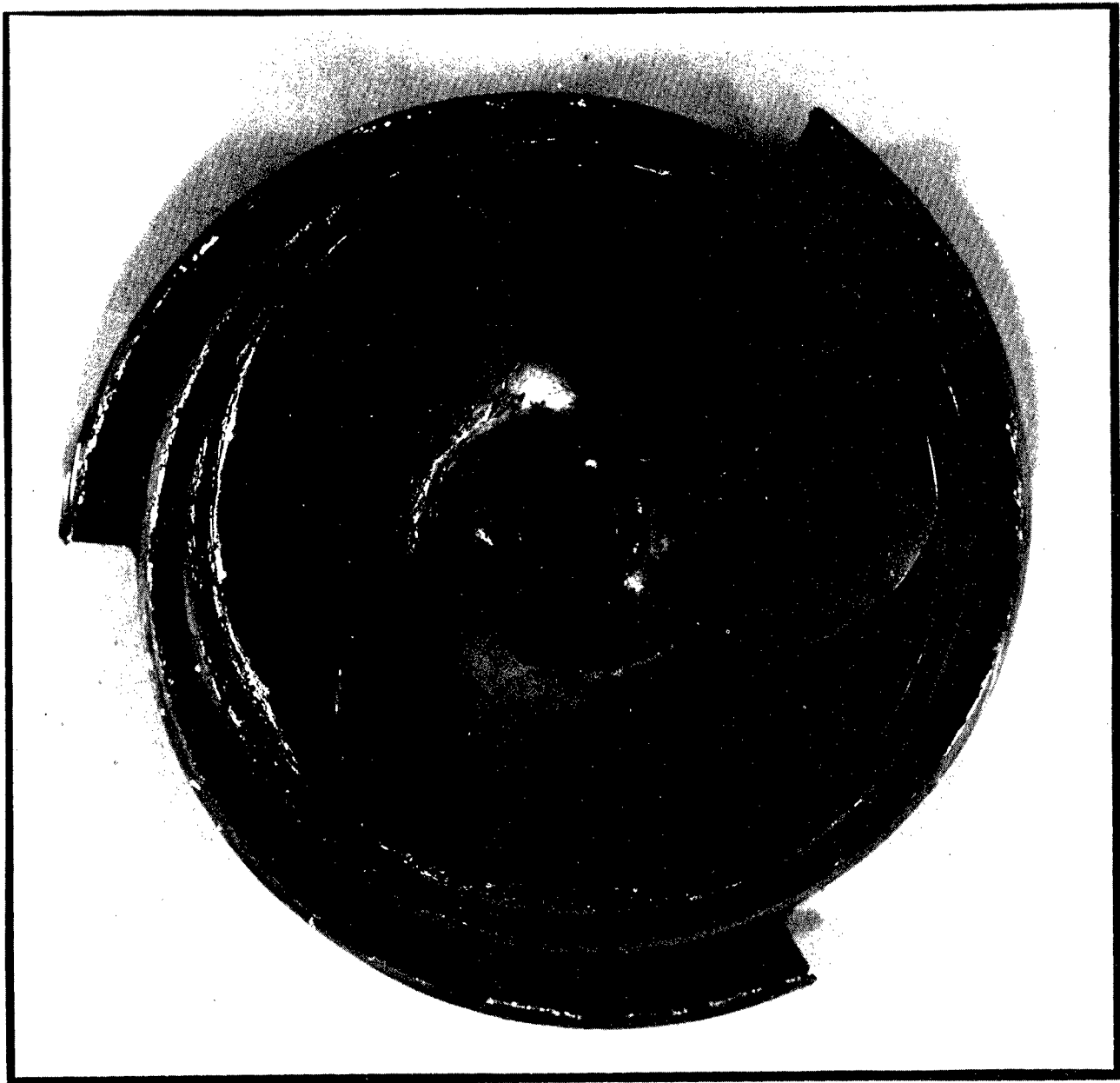


FIG 61

ZYGLO INSPECTION OF POSTTEST IMPELLER (INLET)



POSTTEST VIEW OF RI-7C3 IMPELLER VANE 2 SURFACE

FIG 62

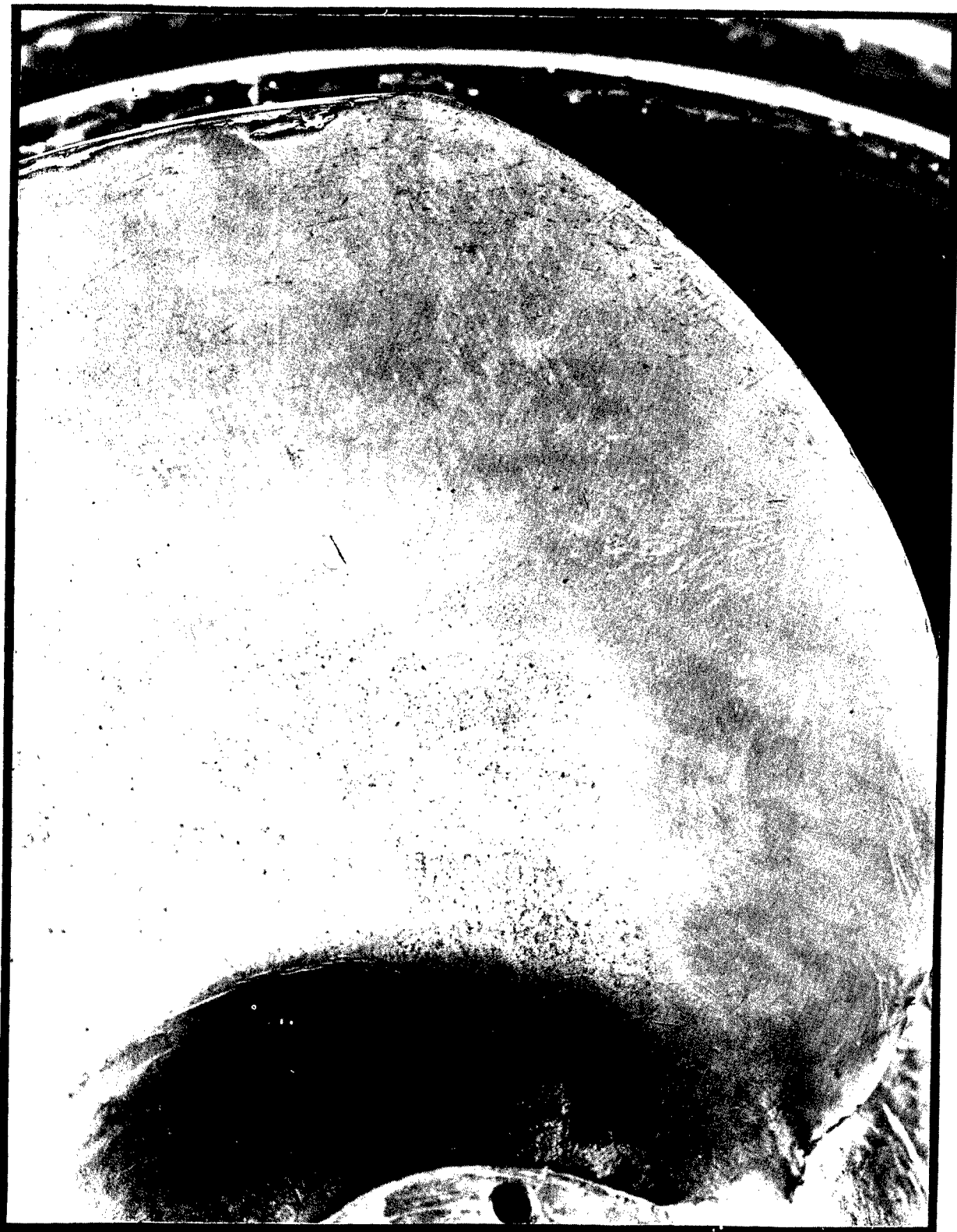
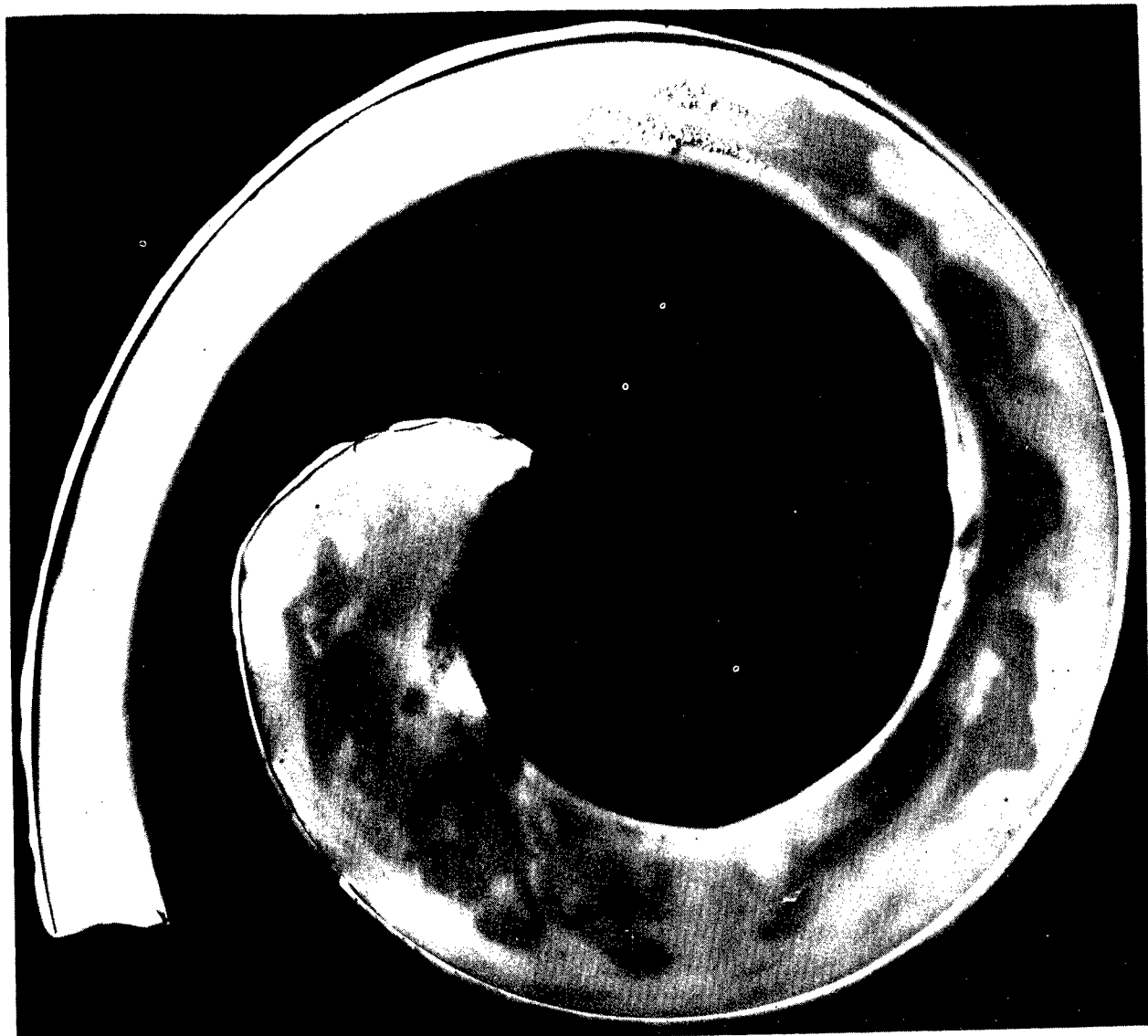


FIG 63

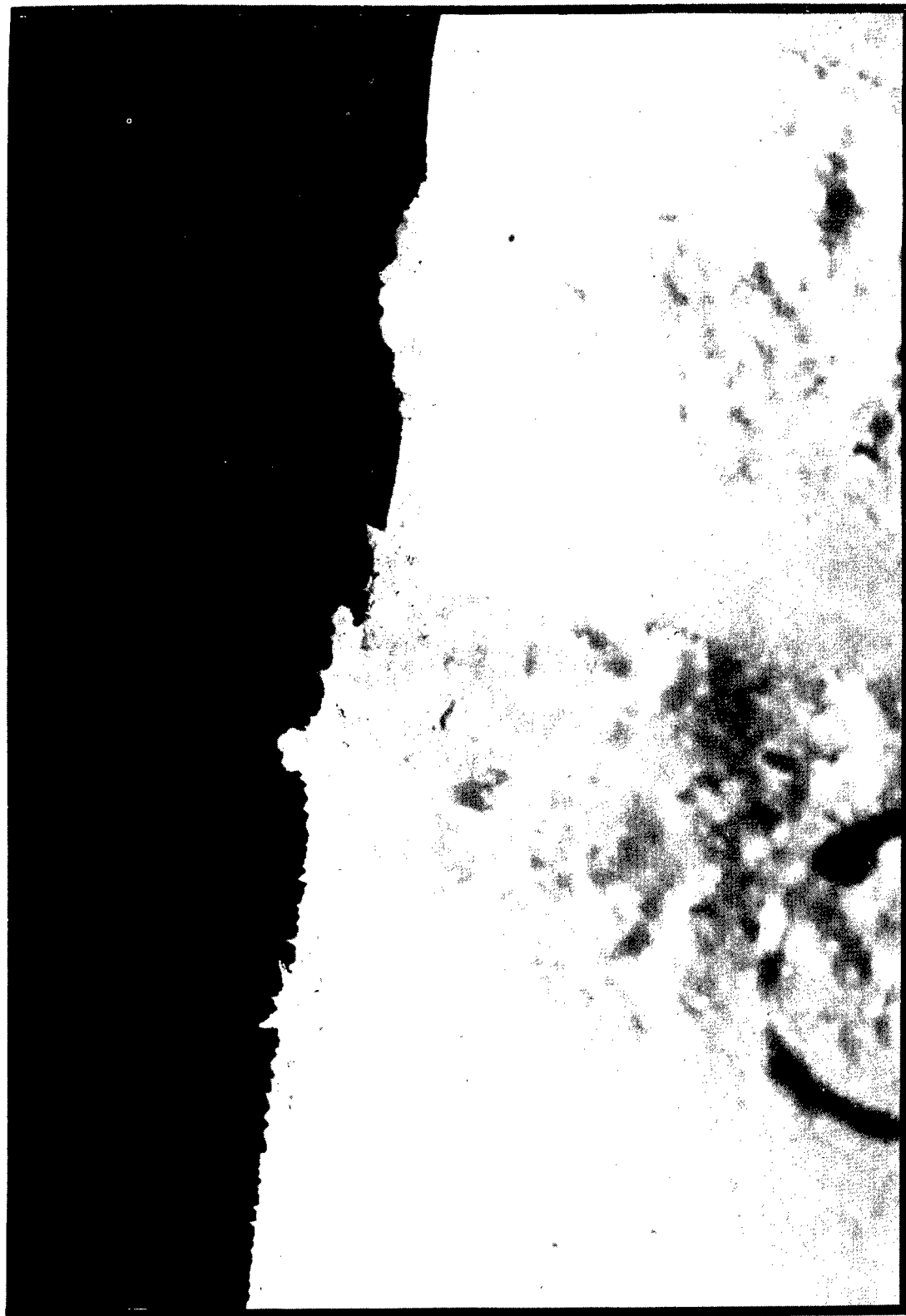
RUBBER MOLD OF IMPELLER VANE SURFACE AFTER POTASSIUM TEST
PRESSURE SURFACE OF VANE 2



RUBBER MOLD OF IMPELLER VANE SURFACE AFTER POTASSIUM TEST

PRESSURE SURFACE OF VANE 2

FIG 63A

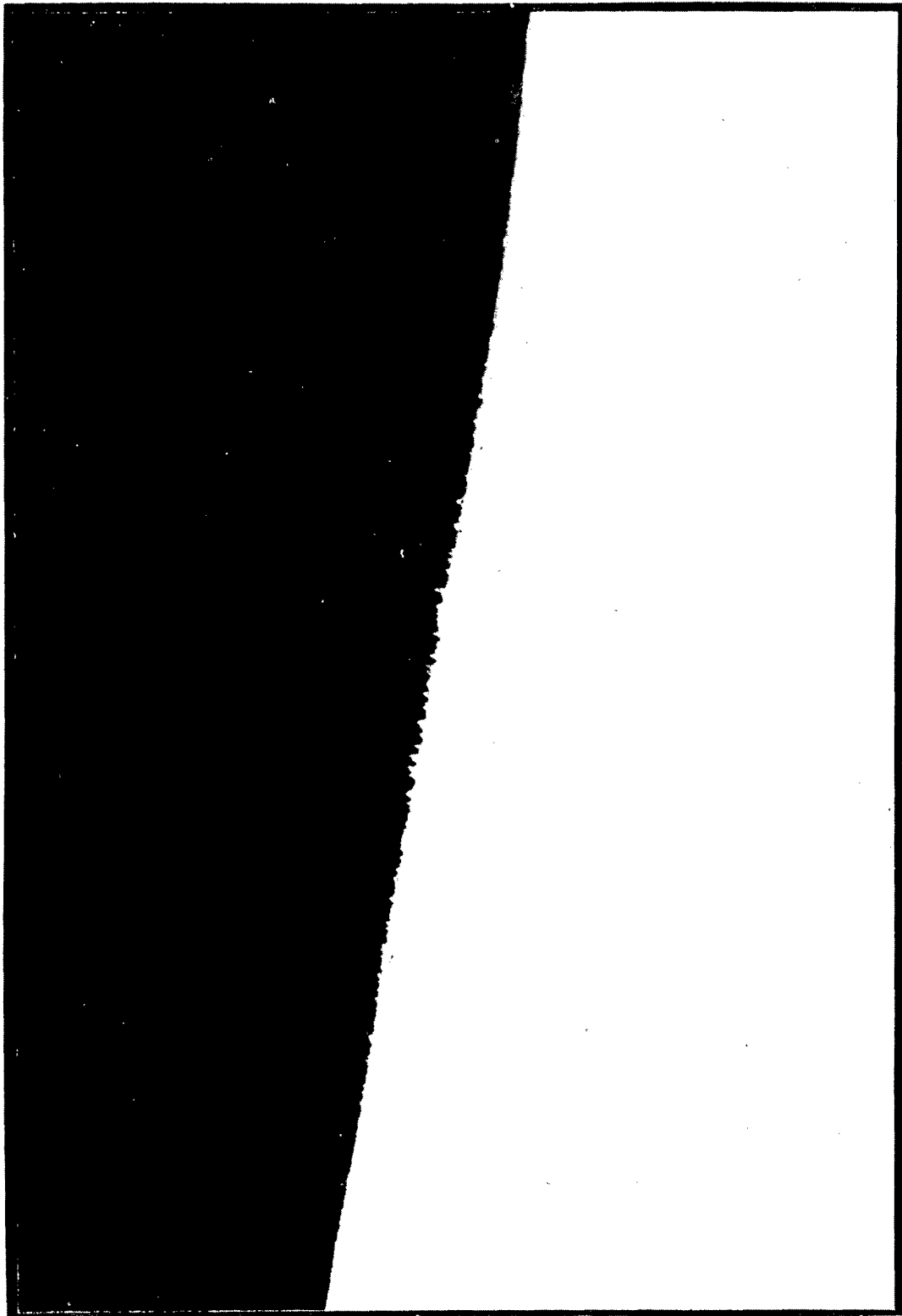


MAGNIFIED: 11X

RUBBER MOLD OF IMPELLER VANE SURFACE AFTER POTASSIUM TEST

PRESSURE SURFACE OF VANE 1

FIG 63B



MAGNIFIED: 23X

PRESSURE SIDE OF VANE 3 REMOVED FROM IMPELLER

FIG 64



SURFACE AT 3 1/2 X

FIG 65

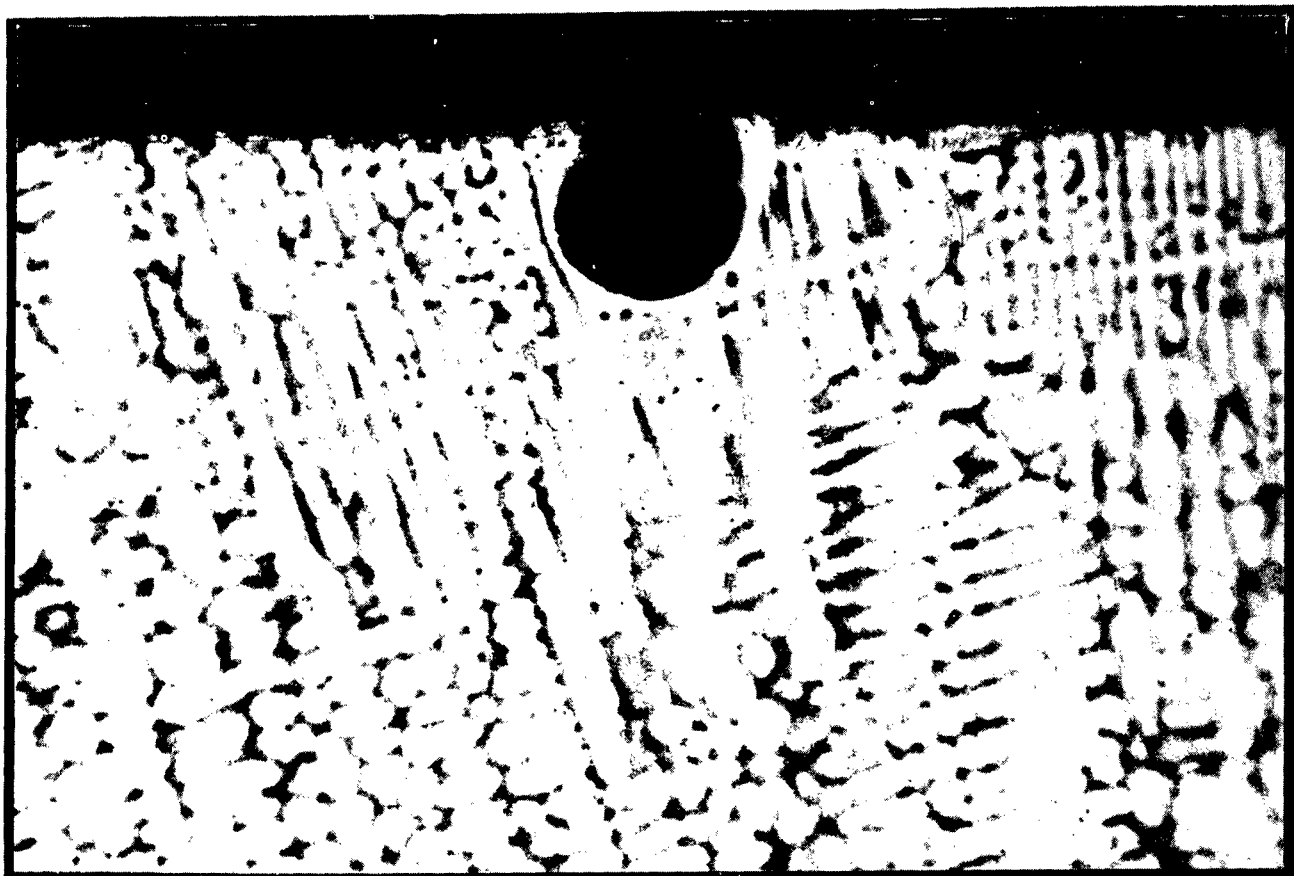
SINGLE EVENT PITTING OF VANE 3 PRESSURE SIDE



SURFACE AT 23X

FIG 66

LARGE PIT OF FIG. 65 IN CROSS SECTION



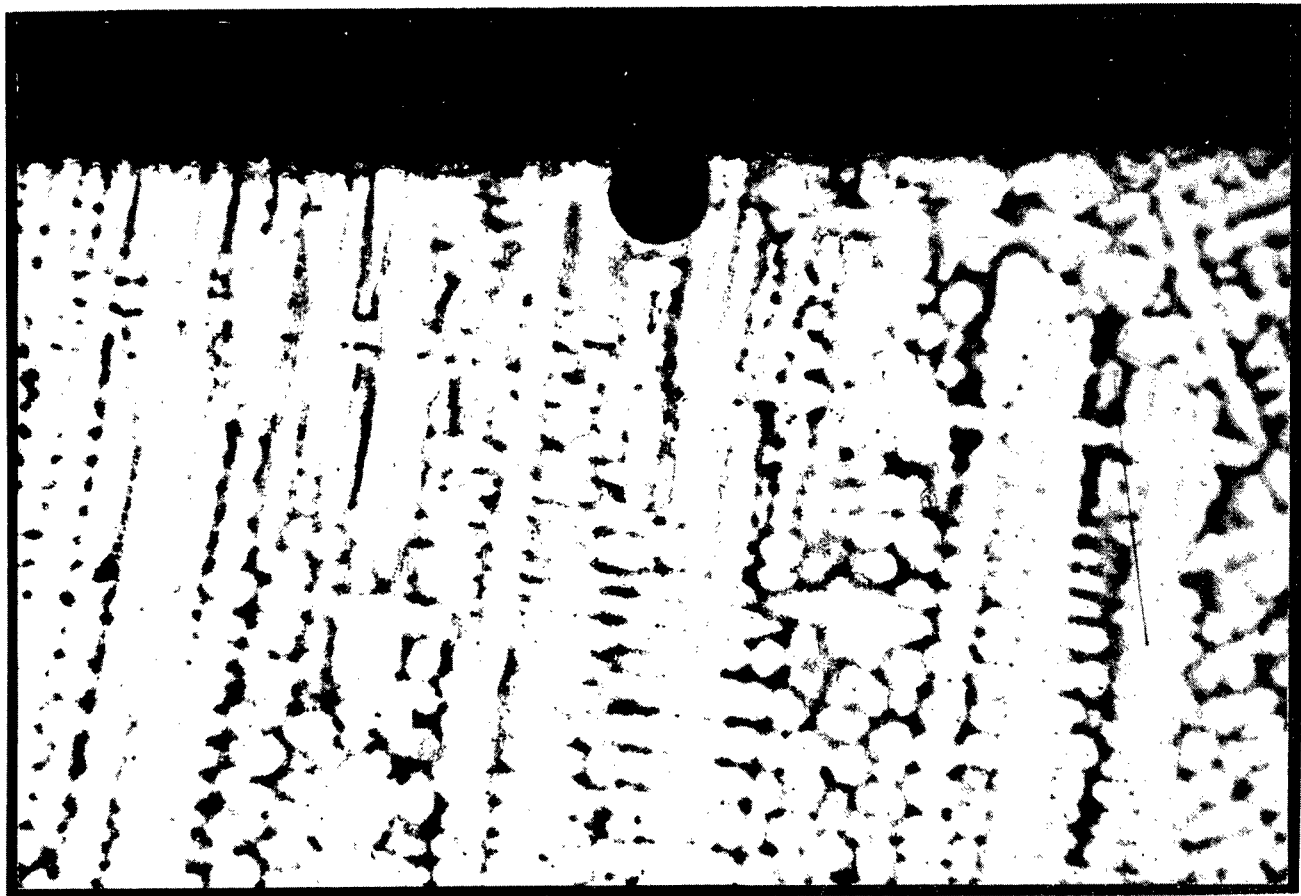
ETCHANT: OXALIC ACID

MATERIAL: 316 SS

MAGNIFIED: 100X

FIG 67

SMALLER PIT OF FIG. 65 IN CROSS SECTION



ETCHANT: OXALIC ACID

MATERIAL: 316 SS

MAGNIFIED. 100X

FIG 68

PHOTOMICROGRAPH OF PRETEST MATERIAL



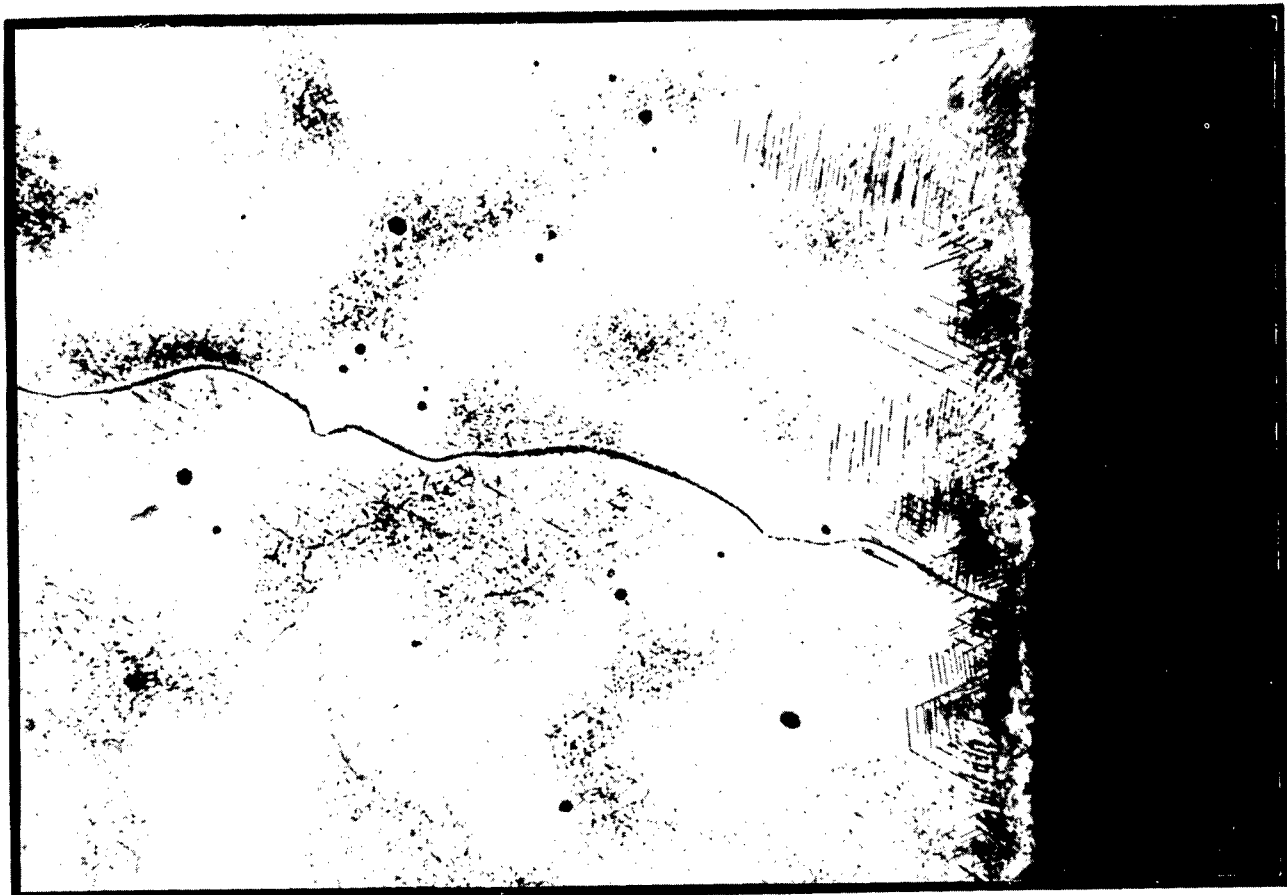
ETCHANT: 10% OXALIC

MAGNIFIED: 500X

CROSS SECTION AREA AT PRESSURE FACE DISPLAYING LARGE GRAINED, CORED 316 SS MICROSTRUCTURE. WIDMANSTÄTTEN CARBIDE PRECIPITATION IS TYPICAL OF ALL SURFACES AND RESULTED FROM THE CASTING PROCESS. RANDOM RECRYSTALLIZATION CAN BE OBSERVED AT THE SURFACE.

FIG 69

PHOTOMICROGRAPH OF POSTTEST UNDAMAGED MATERIAL



ETCHANT: 10% OXALIC

MAGNIFIED: 500X

CROSS SECTION AREA AT PRESSURE FACE, NO APPARENT ATTACK MICROSCOPICALLY. MATRIX CARBIDE PHASE MORE HOMOGENEOUSLY DISTRIBUTED THAN IN PRETEST CONDITION DUE TO TEST TIME AND TEMPERATURE.

FIG 70

PHOTOMICROGRAPH OF POSTTEST MATERIAL OF FIG. 69 AT HIGHER MAGNIFICATION



ETCHANT: 10% OXALIC

MAGNIFIED: 2000X

TYPICAL AREA AT PRESSURE SIDE WHICH DELINEATES EXTREMELY SMALL RECRYSTALLIZED GRAIN STRUCTURE WITH SPHEROIDAL CARBIDE PRECIPITATION IN THE GRAIN BOUNDARIES

PHOTOMICROGRAPH OF VANE 2 CAVITATION DAMAGE

FIG 71



TRANSVERSE
SECTION

VANE PRESSURE
SURFACE

LONGITUDINAL
SECTION

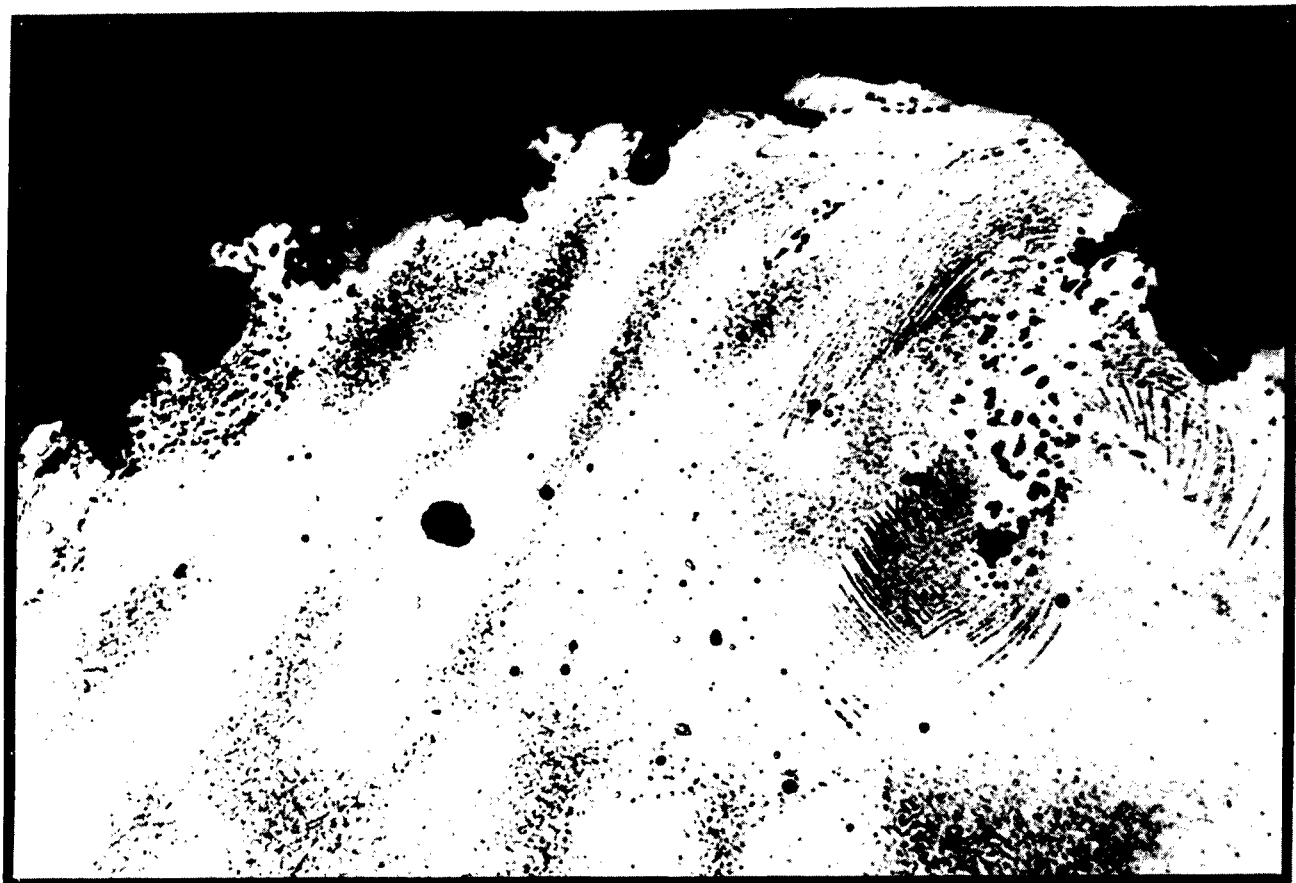
ETCHANT: 10% OXALIC

30X

MAXIMUM DEPTH OF DAMAGE OBSERVED WAS 0.050 INCHES. NOTE DEFORMATION AT CAVITATED SURFACES.

FIG 72

PHOTOMICROGRAPH OF VANE 2 CAVITATION DAMAGE AT
500X



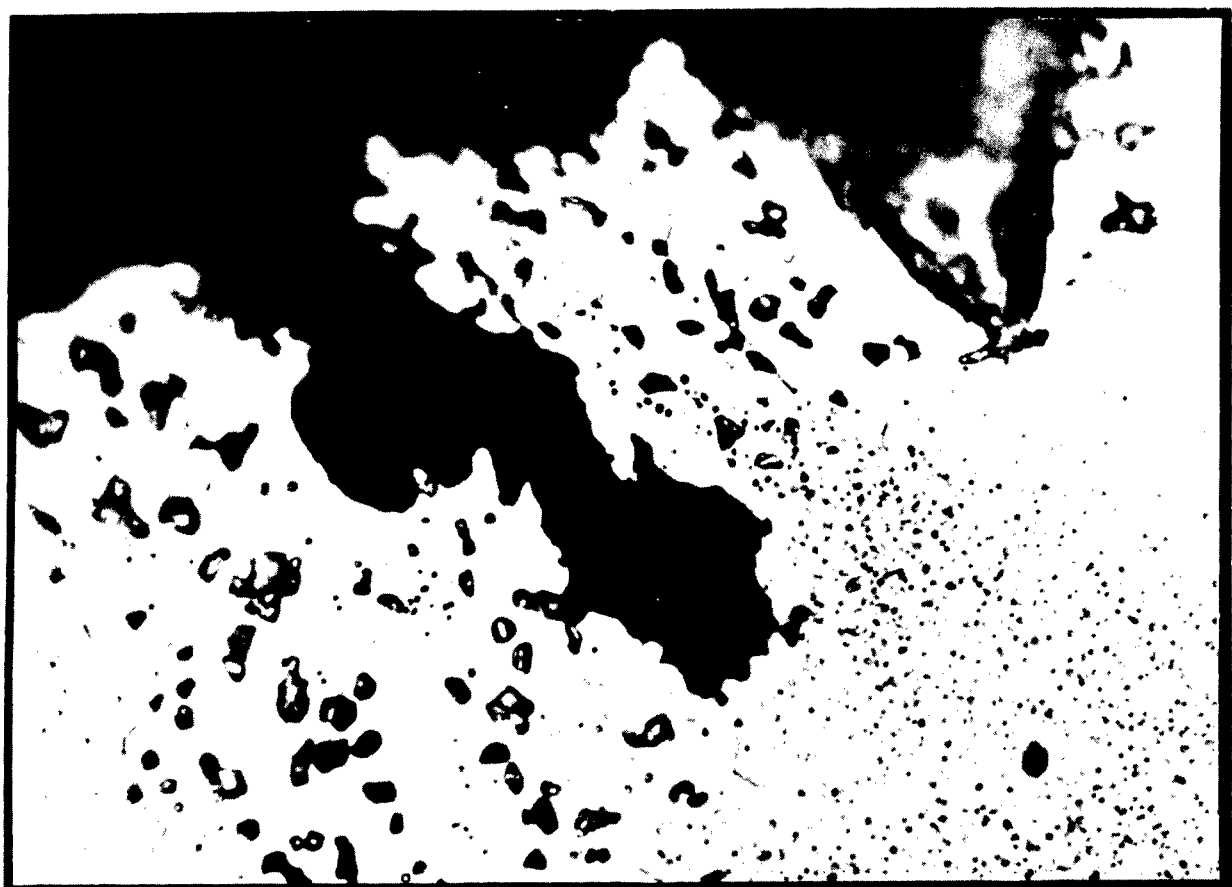
ETCHANT 10% OXALIC

MAGNIFIED: 500X

DEFORMATION AND RE-PRECIPITATION OF CARBIDE PHASE
IS OBSERVED AT CAVITATION DAMAGED SURFACE

FIG 73

PHOTOMICROGRAPH OF VANE 2 CAVITATION DAMAGE
AT 2000X



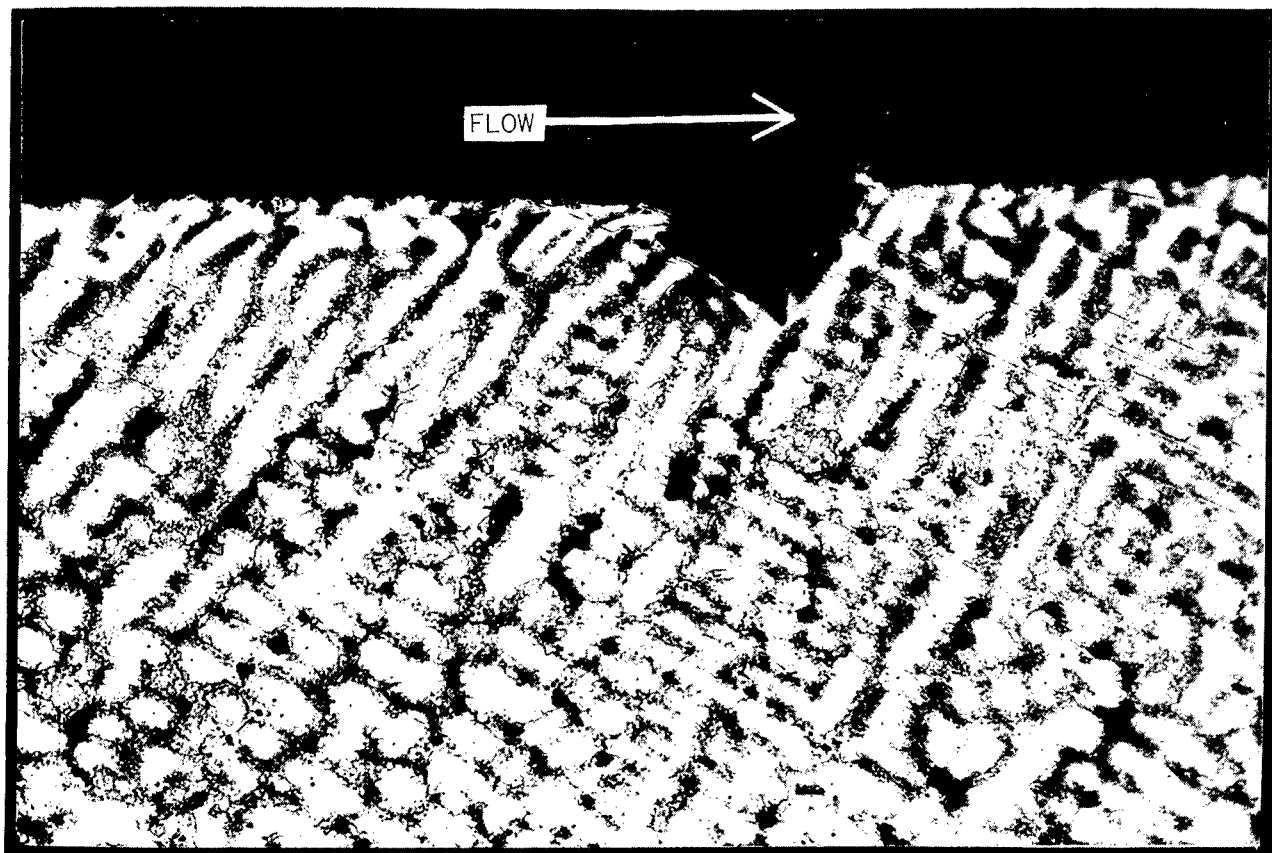
ETCHANT: 10% OXALIC

MAGNIFIED: 2000X

RECRYSTALLIZATION AND GRAIN BOUNDARY PRECIPITATION
OF CARBIDE PHASE AT CAVITATION SURFACE IS CLEARLY
NOTED.

FIG 74

PHOTOMICROGRAPH OF PROJECTION CAUSING CAVITATION DAMAGE



ETCHANT: 10% OXALIC

MAGNIFIED: 100X

AREA OF INDUCED CAVITATION SHOWING RAISED LIP AT
EDGE OF PIT BELIEVED RESPONSIBLE FOR MINOR CAVITATION
DAMAGE ON SUCTION SURFACE OF VANE 2

FIG 75

PRETEST PHOTOGRAPH OF VANE 2

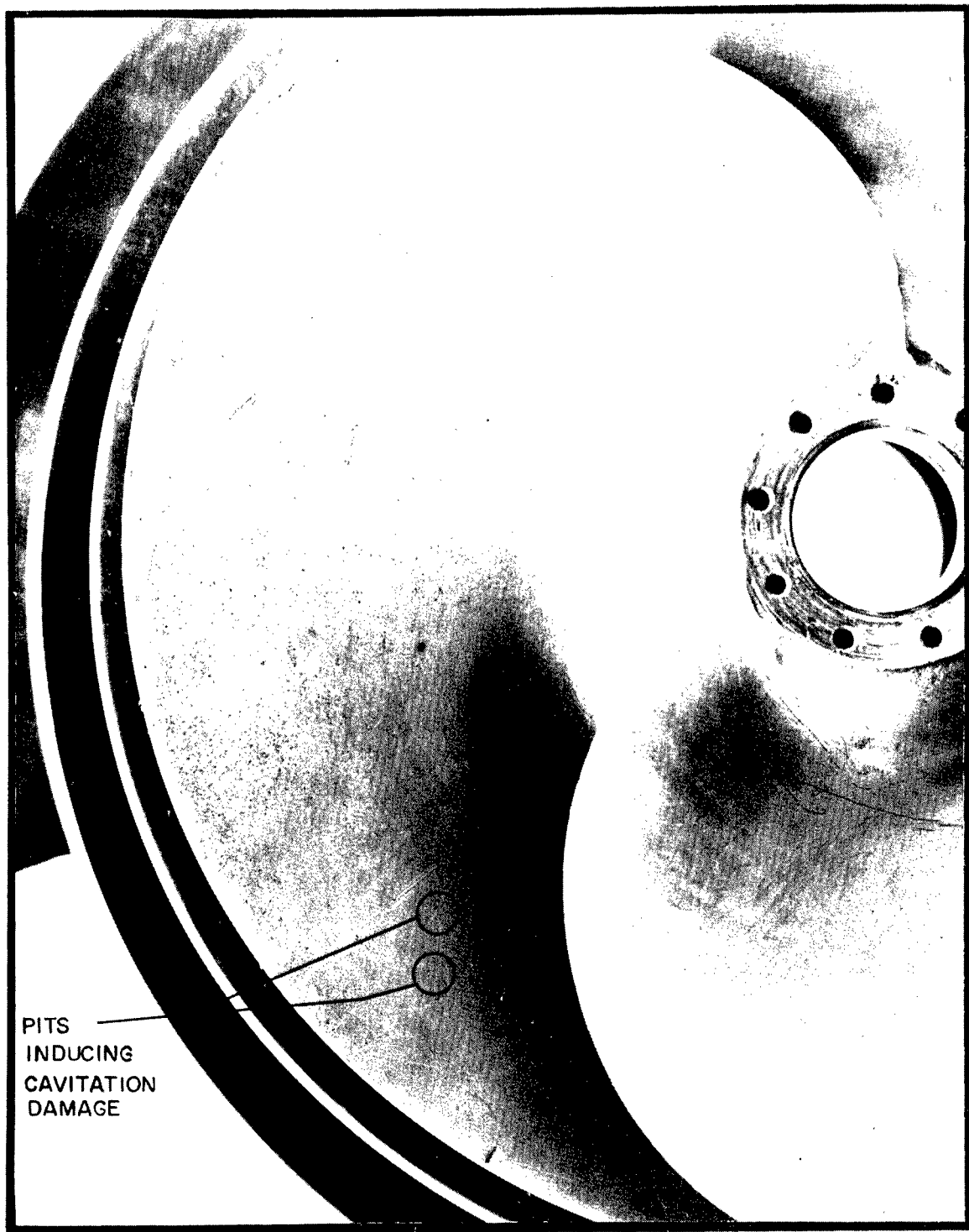
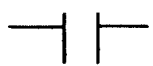


FIG 76

PHOTOMICROGRAPH OF PIT INDUCING CAVITATION DAMAGE
AT 1500X



ETCHANT: 10% OXALIC



MAGNIFIED: 1500X

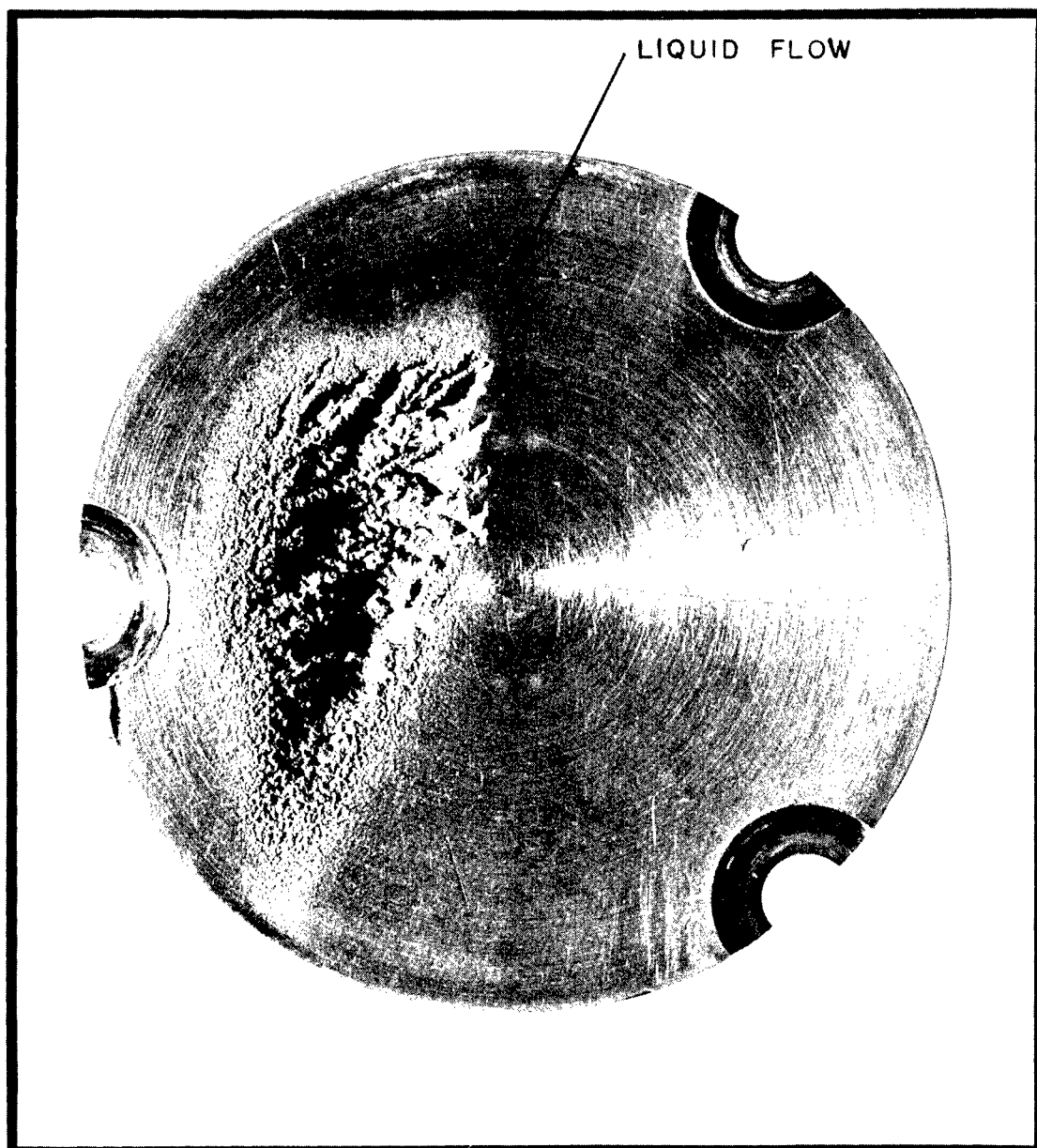
NICKEL-RICH ZONE
AT BOTTOM OF PIT

STRUCTURAL CHANGE AROUND THE EDGE OF SECONDARY
CAVITATION PIT.

FIG 77

DISK SPECIMEN FROM ROTATING DISK CAVITATION
DAMAGE TESTS IN WATER

TIME: 75 HOURS TEMPERATURE: 100F MATERIAL: 316 SS

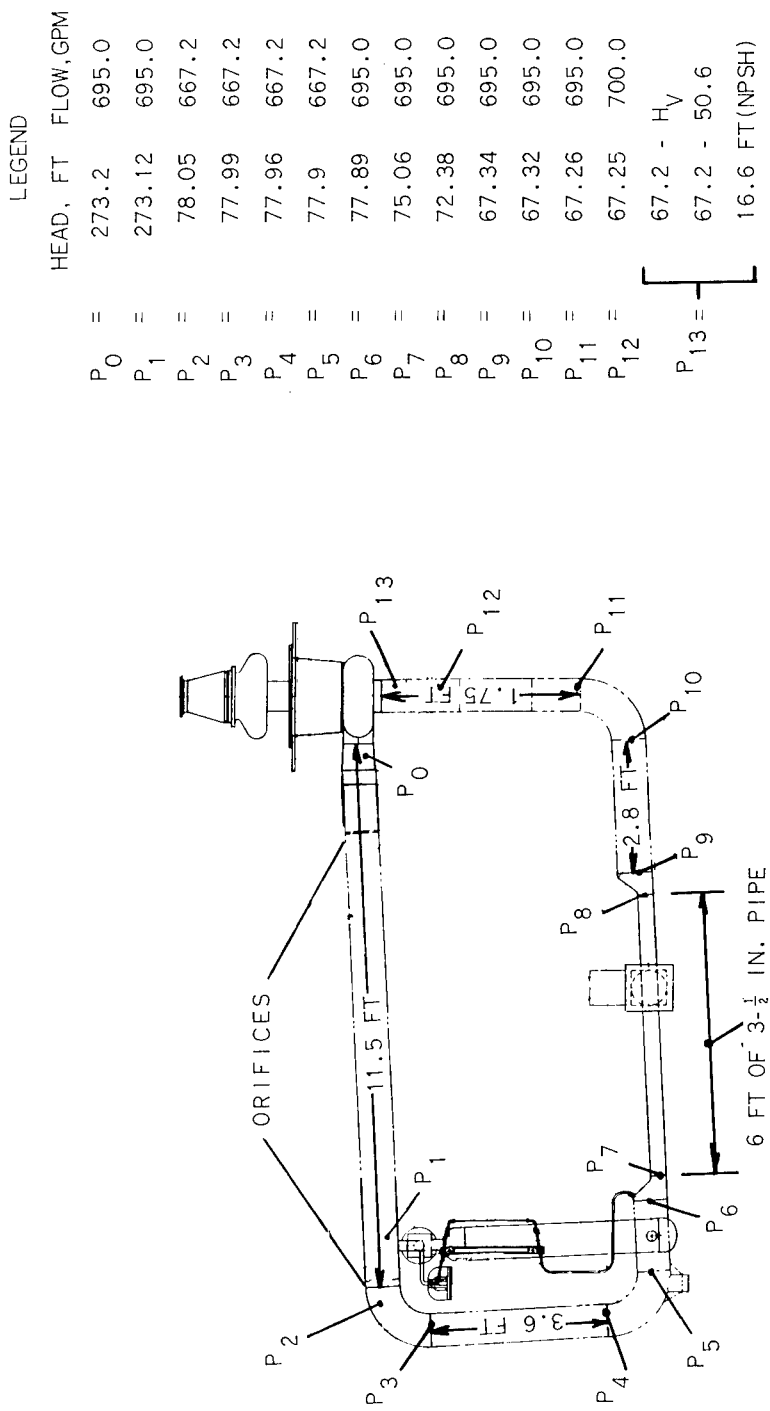


REF: ASME PAPER NO. 63 AHGT-26

MAGNIFIED: 7X

CALCULATED HEAD LOSSES AROUND LIQUID METAL PUMP LOOP

FIG 78



A motion-picture film supplement CRC-1 is available on loan. Requests will be filled in the order received. You will be notified of the approximate date scheduled.

The film (16 mm, $15\frac{1}{2}$ min, B&W, silent but projected at sound speed) shows 25 actual tests of cavitation in water. Five tests with varying degrees of cavitation are shown for each of the five flow rates tested. Sufficient information on the test impeller, test stand, and test conditions are presented to make this supplement self explanatory.

Film supplement CRC-1 is available on request to

Chief, Technical Information Division (5-5)
NASA Lewis Research Center
21000 Brookpark Road
Cleveland, Ohio 44135

CUT

Date _____

Please send, on loan, copy of film supplement CRC-1 to
NASA CR-165.

Name of organization _____

Street number _____

City and State _____

Zip code _____

Attention: Mr. _____
Title _____

Place
stamp
here

Chief, Technical Information Division (5-5)
NASA Lewis Research Center
21000 Brookpark Road
Cleveland, Ohio 44135

"The aeronautical and space activities of the United States shall be conducted so as to contribute . . . to the expansion of human knowledge of phenomena in the atmosphere and space. The Administration shall provide for the widest practicable and appropriate dissemination of information concerning its activities and the results thereof."

—NATIONAL AERONAUTICS AND SPACE ACT OF 1958

NASA SCIENTIFIC AND TECHNICAL PUBLICATIONS

TECHNICAL REPORTS: Scientific and technical information considered important, complete, and a lasting contribution to existing knowledge.

TECHNICAL NOTES: Information less broad in scope but nevertheless of importance as a contribution to existing knowledge.

TECHNICAL MEMORANDUMS: Information receiving limited distribution because of preliminary data, security classification, or other reasons.

CONTRACTOR REPORTS: Technical information generated in connection with a NASA contract or grant and released under NASA auspices.

TECHNICAL TRANSLATIONS: Information published in a foreign language considered to merit NASA distribution in English.

TECHNICAL REPRINTS: Information derived from NASA activities and initially published in the form of journal articles.

SPECIAL PUBLICATIONS: Information derived from or of value to NASA activities but not necessarily reporting the results of individual NASA-programmed scientific efforts. Publications include conference proceedings, monographs, data compilations, handbooks, sourcebooks, and special bibliographies.

Details on the availability of these publications may be obtained from:

SCIENTIFIC AND TECHNICAL INFORMATION DIVISION

NATIONAL AERONAUTICS AND SPACE ADMINISTRATION

Washington, D.C. 20546